DISSERTATIONES
MEDICINAE
UNIVERSITATIS
TARTUENSIS
339

KHAN NGUYEN VIET

Chemical composition and bioactivity of extracts and constituents isolated from the medicinal plants in Vietnam and their nanotechnology-based delivery systems

DISSERTATIONES MEDICINAE UNIVERSITATIS TARTUENSIS
339

DISSERTATIONES MEDICINAE UNIVERSITATIS TARTUENSIS
339

KHAN NGUYEN VIET

Chemical composition and bioactivity of extracts and constituents isolated from the medicinal plants in Vietnam and their nanotechnology-based delivery systems

UNIVERSITY OF TARTU
Press
1632

Institute of Pharmacy, Faculty of Medicine, University of Tartu, Estonia

Dissertation is accepted for the commencement of the degree of Doctor of Philosophy (in Pharmacy) on 21.12.2022 by the Council of the Faculty of Medicine, University of Tartu, Estonia.

Supervisors: Professor Ain Raal, PhD
Institute of Pharmacy, Faculty of Medicine,
University of Tartu, Estonia

Professor Hoai Thi Nguyen, PhD
Faculty of Pharmacy,
Hue University of Medicine and Pharmacy, Vietnam

Professor Jyrki Heinämäki, PhD
Institute of Pharmacy, Faculty of Medicine,
University of Tartu, Estonia

Reviewed by: Associate Professor Külli Jaako, PhD
Department of Pharmacology, Institute of Biomedicine and Translational Medicine, Faculty of Medicine,
University of Tartu, Estonia

Associate Professor Uno Mäeorg, PhD
Institute of Chemistry, Faculty of Science and Technology,
University of Tartu, Estonia

Opponent: Associate Professor Yvonne Holm, PhD
Division of Pharmaceutical Biosciences, Faculty of Pharmacy,
University of Helsinki, Finland

Commencement: 14.02.2023

Publication of this dissertation is granted by the University of Tartu.

This research was supported by the Erasmus Plus, Edushare Funding Programme, the national research projects in Estonia IUT34-18 and PUT1088, the National Foundation for Science and Technology Development (NAFOSTED) of Vietnam, and Hue University.

ISSN 1024-395X (print) ISSN 2806-240X (pdf)
ISBN 978-9916-27-125-4 (print) ISBN 978-9916-27-126-1 (pdf)

University of Tartu Press
www.tyk.ee

CONTENTS

LIST OF ORIGINAL PUBLICATIONS

The thesis is based on the following publications, which are referred to in the text by their Roman numerals (I–V):

I **Nguyen, K.V**., Ho, D.V., Nguyen, H.M., Do, T.T., Phan, K.V., Morita, H., Heinämäki, J., Raal, A., Nguyen, H.T., 2020. *chiro*-Inositol derivatives from *Chisocheton paniculatus* showing inhibition of nitric oxide production. *Journal of Natural Products*, 83 (4), 1201–1206.

II **Nguyen, K.V.**, Ho, DV, Le, AT, Heinämäki, J., Raal, A, Nguyen, H.T., 2021. Secondary metabolites from *Alphonsea tonkinensis* A.DC. showing inhibition of nitric oxide production and cytotoxic activity. *Journal of Pharmacy & Pharmacognosy Research*, 9 (1), 24–32.

III **Nguyen, K.V.**, Nguyen, T.O.T., Ho, DV, Heinämäki, J., Raal, A., Nguyen, H.T., 2021. *In-vitro* acetylcholinesterase inhibitory and antioxidant activity of *Alphonsea tonkinensis* A.DC. *Natural Product Communications*, 16 (9), 1–5.

IV **Nguyen, K.V.**, Ho, D.V., Le, N.T., Phan, K.V., Heinämäki, J., Raal, A., Nguyen, H.T., 2020. Flavonoids and alkaloids from the rhizomes of *Zephyranthes ajax* Hort. and their cytotoxicity. *Scientific Reports*, 10, 22193.

V **Nguyen, K.V.**, Laidmäe, I., Kogermann, K., Lust A., Meos, A., Ho, D.V., Raal, A., Heinämäki, J., Nguyen, H.T., 2019. Preformulation study of electrospun haemanthamine-loaded amphiphilic nanofibers intended for a solid template for self-assembled liposomes. *Pharmaceutics*, 11, 499, 1–13.

Contribution of Khan Viet Nguyen to original publications (I-V):

I Participation in the study design, extraction and isolation, performing part of characterization of compounds, coordinating experiments and participating in sample preparation for bioactivity tests, performing data analysis, writing the paper.

II Participation in the study design, extraction and isolation, performing part of characterization of compounds, coordinating experiments and participating in sample preparation for bioactivity tests, performing data analysis, writing the paper.

III Participation in the study design, extraction and isolation, performing bioactivity tests, performing data analysis, writing the paper.

IV Participation in the study design, extraction and isolation, performing part of characterization of compounds, coordinating experiments and participating in sample preparation for bioactivity tests, performing data analysis, writing the paper.

V Participation in the study design, preparation of electrospun nanofibers, optical microscopy, FTIR spectroscopy, DSC, *in-vitro* drug release, coordinating experiments and participating in sample preparation for the analyses (SEM, XRPD, HPLC), performing data analysis, writing the paper.

ABBREVIATIONS

Ach	acetylcholine
AChE	acetylcholinesterase
AD	Alzheimer's disease
AGS	human stomach gastric adenocarcinoma cell line
API	active pharmaceutical ingredient
ATP	adenosine 5'-triphosphate
BC	before Christ
CD	circular dichroism
CH_2Cl_2	dichloromethane
CNS	central nervous system
COSY	correlation spectroscopy
DDS	drug delivery system
DMEM	Dulbecco's modified eagle medium
DMSO	dimethyl sulfoxide
DNA	deoxyribonucleic acid
DPPH	1,1-diphenyl-2-picrylhydrazyl
DTNB	5,5′-dithiobis-nitrobenzoic acid
DSC	differential scanning calorimetry
EC	ethyl acetate (portion)
ES	electrospinning
EtOAc	ethyl acetate
FBS	fetal bovine serum
FDA	Food and Drug Administration
FTIR	Fourier-transform infrared
HAE	haemanthamine
HCl	hydrochloric acid
HeLa	Henrietta Lacks
HepG2	human hepatocellular carcinoma cell line
HMBC	heteronuclear multiple bond correlation
HPLC	high-performance liquid chromatography
HPLC/MS/MS	high-performance liquid chromatography with tandem mass spectrometry
HRMS	high-resolution mass spectrometry
HRESIMS	high-resolution electronspray ionization mass spectrometry
HSQC	heteronuclear Single Quantum Coherence
IC_{50}	half maximal inhibitory concentration
IR	infrared
KB	human carcinoma in the mouth cell line
L-NMMA	N^G-methyl-L-arginine acetate
LPS	lipopolysaccharide
Me	methyl
MeOH	methanol

MTT	3-(4,5-dimethylthiazole-2-yl)-2,5-diphenyltetrazolium bromide
NF	nanofiber
NLT	not less than
NMR	nuclear magnetic resonance
NO	nitric oxide
NP	nanoparticle
NOESY	nuclear overhauser effect spectroscopy
OMe	methoxy
PC	phosphatidylcholine
PCS	photon correlation spectroscopy
PVP	polyvinylpyrrolidone
SEM	scanning electron microscope
SK-LU-1	human lung carcinoma cell line
SRB	sulforhodamine B assay
SW480	human colon carcinoma cell line
TLC	thin-layer chromatography
US	United States
UV-Vis	ultraviolet-visible
XRPD	X-ray powder diffraction
WHO	World Health Organization
W/O	water-in-oil

1. INTRODUCTION

Chronic diseases are becoming a true global challenge and burden for a health care, and today they are the leading causes of death and disability (Murray et al., 2020). Such diseases include e.g., different types of cancers, asthma, heart diseases, neurodegenerative central nervous system (CNS) diseases and type 2 diabetes. The treatment of the present diseases is increasingly promoted by a modern drug therapy based on either synthetic (chemistry-based) or medicinal plant origin therapeutic agents.

Medicinal plants that have been used since prehistoric times have been proved to be the highly successful source for the discovery of new drugs with chemical and biological diversity (Atanasov et al., 2015). It is estimated that approximately 94% of existing plant species have not been pharmacologically studied to date. Thereby, medicinal plants still offer an important and potential pool with a huge number of unknown compounds to be discovered and studied (Cragg & Newman, 2013). Today, the powerful isolation, identification and structure elucidation techniques enable us to discover and investigate promising new drug candidates of plant origin. The modern isolation techniques such as preparative high-performance liquid chromatography (HPLC), centrifugal partition chromatography or support-free liquid-liquid chromatography have facilitated the isolation of active compounds from natural products (Renault, 2015). Furthermore, nuclear magnetic resonance (NMR) spectroscopy or high-resolution mass spectrometry (HRMS) or combined methods such as liquid chromatography–HRMS or the integration of HRMS and NMR spectroscopies have been applied to simplify structure elucidation of organic compounds even very small amount (less than 10 μg) (Elyashberg, 2015; Atanasov et al., 2021).

The drug substances isolated from plants could present poor water solubility, limited dissolution rate, poor absorption in the body, limitations in target-specific drug delivery, high level of metabolization and fast excretion process, thus leading to a low oral bioavailability and reduced therapeutic effect. These limitations significantly restrict their utility in clinical practice (Júnior et al., 2018).

Nanotechnology is an emerging field of science, and it has found uses in a wide range of applications in medicine, especially in the development of advanced drug delivery systems (DDSs). Nanoscale DDSs provide a novel and powerful alternative for conventional dosage forms intended for the delivery of potential new drugs of plant origin (Patra et al., 2018; Zhang et al., 2018). Nanotechnology-based DDSs enable to enhance the water-solubility of drugs, to improve the stability of herbal medicines from enzymatic degradation, to enhance the delivery of actives to the desired target and/or inside the cell membrane, to reduce therapeutic dose and to reduce adverse effects (Ertas et al., 2021; Teja et al., 2022). Nanotechnology-based DDSs for plant-origin actives have been proven to increase several to hundred times oral bioavailability compared to active pharmaceutical ingredient (API) alone (Teja et al., 2022). Hence, it is expected that a combination of herbal medicines with pharmaceutical

nanotechnology can be a key tool for the advancement of medicinal plant research and therapy (Teja et al., 2022).

Electrospinning (ES) is a versatile and viable method for fabricating uniform and ultrathin fibers (Xue et al., 2019). The electrospun nano- and microfibers enable to generate flexible DDSs and to achieve versatile drug release kinetics to accomplish multiple therapeutic needs. Such polymeric nano- and microfibers as DDSs can improve for example oral bioavailability and therapeutic effects of API(s) owing to the appropriate site, timing and rate for a drug release (Kajdič et al., 2019).

Vietnamese traditional medicine has a long and prestigious history, and it still plays a primary role in the healthcare system of Vietnam. Vietnamese traditional medicine consists of a number of herbal medicines, indigenous folk therapies, and practices from total 54 Vietnamese ethnic groups (Woerdenbag et al., 2012; Nguyen et al., 2016). In particular, the three species of higher plants such as *Chisocheton paniculatus* Hiern, *Alphonsea tonkinensis* A.DC. and *Zephyranthes ajax* Hort. growing in Vietnam are known as medicinal plants in traditional medicine, but only *C. paniculatus* has been studied scientifically. In the present doctoral research work, the first aim was to gain knowledge on the chemical composition and bioactivity of herbal extracts and compounds isolated from these medicinal plants. The chemical structure of the compounds was first determined/elucidated, and then the *in-vitro* bioactivity was evaluated (including anti-cancer cytotoxicity, anti-inflammatory and anti-acetylcholinesterase (AChE) activity). The second objective of the study was to develop novel nanotechnology-based DDSs for the present herbal extract(s) and constituent(s). More specifically, the goal was to design and fabricate electrospun amphiphilic nanofibers (NFs) loaded with a plant-origin API intended for the solid template of self-assembled liposomes. The physicochemical solid-state properties, *in-vitro* performance (dissolution) and stability of the present nanoformulation, were investigated.

2. LITERATURE REVIEW

2.1. Medicinal plants and traditional medicine

Natural products and especially medicinal plants have been utilized to prevent, alleviate and treat diseases since prehistoric times (Yuan et al., 2016). Evidence from fossil records shows that 8 plants were used as medicines at least 60,000 years (White, 2009). Plants provide a major source for drug discovery (Mushtaq et al., 2018), and it is estimated that more than 300,000 secondary metabolites potential for new drug candidates are present in the nature (Buxani et al., 2014). The first pharmacologically active compound, morphine, was isolated from opium in the beginning of the nineteenth century, and since then numerous active compounds have been isolated and identified from plants (Atanasov et al., 2015). Within the past decades, however, the importance of medicinal plants has decreased due to the development of synthetic techniques. Since synthetic compounds are easy to produce and resupply, and since they have a good compatibility with established high-throughput screening platforms, pharmaceutical industry has started to pay particular attention on synthetic compound libraries as drug discovery source (Atanasov et al., 2015). In spite of this, medicinal plants still play an important role in the identification of novel drug leads, and natural products are still in a constant and wide use (Yuan et al., 2016; Newman & Cragg, 2020; Atanasov et al., 2021). According to the World Health Organization (WHO), approximately 80% of the world's population relies on herbs for their medicine needs (Sayed et al., 2021).

Phytotherapy ("therapy by plants") is a field of medicine that uses plants to cure diseases, relieve symptoms or as health-promoting agents (Falzon & Balabanova, 2017; Leite et al., 2021). Phytotherapy relies on a long-term popular knowledge and scientific experience. Since 8,500 BC, the phytotherapeutic practices have represented the fundamental care in the developing countries, and popular complementary and alternative medicine in the developed countries (Leite et al., 2021).

Similarly, traditional medicine has significantly contributed to modern medicine. Traditional medicines of different countries, such as traditional Chinese medicine, Kampo, Indian Ayurveda, Arabic Unani medicine, traditional Korean medicine and traditional Vietnamese medicine, have been practiced for thousands of years (Alves & Rosa, 2007; Yuan et al., 2016). Traditional medicine represents the oldest form of health care, and the use of natural products has incomparable advantages. In addition, traditional medicine comprises of thousands of medicines with a diversity of chemical structures and pharmacological activities (Alves & Rosa, 2007; Zhang et al., 2012). Today, despite some defects, traditional medicine still plays an essential role in the prevention and treatment of physical and mental illnesses of many countries, and it is still a valuable repository of human knowledge (Yuan et al., 2016).

The inextricable link to traditional medicine and phytotherapy is phytochemistry (Cordell, 2011b; Egbuna et al., 2018). Phytochemistry is defined as

study of chemical composition of plants, particularly the secondary metabolites such as phenolics, terpenes, plant steroids, alkaloids, flavonoids, lignans, curcumines, saponins, flavonoids and glucosides, which are synthesized as a measure for self-defense against invasive factors. Phytochemistry investigates the structural constitutions of these metabolites, mechanisms of action, biosynthetic pathways, functions and medicinal and commercial applications (Egbuna et al., 2018). Practice shows that phytochemistry provides strong evidence bases for traditional medicine and phytotherapy, and plays a crucial role in fostering drug discovery and in the development of novel therapeutic agents (Cordell, 2011b; Egbuna et al., 2018).

2.2. Medicinal plants as resources of new drugs

Today, many chronic diseases, such as cardiovascular disease, cancer, Alzheimer's disease (AD), chronic respiratory diseases and diabetes are becoming true global health problems. The above-mentioned diseases attributing to three out of five deaths are the leading causes of death and disability worldwide (Yach et al., 2005; Wang et al., 2016).

2.2.1. Advantages and limitations of plant-based drug discovery

Higher plants that have been used since ancient times are well known to be a rich source for drug discovery. A high number of species enable also to generate a diversity of bioactive compounds for medicinal applications (Lachance et al., 2012). It is estimated that only 6% of existing plant species have been systematically investigated pharmacologically and only about 15% have been studied in phytochemistry (Cragg & Newman, 2013). Thus, there are a huge number of unknown compounds in higher plants for the scientists to be discovered and studied. Such plant-origin compounds are also made from living organisms that are evolutionarily optimized to operate specific biological functions comprising adjustment of defense mechanisms and the competitive interaction with other organisms, thus possessing properties with high relevance to disease treatment (Atanasov et al., 2015, 2021). The bioactive compounds isolated from medicinal plants could have unique pharmacokinetics and selective biological effects owing to their biosynthesis (Clardy & Walsh, 2004; Koehn & Carter, 2005). This explains the fact that more than half of the approved small-molecule drugs have been derived from or inspired by natural products (most from plants) in the last four decades (Newman & Cragg, 2020; Dehelean et al., 2021). It is also worth to mention that the knowledge of local ethics in medicine is a big advantage in discovering new medicines from herbs, since it saves a lot of time, effort and money. Therefore, searching active compounds from medicinal plants based on the experience of ethnic minorities could contribute the development of new drugs for human society (Mohanity et al., 2017).

Despite these advantages and the past success, many pharmaceutical companies have cut back on their use of natural products and medicinal plants in drug discovery due to several drawbacks (Atanasov et al., 2021). The assessment of plant material therapeutic claims is obstructed due to unstable quality and composition. The chemical constitution is dependent on many factors including species identity, harvest time, soil composition, altitude, actual climate, processing, and storage conditions. Moreover, the transformation and degradation of compounds can arise in the extraction and isolation processes (Bucar et al., 2013). A major challenge for plant-based drug discovery is that the amount (quantity) of numerous compounds isolated from higher plants are often insufficient for testing for a wide range of biological activities, particularly for characterizing the pharmacological activity of components. This challenge becomes even more serious, if some compound is identified as a very promising pharmaceutical lead. Recollections of wild species may be complicated due to changes of plant habitats of season-dependent chemical composition (David et al., 2015). In many cases, plant populations become threatened because of large-scale wild-crafting when it becomes commercialization of herbal medicines or one of its constituents recognized as a drug candidate (Cordell, 2011a), such as the "taxol supply crisis" (Cragg et al., 1993). Another major challenge is that natural products with complex chemical structures (i.e., numerous oxygen-containing substituents and chiral centers) lead to the challenges in total synthesis or derivatization, thus arising complications related to the resupply of bioactive natural (Atanasov et al., 2015). Further limitations related to drug discovery programs may occur from the fact that medicinal plants are commonly incompatible with high-throughput screening (Koehn & Carter, 2005). The well-known drawbacks of plant-origin drug candidates are related to their poor water solubility, restricted rate of dissolution, instability in low pH values, fast metabolization and rapid clearance process, thus resulting in limited oral bioavailability and less or no therapeutic effect. These challenges limit their application in clinical practice (Júnior et al., 2018).

In spite of the limitations mentioned above, medicinal plants remain a promising resource of drug candidates in the current and future development pipeline. The scientific and technological advances associated with a natural product research will enhance the discovery of new drug candidates especially from previously inaccessible plant sources. The chemical and biological diversity of medicinal plants is an appropriate source to supply the core scaffolds for future drugs. Therefore, plant-based drug discoveries are expected to make a substantial contribution to human health (Atanasov et al., 2021).

As mentioned above, cancer, AD and a number of other chronic diseases accompanied with inflammation (such as asthma, heart diseases, type 2 diabetes, etc.) are among the most common diseases in the world. Since medicinal plants in Vietnam have been shown to have potential in treating these diseases (Hoai et al., 2018; Le et al., 2018; Nguyen et al., 2019; Nguyen et al., 2021), they have been prioritized and under the focus as diseases in the present doctoral work.

2.2.2. Medicinal plants with anti-cancer activity

Cancer is a genetic disease whereby its abnormal signaling results in excessive cell proliferation (Vogelstein & Kinzler, 2004; Yaffe, 2019). Alterations in three types of genes including oncogenes, tumor-suppressor genes and stability genes are responsible for tumorigenesis (Vogelstein & Kinzler, 2004). Oncogenes are involved in controlling the proportion of cell growth (Aragues et al., 2008). In contrast, tumor suppressor genes play an important role in inhibiting cell proliferation and tumor development (Acosta et al., 2018). The third type of genes, stability genes, control the rate of DNA mutation, and their alteration may contribute to the development of cancer (Aragues et al., 2008).

Cancer generally causes the uppermost clinical, social, and economic load among all human diseases (Mattiuzzi & Lippi, 2019). For example in 2020, cancer was a leading cause of death globally with nearly 10 million deaths. The most prevalent cancer types causing a death in 2020 were lung, colon and rectum, liver, stomach and breast cancer (WHO, 2022), and cancer mortality rate is predicted to double by 2040 (Ertas et al., 2021). Today, the most widespread cancers are breast, lung, colon and rectum and prostate cancers (WHO, 2022).

Chemotherapy, along with radiotherapy, surgery, hormonal treatments and targeted biological therapies, either alone or in combination are successfully used to treat cancer today (WHO, 2022). Attractively, medicinal plants and plant-origin compounds have been under the spotlight of cancer research since the first antineoplastic drugs were discovered (i.e., leucovorin in 1950, carzinophilin in 1954, vincristine in 1963, and actinomycin D in 1964). Such plant-derived natural compounds include e.g., paclitaxel and its derivatives from yew (*Taxus*) species, vincristine and vinblastine from Madagascar periwinkle (*Catharanthus roseus* (L.) G. Don), and camptothecin and its analogs from *Camptotheca acuminata* Decne (Cragg & Newman, 2013).

Today, a number of compounds isolated from medicinal plants have exhibited promising anticancer effects in clinical trials such as pomiferin for growth inhibition in six human cancer cell lines: ACHN (kidney), NCI-H23 (lung), PC-3 (prostate), MDA-MB-231 (breast), LOX-IMVI (Melanoma), HCT-15 (colon); epigallacotechin-3-gallate for prostate cancer treatment; flavopiridol for solid tumors, lymphomas, leukaemias; noscapine inhibiting tumour growth and progression; roscovitine with inhibition of cyclin dependent kinases, reduction of cell cycle progression (Greenwell & Rahman, 2015). Besides, medicinal plants can provide also effective substances against drug resistance owing to their diverse chemical structures and pharmacological effects (Yuan et al., 2017). Many studies indicate that phytochemicals, such as curcumin, quercetin and baicalein, are able to reverse drug resistance by regulating drug-resistant proteins (Efferth et al., 2002). Furthermore, by targeting nonapoptotic cell death, they can bypass drug resistance (Yuan et al., 2017). More research work, however, is needed to prove that the plant-derived substances possessing inhibitory effect against drug resistance are effective in clinical trials as well.

2.2.3. Medicinal plants with anti-inflammatory activity

Inflammation is the immune response of a human body that is activated by harmful stimuli and conditions such as tissue injury, toxic compounds, and pathogens (Medzhitov, 2008; Geetha & Ramachandran, 2021). Thus, it results in cellular changes and immune responses to repair the damaged tissue and cellular growth at the site of the injured tissue (Singh et al., 2019). Interestingly, it is a healthy protective reaction of cells/tissues with the symptoms namely pain, heat, redness, swelling and loss of function. In an inflammation process, multiple pathways take place combining for example a synthesis of prostaglandin, interleukin or other chemo toxin, adhesive protein receptor action, and platelet-activating factors (Vishal et al., 2014). Among them, nitric oxide (NO), one of pro-inflammatory mediators, is released to assist against infectious pathogens and to regulate immunity. An excessive production of NO, however, can cause cell death and even destruction of tissue homeostasis due to the formation of reactive nitrogen species (Min et al., 2009).

Inflammation can be either acute inflammation (with undergoing a short-term process) or a chronic one. The adaptive process of acute inflammation takes responsibility for killing of bacteria, viruses and parasites as well as facilitating for example wound repair (Toth et al., 2005). In case of the persistence of the inflammatory cause or the failure of control mechanisms in charge of shutting down the process, inflammation can become chronic (Singh et al., 2019). Noticeably, the chronic inflammation predispose the body to the development of a wide range of diseases like cancer, AD and other neurodegenerative CNS diseases (Toth et al., 2005; Vishal et al., 2014). Currently, two major types of anti-inflammatory drugs are glucocorticoids and non-steroidal anti-inflammatory drugs. The latter is more widely utilized in curing acute and chronic inflammatory diseases. However, anti-inflammatory drugs have adverse effects such as gastrointestinal toxicity (perforation, dyspepsia, gastroduodenal ulcers, and gastrointestinal bleeding), cardiovascular side effects (hypertension, myocardial infarction, stroke, congestive heart failure, and other thrombotic events), and nephrotoxicity (electrolyte imbalance, reduce glomerular filtration rate, nephrotic syndrome and chronic kidney diseases) (Wongrakpanich et al., 2018; Geetha & Ramachandran, 2021).

To date, many studies have shown that numerous plant-origin compounds (i.e., alkaloids, polyphenols, terpenoids, steroids, fatty acids, and macrolides) have potent anti-inflammatory activity, and thus they are promising novel anti-inflammatory drug candidates. Plant-origin agents possessing clinically tested anti-inflammatory effects were such as curcumin, epigallocatechin-3-gallate, berberine, quercetin, resveratrol, docosahexaenoic acid, and macrolides (erythromycin, rapamycin and tacrolimus) (Wang et al., 2021). Their anti-inflammatory activity are attributed to interaction with a wide range of molecular targets relevant to inflammatory response, such as cytokines, enzymes (e.g., COX-2, 5-LOX, and iNOS), transcription factors, signaling pathways, chemokines, adhesion molecules, immune cells (Geetha & Ramachandran, 2021). According to Geetha

& Ramachandran (2021), plants as huge reservoirs of secondary metabolites have been used to reduce inflammation with fewer adverse effects, but the authors did not provide any clinical evidence nor they did not clarify it, how adverse effects are correlated with anti-inflammatory effects (Geetha & Ramachandran, 2021).

2.2.4. Medicinal plants with action against Alzheimer's disease

AD, the most common cause of dementia, is a progressive neurodegenerative disorder which is an organic disorder with a gradual loss of memory, language and intellectual abilities affecting daily life. With the increment within the number of elderly inhabitants, the incidence of AD increases considerably in the forthcoming decades, and this disease is becoming epidemic proportions globally (Mount & Downton, 2006; Khan et al., 2020).

A reduction of acetylcholine (ACh) levels in the brain is one of the pathologies of AD (Yeung et al., 2018). ACh is a neurotransmitter, which is present at many synapses in the CNS, all autonomic ganglia, the neuromuscular junction, and many autonomically innervated organs. It plays a vital role in processing memory and cognitive skills. In the central and peripheral nervous systems, AChE hydrolyses rapidly ACh in numerous cholinergic pathways for the termination of impulse transmission (Khan et al., 2020). The degeneration of this pathway leading in cognitive impairment is one of the most important event associated with AD (Pepeu & Giovannini, 2010). Correspondingly, the inhibition of AChE can contribute to ACh accumulation in the brain, thus improving cholinergic functions in AD patients (Murray et al., 2013).

To date, the US FDA has approved the following drugs for AD and other dementia: aducanumab (Aduhelm), donepezil (Aricept), rivastigmine (Exelon), galantamine (Razadyne), and memantine (Namenda) (Briggs et al., 2016). Aducanumab is a monoclonal antibody inducing the clearance of AD-associated β-amyloid deposits in the brain. Donepezil, rivastigmine and galantamine are alkaloids, and the last two are also derived from plant alkaloids. They act as AChE inhibitors. Memantine, a nitrogen-containing molecule, acts by blocking a neurotransmitter called glutamate (Konrath et al., 2013; Tanzi, 2021). The average overall effect of these drugs, however, is not high, and they could not improve the underlying neurodegenerative process (Briggs et al., 2016; Walsh et al., 2021).

Interestingly, numerous medicinal plant compounds have been demonstrated to serve as potential therapeutic agents in the treatment of AD (Zieneldien et al., 2022). In the *in vivo* study and/or clinical trials, curcumin (isolated from *Curcuma longa*), convolvine and convolamine (isolated from *Convolvulus pluricaulis*), asiatic acid and asiaticoside (isolated from *Centella asiatica*), celapanin and celapanigin (isolated from *Celastrus paniculatus*), valeranone and nardosinone (isolated from *Nardostachys jatamansi*), (isolated from), bilobalide and ginkgolide (isolated from *Ginkgo biloba*), glycyrrhizin (isolated from *Glycyrrhiza glabra*), huperzine (isolated from *Huperzia serrata*), benzylisoquinoline (isolated from *Cissampelos pareira*), S-allylcysteine (isolated from *Allium sativum*) possess potent action against AD (Ovais et al., 2018).

2.3. Selection of medicinal plants of Vietnam origin for phytotherapy

C. paniculatus, *A. tonkinensis* and *Z. ajax* are ethnomedicinal plants used to prevent and treat many diseases in some rural and remote areas in Vietnam. These medicinal plants are used as folk remedies, and these practices have passed down from generation to generation and from person to person. *C. paniculatus* has been used to treat stomach disorders, fever and malaria. *A. tonkinensis* has been used as anti-tumor, anti-fungal and anti-inflammatory therapy. *Z. ajax* has been exploited as remedies for inflammation, anti-tumor and neurological diseases. The present ethnomedicinal plants, however, are not described in the medical literature, and consequently, there is a lack of scientific knowledge on these treatments up to date. We selected these plants to gain understanding of their potent as resources of new drug candidates and to provide scientific databases of their phytochemical constituents and bioactivities for developing and conserving them in the future.

2.3.1. *Chisocheton paniculatus*

The genus *Chisocheton* belongs to the family Meliaceae with more than 53 species, and these species are distributed in the tropical and subtropical regions of Asia (Hoai et al., 2018). According to the literature, *Chisocheton* genus consists of protolimonoids, limonoids, alkaloids, steroids, sesquiterpenes, triterpenes, anthraquinones, spermidine coumarins and phenolic compounds (Shilpi et al., 2016). It has been also reported that *Chisocheton* genus has potential anticancer, anti-inflammatory, antibacterial, antiobesity, antifungal, and antimalarial properties (Shilpi et al., 2016; Supriatno et al., 2018).

C. paniculatus appears as a tree, and its fruit is capsule (3.5–8.0 cm across) comprising of globose with pyriform base (Figure 1) (Bhattacharyya & Kataky, 2014). It has been attracted much interest by numerous researchers because of novel structures along with potential bioactivities. The phytochemicals and bioactivity of *C. paniculatus* are summarised in Table 1.

Figure 1. *Chisocheton paniculatus*: (A) habitat, (B) across section of immature fruit and (C) fruit.

Table 1. Phytochemicals and bioactivity of *Chisocheton paniculatus*

Compound	Bioactivity	Part used	Reference
6*α*-Acetoxyazadirone; 6*α*-acetoxy-16-oxoazadirone; 6*α*,7*α*-dihydroxymeliaca-1,14,20,22-tetraene-3,14-dione		Fruits	(Saikia et al., 1978)
6*α*-Acetoxygedunin; 6*α*-acetoxyepoxyazadiron; 17*β*-hydroxy-6*α*-acetoxyazadiradione		Seeds	(Chatterjee et al., 1989)
Tetranortriterpenoid vilasinin 1,3-diacetate; *β*-sitosterol; *y*-lactone; hemiacetal; *y*-hydroxybutenolide; 17*β*-hydroxy-6*α*-acetoxynimbinin; melianodiol; vilasinin triacetate; 14,15-deoxyhavanensin 3,7-diacetate; 6*α*-acetoxy-14,15- epoxyazadiradiol; gedunin; 6*α*-acetoxygedunin		Wood and seeds	(Connolly et al., 1979)
1,2-Dihydro-6*α*-acetoxyazadirone		Heart wood	(Bordoloi et al., 1993)
Paniculatin B; paniculatin C; paniculatin D; paniculatin G; paniculatin H; paniculatin B; arunachalin		Root wood	(Yadav et al., 1999)
Chisonimbolinins A; chisonimbolinins B; chisonimbolinins C; chisonimbolinins D	Moderate cytotoxic activity against the HeLa cell line	Twigs	(Kong, 2010)
chisonimbolinins E, chisonimbolinins F, chisonimbolinins G			
Chisopanins A; chisopanins B; chisopanins C; chisopanins D; chisopanins E; chisopanins F; chisopanins G; chisopanins H; chisopanins I; chisopanins J; chisopanins K; Chisiamols D; chisiamols C; chisiamols E; chisopanins L; chisopanins M; chisopanins N; chisopanins O	Potent inhibition of NO production with IC_{50} value lower than 10 μM	Twigs	(Yang et al., 2011) (Yang et al., 2012)
3-*O*-Acetyl-21-*O*-methyltoosendanpentol; 21*α*-methylmelianodiol; 21*β*-methylmelianodiol; 21*β*-melianodiol; 21*α*,25-dimethylmelianodiol; [21-*α*-methylmelianol (21*R*,23*R*)-epoxy-23-hydroxy-21*α*-methoxyl]triucalla-7,25-dien-3-one; chisiamol B; bourjotinoline A; paniculatin C isolated			
Chisiamol A; chisiamols G; chisiamols H; sapelin B; 3*α*-acetoxy-21,24*R*-epoxyapotirucall-14- ene-7*α*,23R,25-triol, 3*α*-acetoxy21,23-epoxyapotirucall-14-ene-7*α*,21R,24,25-tetrol		Twigs	(F. Zhang et al., 2012)

Compound	Bioactivity	Part used	Reference
Paniculatol		Fruits	(Bhattacharyya & Kataky, 2014)
Pentandricine; limonoids; ceramicine B; 6-de(acetyloxy)-23-oxochisocheton; 6-de(acetyloxy)-23-oxo-7-*O*-deacetylchisocheton		Stem bark	(Supriatno et al., 2018)
6*α*,7*α*-Diacetoxy-3-oxo-24,25,26,27-tetranorapotirucalla-1,14,20(22)-trien-21,23-lactam; 5*α*,8*α*-epidioxysterols; (22*E*,24*R*)-5*α*,8*α*-epidioxy-24-methyl-cholesta-6,22-dien-3*β*-ol; (22E,24R)-5*α*,8*α*-epidioxy-24-methyl-cholesta-6,9(11),22-trien-3*β*-ol	Moderate NO production inhibitory activity	Fruits	(Hoai et al., 2018)
chiro-Inositol-4,5-di-5-hydroxytiglate-1,3-di-tiglate; *chiro*-inositol-2-acetate-4,5-di-5-hydroxytiglate-3-tiglate; *chiro*-inositol-2-acetate-4,5-di-5-hydroxytiglate-3-2-methylbutyrate;		Leaves	(Nguyen et al., 2019)
6*α*,7*α*-Diacetoxy-23-hydroxy-3-oxo-24,25,26,27-tetranorapotirucall-1,14,20(22)-trien-21,23-olide	Potent cytotoxicity against the human lung cancer A549 and cervical cancer HeLa cell lines		
(24*E*)-3-Oxo-dammara-20,24-dien-26-ol	Moderate cytotoxicity against the A549, HeLa, and human stomach cancer GSU cell lines		
Vismiaefolic acid, *δ*-tocopherol	Weak cytotoxicity against the A549, HeLa, and human stomach cancer GSU cell lines		

The studies mentioned above show that *C. paniculatus* is a rich source of limonoids, triterpenoids, protolimonoids and inositol derivatives. These studies also show that the constituents isolated from *C. paniculatus* have potent anti-inflammatory properties *in vitro*.

2.3.2. *Alphonsea tonkinensis*

A. tonkinensis is one of the species with a single specimen over two sheets (Figure 2) which has just recently been found in Vietnam and Laos (Turner et al., 2018). To the best of our knowledge, this species has been investigated only for essential oils with main compounds comprising of germacrene D (17.4%), *β*-caryophyllene (9.9%), *α*-pinene (9.5%), *β*-elemene (9.3%) and *β*-pinene (9.2%) in the stem oil, and *β*-caryophyllene (27.8%), *β*-elemene (15.6%) and caryophyllene oxide (14.5%) in the leaf oil (Nguyen et al., 2018). To date, no reports have been published on the pharmacological activity of the herbal extracts or new constituents isolated from *A. tonkinensis*.

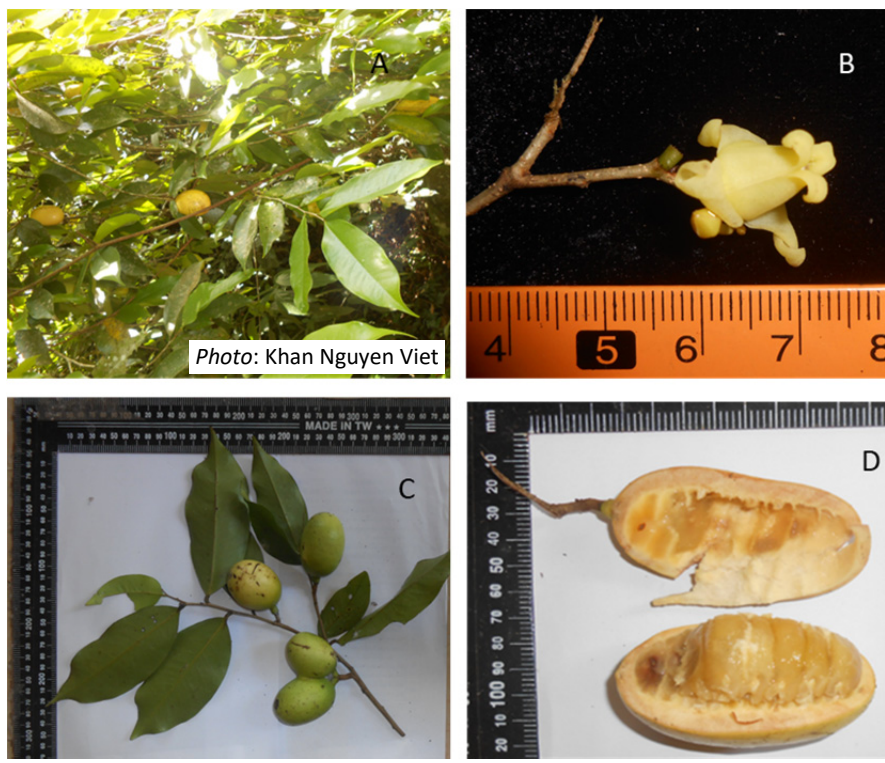

Figure 2. *Alphonsea tonkinensis*: (A) habitat, (B) flower, (C) fruit, stems, leaves and (D) across section of mature fruit.

A. tonkinensis is a member among 30 species of the *Alphonsea* genus of *Annonaceae* family. This genus is distributed in Northeastern India, Southeast Asian countries and Southern China (Bakri et al., 2017; Srivastava and Mehrotra, 2013). According to the literature, *Alphonsea sp.* contains alkaloids, steroids, lignan, sesquiterpenes and monoterpenes (Bakri et al., 2017). Several plants of this genus have been reported to reveal cytotoxic, anti-oxidant, anti-fungal, anti-inflammatory and anti-trypanosomal activity (Bakri et al., 2017). Interestingly, *A. tonkinensis* has been used as folk remedies in remote areas in Vietnam for reducing tumor growth, inflammation and anti-fungal treatment.

2.3.3. *Zephyranthes ajax*

Zephyranthes is the genus of bulbous perennials in the Amaryllidaceae family, and this genus consists of about 90 species. The genus is distributed widely in the temperate and tropical regions, and it is well known for its ornamental with attractive flowers and considerable medicinal values (Katoch D & Singh B, 2015). Many species of this genus have been traditionally utilized in many countries as remedies for tumor, diabetes mellitus, viral infections, inflammation, circulatory and neurological diseases (Katoch & Singh, 2015; Ding et al., 2017). Previous phytochemical investigations of *Zephyranthes* genus have shown that the present plant contains numerous alkaloids, flavonoids, sterols, fatty acids, phospholipids and their glycosides. Its pharmacological properties have been reported to include e.g., potential AChE inhibition, and anticancer, antifungal, antiviral and antibacterial activities (Katoch & Singh, 2015).

Z. ajax (Figure 3) is an amaryllidaceous bulbous perennial used as an ornamental and medicinal plant in Vietnam (Ho, 2003). Noteworthy, *Z. ajax* has been used as folk remedies for anti-inflammatory, anti-cancer and neurological disease therapy in some rural and remote areas in Vietnam. Even though the plant is well-known in Vietnam, the knowledge on the phytochemical and pharmacological properties of this species is still very limited.

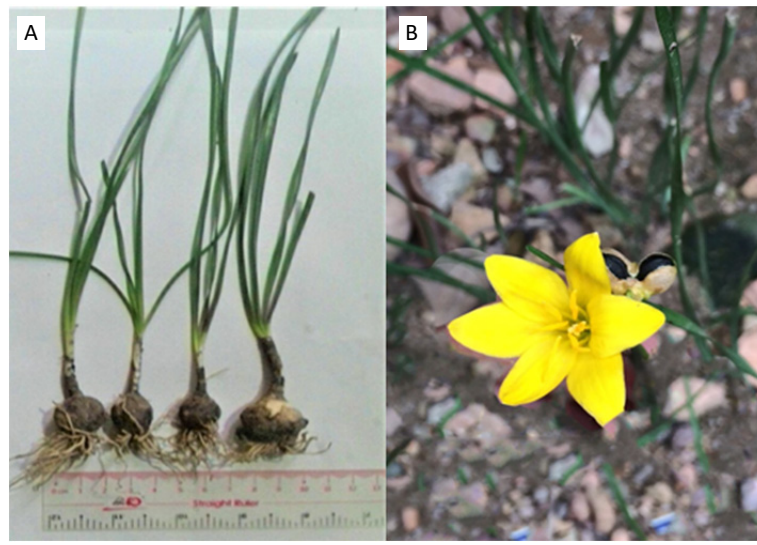

Photo: Nhan Le Trong & Khan Nguyen Viet

Figure 3. *Zephyranthes ajax*: (A) plant compared with a hand and (B) face view of flower in natural habitat.

To date, little is also known about the phytochemical and bioactivities of *Z. ajax* and *A. tonkinensis*.

2.4. Design of nanotechnology-based drug delivery systems for plant-origin actives

Many studies have shown that herbal medicines or natural compounds exhibiting a good activity in *in-vitro* assays, do not possess similar properties *in vivo* due to a poor water-solubility, poor oral bioavailability, limitations in target-specific drug delivery, and *in-vivo* instability (Bonifácio et al., 2013; Patra et al., 2018b). Such limitations greatly restrict the applicability of medicinal plants (Teja et al., 2022). Noteworthy, the development of novel DDSs for herbal extracts or natural compounds have recently proved the potential approach to overcome these challenges (Ansari et al., 2012; Bonifácio et al., 2013; Patra et al., 2018; Teja et al., 2022).

Since 2010, there has been a remarkable boost in herbal nanoformulation research. Compared to conventional dosage forms (such as tablets, capsules, syrups, and decoctions), herbal nanomedicines have demonstrated great advances and success in drug delivery (Farooq et al., 2019). The design and development of novel nanotechnology-based DDSs lead to decrease in particle size and increase in outer surface area, thus increasing the water-solubility of drugs (Sharma et al., 2016). The nanotechnology-based DDSs with a particle size ranging between 100 nm to 200 nm are likely to avoid efflux pumps, and the

cellular intake of the drug by a receptor-mediated endocytosis supports against drug resistance, thus ensuring a maximum drug release inside the cell membrane (Danaei et al., 2018).

Regarding cancer therapy, most drugs administered with a conventional dosage forms are not specifically targeted to cancer cells, thus causing patients to suffer from serious undesired side effects (Mokhtarzadeh et al., 2017). Recently, nanotechnology-based herbal medicines such as tumor microenvironment sensitive intelligent nanomicelles, pH-sensitive self-assembled nanoparticles (NPs), bio-orthogonal copper-free click chemistry approaches, and monoclonal antibodies coupled liposomes have been introduced for enhancing drug targeting. NPs act as an effective carrier system for targeted drug delivery enabling the efficient delivery of drug to the site of disease due to their extremely small size and ability to penetrate the tissue and cell membranes (Ertas et al., 2021; Teja et al., 2022). Moreover, the drug-loaded NPs can be formulated by surface conjugating with multifunctional antibodies and ligands (Ertas et al., 2021; Teja et al., 2022). NPs have been also shown to enhance the stability of herbal medicines which is based on the protection of the cargo from enzymatic degradation (Ertas et al., 2021). Furthermore, modified drug release can be achieved thanks to the size and surface characteristics of NPs coated with biodegradable polymers and/or polyethylene glycols, PEGylation, thus allowing the drug to be released for an extended time (Kalaydina et al., 2018). Therefore, the application of nanotechnology in herbal medicine results in an increase in bioavailability and bioactivity of APIs of herbal origin (Gunasekaran et al., 2014), and reduced dose-related toxicity and adverse effects (Teja et al., 2022).

According to the literature, numerous nanotechnology-based DDSs have been introduced to date in herbal medicine for enhancing the delivery of herbal extracts, fractions and/or constituents. These DDSs include e.g., polymeric herbal NPs, nanoemulsions, phytosomes, liposomes, solid lipid nanoparticles, nanomicelles, self-emulsifying nano-scale DDSs, NFs, dendrimers, ethosomes, nanosuspensions, and carbon nanotubes. The evaluation parameters, opportunities and challenges of these systems have been extensively reported in the state-of-the-art literature. Polymeric NPs, nanoemulsions and phytosomes are the most widely used nanotechnology-based DDSs for medicinal plants (Teja et al., 2022). For example, total 89 different herbal nanoformulations have been reported for curcumin, which is the most widely studied herbal drug. Curcumin is poorly soluble in water, thus having a limited oral bioavailability. Interestingly, poly(lactic-co-glycolic acid) NPs loaded with curcumin presented 640 times increased water solubility and 5.6 fold enhancement in oral bioavailability compared to curcumin as a powder form (Xie et al., 2011). Shelat et al. (2015) reported that this herbal API in solid lipid NPs showed the increase in oral bioavailability to 12 folds with respect to curcumin alone. Berberine-loaded nanomicelles possessed 20-fold higher hepatoprotective activity on bile duct ligation (a condition of liver cirrhosis) in rats than berberine as a pure drug (Pishva et al., 2018). According to Teja et al. (2022), a combination of herbal medicines with pharmaceutical nanotechnology can be a key tool in the future

for the advancement of medicinal plant research with significantly enhanced bioavailability, therapeutic effect and safety.

2.5. Electrospun nanofiber-based drug delivery systems

2.5.1. Electrospinning

NFs can be generated with three different techniques: ES, self-assembly, and phase separation (Shahriar et al., 2019). Today, ES (as shown in Figure 4) is the most promising technique in generating nano- and microfiber-based constructs and DDSs for pharmaceutical and biomedical applications. ES is an electro-hydrodynamic process where a jet is produced from a charged droplet of polymer solution (or polymer melt) by stretching and elongating it under the exposure of high electric field voltage. The ES setup consists of four major components: a high-voltage power supply, a syringe pump, a needle/spinneret for the ejection of a polymer solution, and a grounded collector (plate/roll). A charged jet of polymer solution or melt is ejected toward a collector as a result of the electro-static repulsion deforming the droplet into a Taylor cone. The jet propagates in an almost straight line and then curves complicated paths due to bending instabi-lities. It is elongated and slimmed (because of electrical forces) followed by a rapid solidification and formation of solid fine fibers on the grounded collector (Reneker & Yarin, 2008; Xue et al., 2019). The formation of electrospun nano- and microfibers is dependent on the the surface tension of a polymer solution.

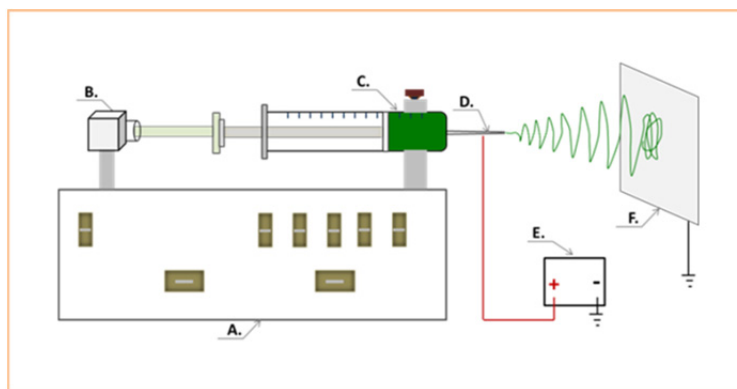

Figure 4. The electrospinning (ES) setup for generating nanofibrous templates for self-assembled liposomes of haemanthamine (HAE). Key: (A) a robotized ES system; (B) programmable syringe pump; (C) polymer solution; (D) spinneret (a needle system); (E) high-voltage power supply; (F) collector plate.

ES technique has gained a lot of attention among scientists owing to (1) the possibility of scaling up for commercial use and affordability, (2) the ease of functionalization of the electrospun fibers for a numerous applications, (3)

superior mechanical properties of the fibers, and (4) relative simplicity and ease of control of an ES process (Braghirolli et al., 2014). ES is a versatile method for fabricating uniform polymeric nano- or microfibers with a high specific surface area, and the chemistry and dimensions of such fibers are similar to extracellular matrix structure (Sahoo et al., 2010). Large and sophisticated 3D fiber structures can be produced to enable the cells to occupy the structure in a 3D behavior under the meticulous setting parameters (Braghirolli et al., 2014). In addition, novel electrospun polymeric structures and DDSs have been generated based on the modifications of a traditional ES method. For example, core-shell-structured composite fibers have been successfully generated by using two concentric nozzles instead of the conventional spinneret (Agarwal et al., 2009; Chakraborty et al., 2009; Sharma et al., 2014). These core-shell structures are shown to be very useful for drug and/or protein delivery and for the encapsulation of cells, bacteria, viruses and growth factors (Agarwal et al., 2009; Chakraborty et al., 2009; Sharma et al., 2014). One extension of ES is the use of an ES setup for electrospraying for the preparation of drug-loaded nano- and microparticles. The formation of a spray is generated between two charged electrodes (Kempski et al., 2008). Today, electrospun preparations are applied widely in many fields, and the nanofiber-based systems have found uses especially in biomedicine (El-Aassar et al., 2021; Xue et al., 2019).

The choice of an appropriate method of preparation and optimized process parameters are crucial in ES drug-loaded NFs for therapeutic applications. The three commonly used solution-based ES techniques for generating drug-loaded nano- and microfibers are (1) blend, (2) coaxial and (3) emulsion ES (Nikmaram et al., 2017).

A conventional blend ES technique is a simple method based on the dispersion or dissolution of drug(s) in the polymer solution prior to ES. This ensures that the drugs incorporated are dispersed throughout the fibers (Bhattarai et al., 2019). In blend ES, however, actives may be denaturated or their bioactivity may be reduced due to solvents. Moreover, their inherent charge may lead them to migrate on the jet surface and disperse on the surface of the NFs rather than the encapsulation of biomaterials within the fibers, thus resulting in the burst release of the APIs (Schoolaert et al., 2016). In order to avoid these deleterious effects or adjust the release profile, the drugs could be encapsulated prior to adding to the ES solution or be incorporated into the fiber core using coaxial ES/emulsion ES (Kai et al., 2014).

Co-axial ES comprises of two nozzle systems connected to the high voltage source. NFs with core-shell morphologies are formed from the pumping of two solutions loaded in each nozzle (Nikmaram et al., 2017). APIs are positioned in an inner jet, while polymer(s) are present in an outer jet, thus forming a cargo system and enabling a prolonged drug release in the physiological environment (Shahriar et al., 2019). Furthermore, the biofunctionality and cell-surface interactions of NFs can be significantly enhanced through the surface of coaxial fibers being modified with biomolecules (Vaidya et al., 2015).

Emulsion ES can produce core-shell NFs based on two immiscible solvents being simultaneously electrospun (Shahriar et al., 2019). Initially, a continuous phase (oil phase in case of using W/O emulsion) is formed. Electrospun drug-loaded NFs designed for a specific drug release (targeted site-specific or time dependent) enable to provide the desired therapeutic effects. Such NFs are usually designed for a specific drug, meaning that if the drug is changed in the NFs the release kinetics can be considerably changed accordingly (Kajdič et al., 2019).

2.5.2. Material selection for nanofiber-based drug delivery systems

Polymers are applied in nanofiber-based DDSs to afford stability, drug release, targeting, enhanced bioavailability and patient acceptability (Ngwuluka et al., 2014). The carrier polymers used in such DDSs can be natural or synthetic polymers, hydrophilic or hydrophobic polymers, and/or biodegradable or non-biodegradable polymers. From the formulation point of view, each polymer has its own specific advantages and disadvantages (El-Aassar et al., 2021).

Natural polymers derived from plants or animals are generally biodegradable, biocompatible and low toxic, and consequently, they have been widely used in biological and therapeutic applications (El-Aassar et al., 2021; Mele, 2016). Perhaps, the major limitations of such biopolymers include weak mechanical properties, ease of microbial degradation, batch to batch variability and the unreserved rate of hydration, which may hinder the use of them e.g., in prolonged-release DDSs (Campiglio et al., 2019; Garg et al., 2018). The native-origin polymers can be classified also as: neutral (e.g., β-glucan, dextran, cellulose), acidic (e.g., hyaluronic acid, alginic acid,), and basic polymers (e.g., chitin, chitosan) (El-Aassar et al., 2021).

Synthetic polymers offer many advantages over natural polymers. Synthetic polymers with a wide range of chemical linkages possess better mechanical properties and they can be flexibly tailored to fabricate various types of DDSs with good mechanical and degradation properties. Synthetic polymers, however, do not have bioactive sites for supporting cell attachment (Bhatia, 2016; Keshvardoostchokami et al., 2021). According to the literature, the following synthetic polymers have been applied as carrier materials for pharmaceutical ES applications: poly(lactic-co-glycolic acid), polylactic acid, polyglycolic acid, poly (vinyl alcohol), poly (ε-caprolactone), poly (ethylene glycol), poly (L-lysine) and polyphosphoesters (Maghsoudi et al., 2020). Hydrophilic polymers are applicable for the nanoformulation of immediate-release DDSs, while hydrophobic polymers are used as carrier materials in controlled or sustained drug release preparations (Abu-Diak et al., 2012). In order to achieve desired fiber properties, controlled drug release and good ES process performance, two or more carrier polymers can be combined and with the addition of surfactant(s). In summary, the selection of carrier polymer(s) for ES plays a fundamental role in the design of novel electrospun DDSs.

2.5.3. Nanofiber-based drug delivery systems

To date, electrospun NFs have found numerous applications in advancing cell migration, stem cell differentiation, peripheral nerve repair, wound healing, cardiac tissue regeneration, vascular tissue regeneration, musculoskeletal tissue regeneration, tissue-to-tissue interface engineering, repair or regeneration of other tissues, as implant coatings, barrier membranes, filtration membranes, diagnosis, and especially in drug delivery (Xue et al., 2019; Fadil et al., 2021).

It is well known that most conventional drugs are hydrophobic, poorly water soluble, and poorly bio-distributable, thus leading to undesired active targeting and therapeutic efficacy (Potrč et al., 2015). In terms of drug delivery, electrospun NFs possess many advantages such as a large surface area to volume proportion, ultrafine fibrous structure, high porosity, high loading capacity, high permeability, high encapsulation efficiency, capacity of simultaneous administration of multiple drugs, simplicity of modification and cost effectiveness (Braghirolli et al., 2014; Sharma et al., 2014; Fadil et al., 2021). Electrospun NFs have been utilized for the oral, inhalation, rectal, sublingual/buccal, parenteral, transdermal, nasal, ocular and vaginal routes to deliver APIs to the target site in the body (Shahriar et al., 2019). According to the literature, the incorporation of anticancer drugs, antibacterial drugs, anti-inflammatory agents, cardiovascular agents, gastrointestinal drugs, antihistamine drugs, contraceptive drugs and palliative drugs into electrospun NFs has numerous benefits in terms of drug therapy (Shahriar et al., 2019).

The release of drug(s) from electrospun fiber matrix can occur via three alternative mechanisms including (1) relaxation – drug release from the electrospun DDSs owing to relaxation of polymer chains, (2) degradation – the deterioration or dissolution or polymer in the release medium resulting in drug release, and (3) diffusion – a concentration gradient within polymer matrix promoting drug to move out (Munj et al., 2017). Notably, the drug release mechanism from electrospun DDS systems is a complicated issue due to the influence of diverse variables including material (such as composition, structure, degradation, swelling), release medium (such as pH, temperature, enzymes, ionic strength), and APIs (such as stability, solubility, interaction with matrix, charges) (Fu & Kao, 2010). An ideal DDS enables to promote the appropriate site, timing and rate for a drug release, thus ensuring an optimal therapeutic effect. Medicated NFs for controlled drug release provide the specific drug release profile for desired therapeutic effect, and this drug release profile can be an immediate release, prolonged release, biphasic release and/or stimulus-activated drug release type (Kajdič et al., 2019).

For immediate drug release, NFs have a simple, homogenous structure and a proper water-soluble polymer is used for forming a nanofiber matrix. The present preparations possess a high surface-to-volume ratio exposing a large contact surface area for dissolution, high porosity, and the effective conversion of a crystalline drug into an amorphous state. These unique material properties jointly enhance the solubility and dissolution rate of the drug resulting in the

improvement of oral bioavailability (Paaver et al., 2015; Potrč et al., 2015; Kajdič et al., 2019).

The NFs intended for modified drug-release applications are designed to present a prolonged or biphasic and/or stimulus-activated drug release behavior. The NFs applied for prolonged drug release applications can be matrix-type NFs (such as monolithic or blended systems), core-shell NFs (such as reservoir-type or multi-matrix systems), or other types of NFs (such as sandwich-type nanofibrous mats or NFs with controlled bead diameters) (Kajdič et al., 2019). Biodegradable or swelling polymers are the materials of choice for such fiber applications and for achieving extended drug release (Zupancic et al., 2015), (Kajdič et al., 2019). Core-shell NFs with multiple drug-loaded layers or an outer polymer layer as rate-controlling barrier have been exploited to promote prolonged drug release (Acevedo et al., 2018). Incorporation of one or more stimulus-responsive polymers in the NFs boosts to achieve stimulus-activated drug release (such as for thermo-, pH-, or electroresponsive release) (Elashnikov et al., 2017). The formulation of a simple matrix-type nanofiber structures, core-shell NFs or the sandwich structures enables also a biphasic drug release (Kuang et al., 2018; H. Lee et al., 2017). This type of release behavior is highly effective, since a high drug content can be rapidly delivered to the target site and subsequently maintained at a high level for a longer time-period in the absence of recurrent drug administration (Kuang et al., 2018).

2.5.4. Characterization of electrospun nanofibers

To ensure a high pharmaceutical quality and functionality, it is of outmost important that the electrospun nanofiber-based DDSs are precisely and rigorously characterized. In most cases, the electrospun NFs are evaluated for their fiber size and shape, surface morphology, molecular structure and mechanical properties (Shojaei et al., 2019). The characterization approaches mentioned above are general for all electrospun NFs, but some approaches are specifically verifying the final performance of the nanofiber-based preparation. For example, if the NFs are intended for as a solid template for self-assembled drug-loaded liposomes, then assessing the spontaneous formation of liposomes is essential. The critical properties of such amphiphilic NFs intended for a solid template for self-assembled liposomes, are listed below.

Size, shape and surface morphology

The diameter, shape and surface morphology of electrospun NFs are typically investigated by scanning electron microscopy (SEM), transmission electron microscopy (TEM), atomic force microscopy (AFM) and optical microscopy (Papkov et al., 2019). SEM is a widely used method for visualizing and investigating the morphology of nanofibers. A gold or platinum coating is needed for improving resolution at higher magnifications. For extremely small fibers (<300 nm), TEM can be particularly helpful to investigate fiber diameters. AFM provides another alternative method to assess fiber diameter, but it is a

complicated method to obtain accurate results because of tip convolution. Optical microscopy is a highly convenient tool for preliminary characterization. However, this technique does not enable to measure the size of fibers at a nano-scale (Širc et al., 2012; Papkov et al., 2019).

Physical solid-state properties

Determination of physical solid state and stability of API(s) and carrier polymer(s) in NFs is a fundamental characterization. The solid-state analytical techniques comprise of X-ray powder diffraction (XRPD), Fourier-transform infrared (FTIR) spectroscopy and differential scanning calorimetry (DSC). XRPD is the primary method for a solid-state characterization, since it is a non-destructive, high sensitive, reliable and depth-profiling technique. As the result of the interaction of X-rays with crystalline material, each material gives distinctive diffraction patterns. XRPD databases can be used to determine polymorphism or the amorphous form (and even the degree of crystallinity) of APIs/excipients (Chauhan, 2014). FTIR spectroscopy is a quick, reliable and safe technique. Its vibrational spectroscopy data give additional details with respect to the solid-state characteristics of APIs/excipients. Particularly, the peak shifts in FTIR spectral profiles enable to determine intermolecular interactions between fiber matrix components (Mader et al., 2016). DSC is a thermal analysis technique to verify the drug-excipient compatibility and interactions between the components. In the thermodynamics profile, endothermic peak is obtained from the latent heat attributed to the thermodynamic transition at the crystalline melting temperature (Shojaei et al., 2019).

Drug content and in-vitro drug release

Determination of drug content and *in-vitro* drug release are important in assessing the final properties and bioavailability of API(s) loaded in the nanofiber-based DDSs. Ultraviolet-visible (UV-Vis) spectroscopy and HPLC are the methods of choice for quantifying the drug content in the samples and for determining drug release behavior. UV-Vis spectroscopy is a simple, rapid, low-cost and readily available method. However, the major limitation of this method is poor selectivity (Begum et al., 2018). The limitations of UV-Vis spectroscopy may be directly solved by using HPLC. HPLC has become a dominant analytical technique in the pharmaceutical research attributing to rapidness, automatic operation, high accuration and selectivity. In addition, recent innovations like ultrahigh-pressure liquid chromatography and HPLC/MS/MS boost its advantages (Swartz, 2010).

3. SUMMARY OF THE LITERATURE

Medicinal plants have many advantages and attributes to promote modern drug discovery and therapy. Therefore, the investigation of active compounds isolated from ethnomedicinal plants is a valuable and up-to-date approach. The characterisation of the phytochemistry and bioactivity of such plant-origin compounds is crucial to obtain scientific justification for their use in modern medicine.

In the present doctoral work, the ethnomedicinal plants *C. paniculatus*, *A. tonkinensis* and *Z. ajax* were investigated in depth, since the phytochemistry and phytotherapy potential of these plants have not been studied earlier. The compounds and/or extracts with potential bioactivity were isolated from the present medicinal plants and the chemical structure (of compounds) was determined/elucidated. The isolated compounds and/or extracts were evaluated with their *in-vitro* bioactivities including anti-cancer cytotoxicity by SRB staining assay, anti-inflammatory activity by NO production inhibition assay, and AChE inhibition activity by anti-AChE activity assay.

Plant-origin drugs may have also some limitations, thus restricting their use in clinical practice. The most common limitations include poor water solubility, poor oral absorption, challenges in target-specific drug delivery, and *in-vivo* instability. These all limitations can significantly reduce the bioavailability and therapeutic effect of potential drug candidate(s) isolated from plants. Pharmaceutical nanotechnology with numerous advanced developments is expected to promote herbal medicines to overcome these challenges. For example, ES is a versatile and viable nanotechnology-based fabrication method for generating polymeric nanofibers as DDSs. In the present doctoral work, ES was used to develop novel amphiphilic NFs and self-assembled liposomes for the herbal extract(s) and constituent(s). The physical solid-state properties and *in-vitro* performance of such nanoformulations were verified.

4. AIMS OF THE STUDY

The present doctoral research work has two main objectives: **(1)** to gain knowledge on the chemical composition and bioactivity of herbal extracts and compounds isolated from the selected medicinal plant(s) used in the traditional medicine of Vietnam, and **(2)** to develop novel nanotechnology-based DDSs for the present herbal extract(s) and constituent(s). The active plants were selected based on their bioactivity potency.

The specific objectives

1. To isolate the individual compounds from the plant extracts of interest and to determine/elucidate (identify) the chemical structure of compounds (I–IV). The compounds and extracts with potential bioactivity were isolated from *C. paniculatus*, *A. tonkinensis* and *Z. ajax* known in ethnomedicine of Vietnam
2. To evaluate the bioactivity of the compounds isolated from the plant extracts (including anti-cancer cytotoxicity, anti-inflammatory, anti-AChE activity) (I-IV).
3. To design and fabricate electrospun plant-origin API loaded amphiphilic NFs intended for a solid template for self-assembled liposomes (V).
4. To evaluate the physicochemical properties, *in-vitro* performance (dissolution) and stability of the abovementioned nanoformulations (V).

5. EXPERIMENTAL

5.1. Materials

5.1.1. Plant materials (I–IV)

The *C. paniculatus* leaves (4.5 kg of dried samples) were collected from Quang Tri province, Vietnam (geographical coordinates: 17°03’20.4"N; 107°04’15.4"E) in August 2018. The *A. tonkinensis* stems and leaves (8.0 kg of dried samples) were collected from Quang Tri province, Vietnam (geographical coordinates: 16°28′45.2″N; 107°00′49.9″E) in July 2017. The plants of *Z. ajax* (5.5 kg of dried bulbs) were collected in Hue city, Vietnam (geographical coordinates: 16°27’43.8"N; 107°33’55.4"E) in May 2017. The plant materials used were authenticated by Dr. Vu Tien Chinh (Vietnam National Museum of Nature, Vietnam Academy of Science and Technology, Vietnam), and voucher specimens (CP-02, AT-01 and ZA-01, respectively) were deposited by the Faculty of Pharmacy, Hue University of Medicine and Pharmacy, Vietnam.

5.1.2. Active pharmaceutical ingredient (V)

Haemanthamine (HAE), a white, crystalline powder with a purity NLT 95%, was used for the preparation of electrospun NFs (Figure 5). HAE was isolated from *Z. ajax* belonging to the family Amaryllidaceae.

5.1.3. Solvents (I–V)

For extraction and isolation of plant materials, the following solvents were used: methanol (MeOH), *n*-hexane, ethyl acetate (EtOAc), acetone, dichloromethane (CH_2Cl_2), hydrochloric acid (HCl), chloroform and water with a reagent grade and HPLC grade (Xilong, China and Sigma-Aldrich C.C., USA). Ethanol (Merck GmbH, Germany) was used as a solvent in the ES of amphiphilic NFs.

5.1.4. Other materials and reagents (V)

Polyvinylpyrrolidone (PVP) (Kollidon 90F K90) was purchased from BASF SE, Germany, and Soybean phosphatidylcholine (PC) (Lipoid S-100) was obtained from Lipoid GmbH, Ludwigshafen, Germany (Figure 5).

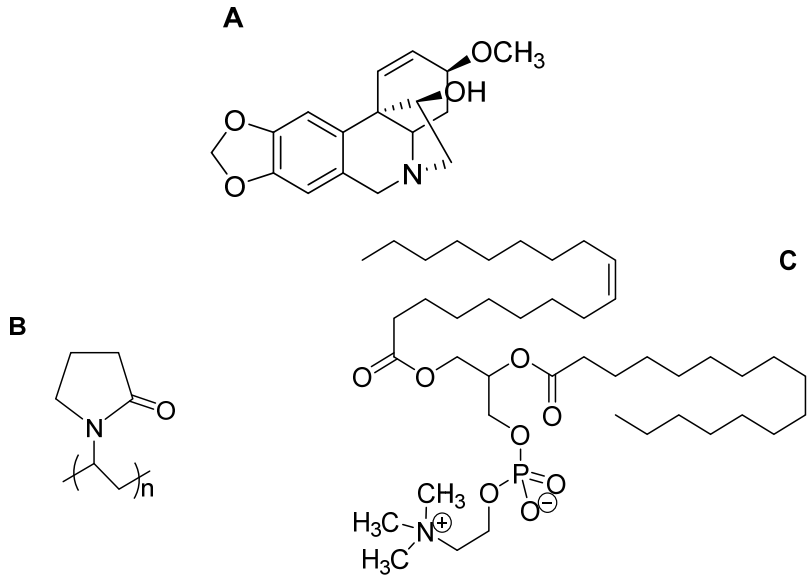

Figure 5. The chemical structure of (**A**) haemanthamine (HAE), (**B**) polyvinylpyrrolidone (PVP) and (**C**) phosphatidylcholine (PC).

5.2. Extraction and isolation of compounds from plant materials

5.2.1. General experimental procedures (I–IV)

Column chromatography was carried out with silica gel (60 N, spherical, neutral, 40-50 μm, Kanto Chemical Co., Inc., Tokyo, Japan), reversed-phase C_{18} (RP-18) (Fuji Silysia Chemical Ltd., Kasugai, Aichi, Japan), and Sephadex LH-20 (Dowex® 50WX2-100, Sigma–Aldrich, St.Louis, MO, USA). Analytical thin-layer chromatography (TLC) was performed with pre-coated silica gel $60F_{254}$ and RP-18 F_{254} plates (0.25 or 0.50 mm thickness, Merck KGaA, Darmstadt, Germany). Preparative HPLC was performed with an Agilent 1260 Infinity II system (Agilent, Santa Clara, CA, USA), using a Zorbax SB–C_{18} column (5μm particle size, 9.4 × 250 mm) and a DAD detector. A P-2000 polarimeter (JASCO, Tokyo, Japan) was used for optical rotation determinations. A Shimadzu UV-1800 spectrophotometer (Shimadzu, Kyoto, Japan) was used to record ultraviolet spectra. Infrared (IR) spectra were collected with an IR Prestige-21 spectrometer (Shimadzu, Kyoto, Japan). NMR spectroscopy studies were conducted with a Bruker Avance 500 spectrometer (500 MHz for ^{1}H NMR, 125 MHz for ^{13}C NMR) (Bruker, Billerica, MA, USA) and with tetramethylsilane as an internal reference. High-resolution electronspray ionization mass spectrometry (HRESIMS) data were obtained with a LCMS-IT-TOF spectrometer (Shimadzu, Kyoto, Japan).

5.2.2. Extraction and isolation of *Chisocheton paniculatus* (I)

The dried leaves (4.5 kg) of *C. paniculatus* were extracted three times using MeOH (10.0 L each) at room temperature to acquire 357 g of solid extract. The extract was suspended in water (2.0 L) and partitioned three times with *n*-hexane and EtOAc (5.0 L each) to obtain the dry *n*-hexane (127 g), EtOAc (105 g), and water (W, 98 g)-soluble portions. The phytochemical investigation of the water-soluble portion by application of repeated column chromatography and prep-HPLC resulted in the isolation of six new compounds **1–6** (Figure 6).

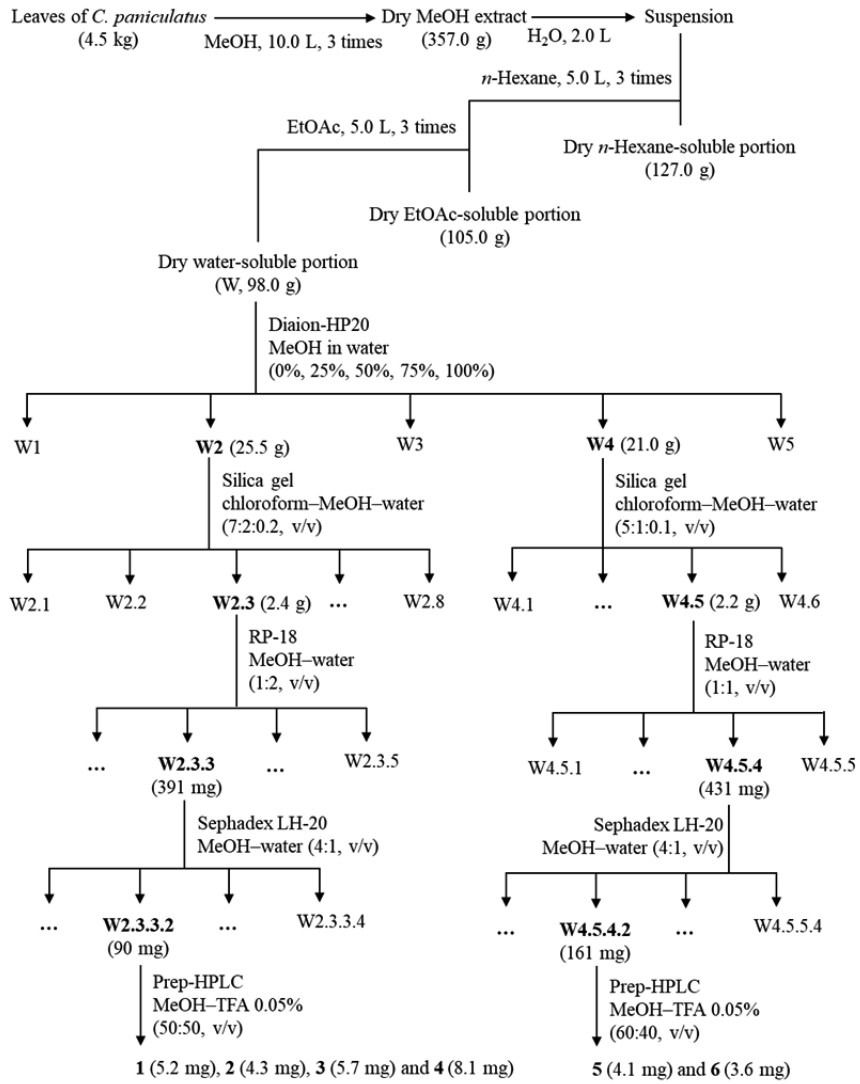

Figure 6. Schematic diagram of the extraction and isolation of compounds **1**–**6** from *Chisocheton paniculatus*.

5.2.3. Extraction and isolation of *Alphonsea tonkinensis* (II–III)

The dried stems and leaves (8.0 kg) of *A. tonkinensis* were extracted with MeOH by maceration (3×20.0 L each) at room temperature to obtain 790.0 g of dry extract. After being suspended in HCl solution (pH 2.0), the dry MeOH extract was extracted with EtOAc to obtain the EtOAc-soluble portion (dry EA extract, 455.70 g). The aqueous phase was adjusted to pH 9 using saturated ammonia solution and then extracted with CH_2Cl_2 to acquire 19.26 g of dry CH_2Cl_2 extract. The dry CH_2Cl_2 extract was subsequently partitioned into the dry *n*-hexane portion (0.14 g), dry EtOAc portion (dry EC extract, 1.34 g), and dry MeOH portion (14.59 g) extract. With application of column chromatography techniques to EA, EC and dry MeOH portion extracts, eight compounds were afforded **7**–**14** (Figure 7).

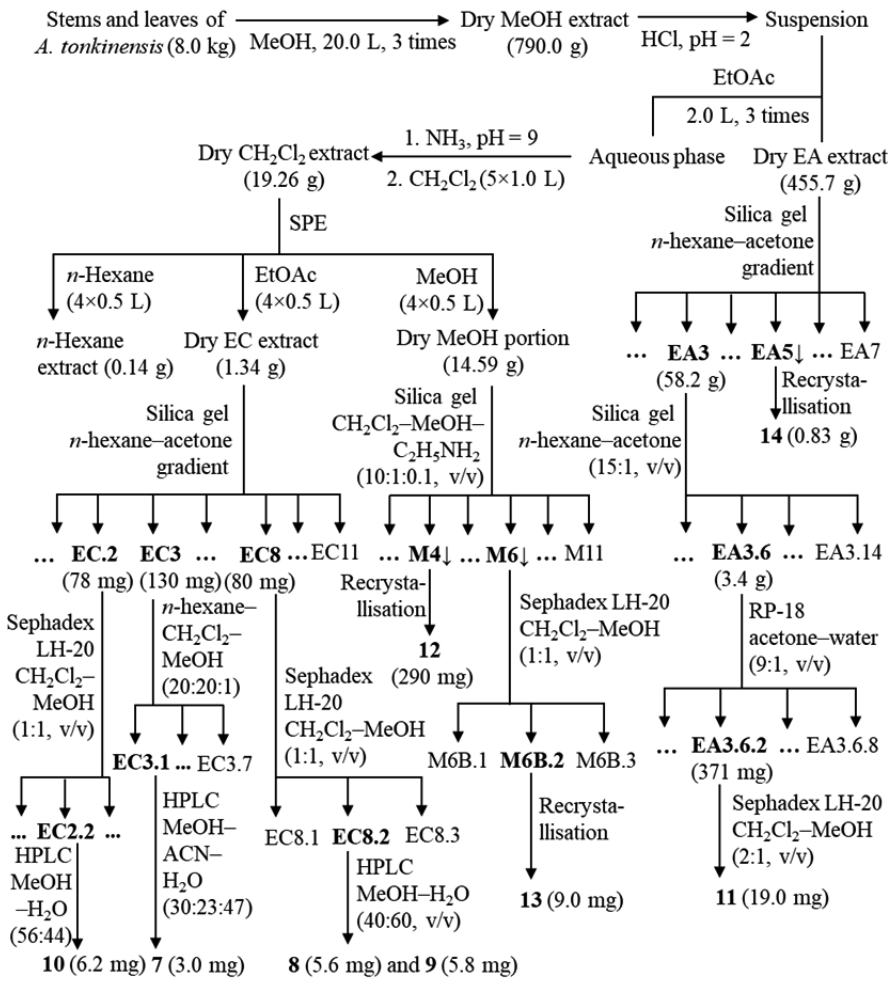

Figure 7. Schematic diagram of the extraction and isolation of compounds **7**–**14** from *Alphonsea tonkinensis*.

5.2.4. Extraction and isolation of *Zephyranthes ajax* (IV)

The powdered bulbs (5.5 kg) of *Z. ajax* were extracted three times with MeOH (10.0 L each) at room temperature. The combined MeOH extract was evaporated under a reduced pressure to give 467 g of dry extract. The extract was suspended using 2.0 L water to partition with CH_2Cl_2, EtOAc, *n*-butanol (3 times, 2.0 L each). The solvents were dried *in vacuo* to obtain the dry CH_2Cl_2 extract (D, 120.3 g), dry EtOAc extract (E, 126.8 g), dry *n*-butanol (43.5 g) extract and dry water (140.3 g) extract. Chromatographic purification of the CH_2Cl_2 extract and EtOAc extract led to the separation of eight compounds consisting of a new flavanol derivative and seven known compounds **15–22** (Figure 8).

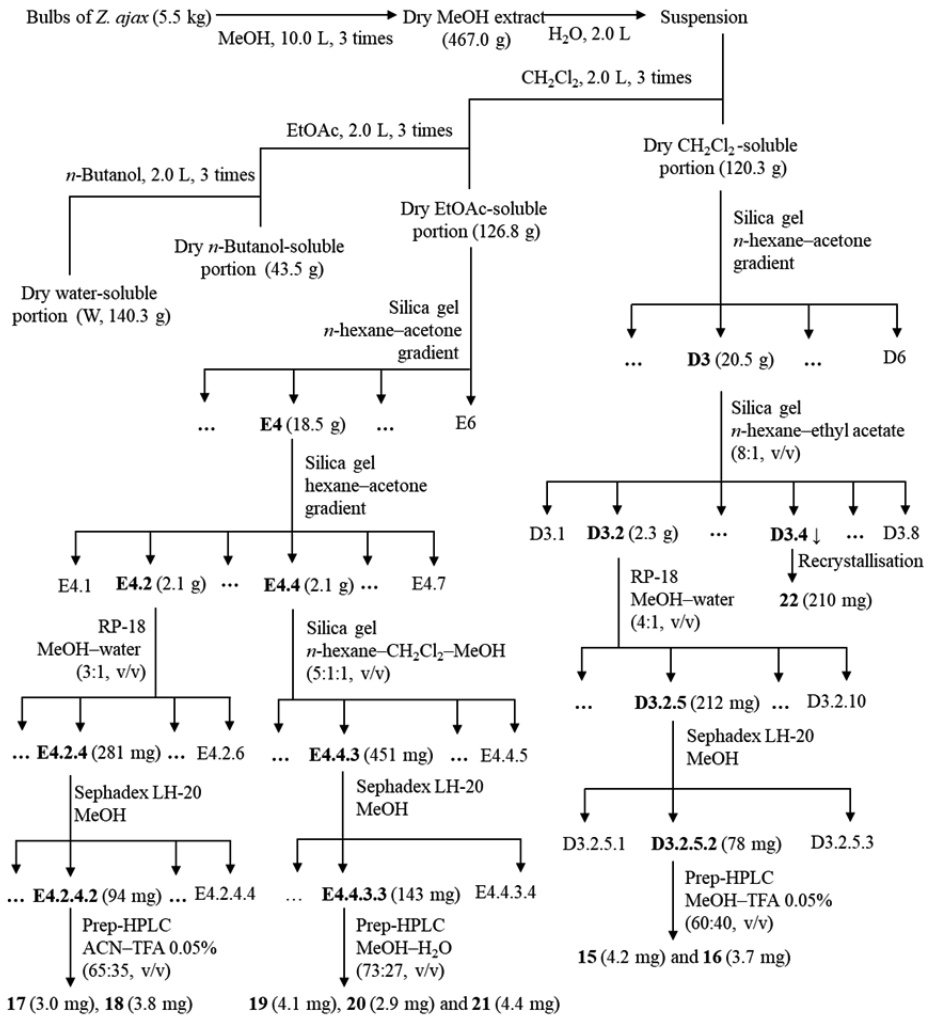

Figure 8. Schematic diagram of the extraction and isolation of compounds **15**–**22** from *Zephyranthes ajax*.

5.2.5. Cytotoxicity assay (I, II, IV)

The cytotoxic activity of isolated secondary metabolites was evaluated by using a SRB assay. The evaluation of cell viability by means of SRB assay is based on the determination of cellular protein content (Monks et al., 1991) against the growth of human cancer cells including human lung carcinoma (the SK-LU-1 cell line), and/or human hepatocellular carcinoma (the HepG2 cell line), and/or human carcinoma in the mouth (the KB cell line), and/or human colon carcinoma (the SW480 cell line), and/or human stomach gastric adenocarcinoma (the AGS cell line).

In the present study, cells were cultured in Dulbecco's modified eagle medium (DMEM) composing of 2.0 mM L-glutamine, 10.0 mM HEPES, 1.0 mM sodium pyruvate, supplemented with 10% fetal bovine serum (FBS) (GIBCO). The cells were dissociated using 0.05% Trypsin-EDTA, sub-cultured every 3–5 days with the ratio of (1:3) and incubated under a 5% CO_2 and 95% air atmosphere. Briefly, each cell line was seeded into each well of the 96-well culture plates and incubated in the respective medium at 37 °C, under a 5% CO_2 and 95% air atmosphere, for 24 h. The cultivation of cells was maintained in a humidified atmosphere of 5% CO_2 at 37 °C for 48 h. The cell line plated at proper density was exposed to the test compound at concentrations of 100, 20, 4 and 0.8 μg/mL under the same conditions for 72 h. Subsequently, the cell monolayers were fixed using cold 20-% (w/v) trichloroacetic acid for 1 h after removal of the medium, and stained by SRB staining solution for 30 min at 37 °C. The 1% (v/v) acetic acid solution was afterwards employed in three times to remove the unbound dye. The optical density measurement at 515 nm on an ELISA Plate Reader (Bio-Rad) was performed for the protein-bound dye dissolved in 10 mM Tris base solution. DMSO 10% and ellipticine were used as a negative control and a positive control, respectively. The determination of half maximal inhibitory concentration (IC_{50}) was assessed by the program TableCurve Version 4.0. Each cytotoxicity assay was carried out in triplicate. The inhibition rate (IR) of cell growth was calculated using the following equation: $IR\% = (100\% - [(At - A_0)/(A_c - A_0)] \times 100)$, where At denotes to an average optical density value at day 3, A_0 denotes to an average optical density value at time-zero, and A_c denotes to an average optical density value of the negative (DMSO) control sample.

5.2.6. Anti-inflammatory assay (I, II)

The nitrite concentration, as an indicator for the presence of NO in the culture medium, was assessed using the Griess reaction. Briefly, in a 96-well plate, the RAW 264.7 cells were cultured at a concentration of 2×10^5 cells/well and incubated at 37 °C and 5% CO_2 for 24 h. DMEM composed of 10.0 mM HEPES, 2.0 mM L-glutamine and 1.0 mM sodium pyruvate without FBS was utilized to replace the culture medium for 3 hours. Subsequently, the cells were treated with or without test compounds at various concentrations of 100, 20, 4

and 0.8 μg/mL and then stimulated with lipopolysaccharide (LPS) (1 μg/mL) for another 24 h at 37 °C in an incubator. The concentration of NO production in the cell culture supernatant was measured using a Griess reagent comprising 1% (w/v) sulfanilamide in 5% (v/v) phosphoric acid and 0.1% (w/v) *N*-1-naphthylethylenediamine dihydrochloride in water (1:1, v/v). The cell-free supernatant (100 μL) was mixed with an equal volume of the Griess reagent and further incubated at room temperature for 10 min. The absorbance of the mixture was determined at 540 nm by a microplate reader (Bio-Rad, Hercules, CA, USA) with a calibration curve prepared from standard $NaNO_2$ serial dilution. N^G-methyl-L-arginine acetate (L-NMMA) was employed as a positive control. Cell viability of the remaining cells was estimated using a MTT-based colorimetric assay (Yeon et al., 2015; Nguyen et al., 2020).

5.2.7. Acetylcholinesterase inhibitory activity assay (III)

The AChE inhibition assay was performed by slightly modifying an Ellman method (Magalhães et al., 2020). Acetylthiocholine is hydrolysed by AChE enzyme to produce thiocholine, and the product reacts with Ellman's reagent (5,5′-dithiobis-nitrobenzoic acid, DTNB) resulting in 5-thio-2-nitrobenzoate which was measured by the spectrophotometric. In a 96-well microplate, 140 μL (100 μM) of sodium phosphate buffer (pH 8.0), 20 μL of tested sample solution (final concentration of 100 μg/mL for the extracts and 100 μM for compounds), and 20 μL of either AChE solution, were added and mixed in the wells, and then incubated for 15 min at room temperature. Subsequently, 10 μL of DTNB was added to the solution. The enzymatic reaction was undertaken with the addition of acetylthiocholine (10 μL). The formation of the yellow 5-thio-2-nitrobenzoate anion for 15 min was analyzed using an ELISA plate reader (BioTek, Winooski, VT, USA) at 405 nm to evaluate the AChE inhibition of tested samples. The concentrations of 100, 20, 4 and 0.8 μg/mL (μM) in MeOH of all samples and the positive control (galanthamine) were carried out in triplicate to calculate dose-response curves. The inhibition value (in %) was determined using the following equation [1]:

$$\% \text{ AChE inhibition} = [(Ac - Abc) - (As - Abs)]/(Ac - Abc) \times 100 \qquad [Eq.\ 1]$$

where Ac is the absorbance of the control, Abc is the absorbance of the control blank, As is the absorbance of the sample, Abs is the absorbance of the sample blank. An IC_{50} value (μM required to inhibit the hydrolysis of the substrate, AChE by 50%) was used to express the inhibition of AChE activity of each sample, as calculated from the log-dose inhibition curve.

5.2.8. Antioxidant activity assay (III)

Free radical-scavenging ability of the extracts and isolates was evaluated using a 1,1-diphenyl-2-picrylhydrazyl (DPPH) radical method (Baliyan et al., 2022). Briefly, 200 µL of each sample at various concentrations of 200, 40, 8 and 1.6 µg/mL was combined with the 200 µL methanolic solution of DPPH (0.135 mM) in a test tube. The tubes were mixed and incubated in total darkness for 30 min. Then, the absorbance was measured at 517 nm by means of a Shimadzu UV-1800 spectrometer (Shimadzu USA Manufacturing, Inc., Canby, OR, USA). Quercetin was used as a positive control. The tests were carried out in triplicate. The scavenging of the DPPH radical was determined by the following equation [2]:

$$I\% = [(A_{blank} - A_{sample})/ A_{blank}] \times 100 \qquad \text{[Eq. 2]}$$

where A_{blank} is the absorbance of the DPPH in MeOH and A_{sample} is the absorbance of the DPPH + sample extract. The extract concentration providing 50% inhibition (IC_{50}) was obtained by plotting inhibition percentage against extract concentrations.

5.3. Preparation and characterization of amphiphilic nanofibers loaded with plant-origin haemanthamine (V)

5.3.1. Preparation of nanofibers (V)

The amphiphilic NFs loaded with HAE were generated with a solvent-based ES method. ES solutions were prepared by first dissolving PC (150.0 mg) in 5 mL of ethanol and stirring in a magnetic stirrer at ambient room temperature (22 ± 2 °C) for one hour. Next, PVP (300 mg/600 mg) was added to the solution and stirred for at least 17 h. At last, HAE (21.0 mg) was added and stirred for 6 h under the same environmental condition. After 24 h, the solutions consisting of soybean PC and PVP at the weight ratios of 1:2 and 1:4 were achieved for producing the amphiphilic NFs.

The NFs were fabricated using an ESR200RD robotized ES system consisting of a programmable syringe pump, a special syringe (spinneret), a high-voltage power supply (Model HV30) and a collector plate covered with aluminum foil, and ES/spraying system (NanoNC, South Korea). For ES, the voltage applied was 10 kV, the distance between the spinneret and a collector plate was 12 cm, and a 2.5-mL syringe equipped with a metal 25G blunt needle was used at an injection rate of 1.0 mL/h. The ES experiments were performed at room temperature (22 ± 2 °C) and relative humidity of 18–20%. All fiber samples collected onto an aluminum foil were kept in a zip-lock plastic bag in a refrigerator (8 °C) and at 0% relative humidity above silica gel in a desiccator for 12 h prior to analysis.

5.3.2. Preparation of liposomes (V)

The mixture consisting of the pre-weighted sample (100 mg) of NFs and distilled water (1.0 mL) was gently manually shaken for 1–2 min at room temperature to afford a homogenous dispersion (Figure 9). The dispersion was then left to be equilibrated for at least 10 min for yielding the HAE-loaded liposomes by self-deposition. Then, the self-assembled liposomes formed in the dispersion were immediately investigated.

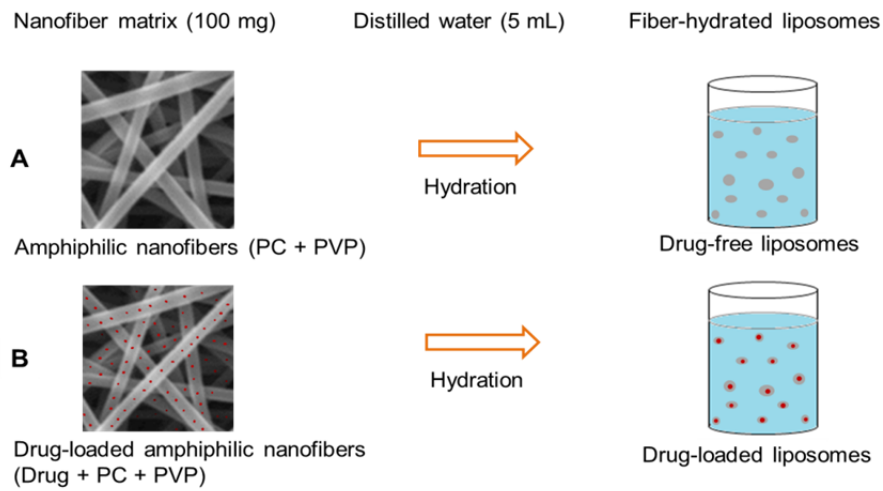

Figure 9. Schematic representation of the prepared liposome dispersions from hydrated nanofibers (NFs), (A) the formation of empty liposomes, and (B) the formation of the drug-loaded amphiphilic liposomes.

5.3.3. The geometric properties and surface morphology of electrospun nanofibers (V)

The shape, surface porosity, fiber size and morphology of NFs were investigated with a scanning electron microscope (SEM) (NanoSEM 450, FEI Corp., Hillsboro, OR, USA). The samples were attached on aluminum stubs coated with a 3 nm gold layer and magnetron sputter coated with platinum (3–5 nm) in an argon atmosphere. The SEM diameter data of NFs were acquired with ImageJ 1.50b software (National Institutes of Health, Bethesda, Rockville, MD, USA). The assessments were carried out for at least 100 individual NFs (n = 100).

5.3.4. Optical microscopy of self-assembled liposomes (V)

Optical microscopy CETI MAGTEX (Medline Sci., Chalgrove, Oxfordshire, UK) was used to assess the spontaneous formation of self-assembled liposomes. After gently manually shaking NFs in distilled water (1:10 m/v) for 1–2 min,

the liposomes were formed by self-deposition for 10 min, and consequently, investigated by optical light microscopy.

5.3.5. Photon correlation spectroscopy (V)

The size and size distribution of liposomes were measured using photon correlation spectroscopy (PCS) submicron particle analyzer (Nicomp model 380, Nicomp Inst Corp, Santa Barbara, CA, USA). The NFs (100 mg) were added 5.0 mL of distilled water, then vortexed (Vortex-Genie 2, G560E, Scientific Industries Inc., Bohemia, NY, USA) for 5 min to obtain white and homogeneous liposome dispersion. The NFs were hydrated, and self-assembled liposomes were formed. The mixture containing liposomes was then ultra-centrifuged in a Beckman Optima LE-80K ultracentrifuge (Beckman Coulter Inc., Fullerton, CA, USA) using a SW55 rotor at 50,000 rpm (at 4 °C for 1 h), and the supernatant with polymer (PVP) was removed. The vesicle dispersion was then diluted (50 × dilution in distilled water) for the PCS analysis.

5.3.6. Fourier transform infrared spectroscopy (V)

Fourier transform infrared (FTIR) spectroscopy studies were carried out using IR Prestige-21 Spectrophotometer (Shimadzu Corp., Kyoto, Japan) and Single Reflection ATR crystal (Specac Ltd., Orpington, United Kingdom). The performing range was from 4000 cm^{-1} to 550 cm^{-1}.

5.3.7. X-ray powder diffraction (V)

The XRPD patterns of samples were conducted on a Bruker D8 Advance diffractometer (Bruker Corporation, Germany) with two 2.5 Soller slits and a LynxEye line-detector. For material powder, a Vario1 focusing primary monochromator, the wavelength of Cu K-alpha 1 radiation = 1.5406 Å, data from 5 to 40° 2θ with a scanning step of 0.0173° 2θ and a total counting time of 324 s per step were applied. While NFs were investigated using a Goebel mirror (the wavelength of Cu K-alpha radiation = 1.39222 Å), a step size of 0.0194°2θ from 5 to 35° 2θ and a total counting time of 328 s per step.

5.3.8. Differential scanning calorimetry (V)

DSC 4000 (Perkin Elmer Ltd., Shelton, CT, USA) was exploited for the thermal properties of samples. Samples were studied under a dry nitrogen flow in crimped aluminum pans with 2 pinholes in a lid. Indium was used as a standard for the calibration of the calorimeter. In the DSC experiments, the fundamental parameters were as follows: the weight of the samples (2–8 mg), the heating rate (20 °C/min), the range for the operating temperature (30 °C–215 °C). Each DSC run was performed three times.

5.3.9. *In vitro* drug release (V)

In-vitro drug release tests were carried out by using a dialysis bag diffusion method (molecular weight cut off 10 kDa, Membrane-Cel, Viskase, Inc., Chicago, IL, USA). Drug-loaded NFs (20 mg) were dispersed into dialysis bag containing 2.0 mL of phosphate buffered saline (PBS), pH 6.8, as release media. The control sample (2.0 mL) including 1.0 mL HAE aqueous solution (1 mg/mL) and 1.0 mL of PBS was placed inside a dialysis bag. The dialysis bag was put in a 50 mL tube containing 20 mL of pH 6.8 PBS which was covered and positioned in a dissolution apparatus vessel (Dissolution system 2100, Distek Inc., North Brunswick Township, NJ, USA). The rotating speed of the paddles was maintained at 100 rpm, at 37 ± 1 °C throughout the experiment. At predetermined time points, samples (1.0 mL) were withdrawn and replaced with equal amounts of a fresh media. All samples were filtered through a 0.45 μm filter membrane and analyzed using HPLC (Shimadzu Corporation, Kyoto, Japan) equipped with a Luna C18 column (25 cm × 4.6 cm, 5 μm particle size) (Phenomenex Inc., Torrance, CA, USA). The HPLC method was applied as described in the literature with slight modifications (López et al., 2002). The mobile phase consisted of a solution A and MeOH (60:40, v/v). The solution A was a water:acetonitrile mixture (33:67, v/v) containing 7 mM sodium dodecylsulphate, 25 mM sodium phosphate and 1 mM ammonium acetate solution, and solvent B was MeOH. The flow rate was kept at 1.0 mL/min and the wavelength was set at 293 nm.

5.3.10. Data analysis

Structure generation of compounds (I–V) was performed using the ChemBio-Draw Ultra (version 13.0) drawing program. Results are expressed as mean ± standard deviation (SD) of three replicates (I–V). Descriptive statistical analyses (I-V) including the calculation of frequencies, the arithmetic means, SDs, students' t-test and one-way analysis of variance (ANOVA) used for testing statistical significance of differences ($p = 0.05$) or plotting figures were carried out using Microsoft Excel 2013 and OriginPro 8.5.0 software (Originlab Corporation, Northampton, MA, USA). The measurement of the particle size (Martin's diameter) and particle size variation (V) were determined by ImageJ (version 1.50b) software. Particle size normality distribution (V) was examined by a Shapiro-Wilk test.

6. RESULTS AND DISCUSSION

6.1. Chemical structure elucidation, cytotoxicity and biological activity of the compounds isolated from the selected plants (I–IV)

Chemical structure of the compounds isolated from *C. paniculatus*, *A. tonkinensis* and *Z. ajax* were elucidated using NMR (1D and 2D) and/or HRESIMS and/or IR and/or UV, circular dichroism (CD) spectra, optical rotation and comparison with the literature data.

6.1.1. *Chisocheton paniculatus* (I)

6.1.1.1. Chemical structure elucidation (I)

Six new *chiro*-inositol derivatives isolated from the leaves of *C. paniculatus* using an in-house extraction and chromatographic techniques were: 4,5-di-*O*-5-hydroxytigloyl-1-*O*-2-methylbutyroyl-3-*O*-tigloyl-*chiro*-inositol (**1**), 4,5-di-*O*-5-hydroxytigloyl-3-*O*-2-methylbutyroyl-1-*O*-tigloyl-*chiro*-inositol (**2**), 4,5-di-*O*-5-hydroxytigloyl-1,3-di-*O*-2-methylbutyroyl-*chiro*-inositol (**3**), 3,5-di-*O*-5-hydroxytigloyl-2-*O*-2-methylbutyroyl-6-*O*-tigloyl-*chiro*-inositol (**4**), 3,5-di-*O*-5-hydroxytigloyl-2,6-di-*O*-2-methylbutyroyl-*chiro*-inositol (**5**), 4,5-di-*O*-5-hydroxytigloyl-3,6-di-*O*-tigloyl-*chiro*-inositol (**6**). Their structural elucidations are present in Figure 10.

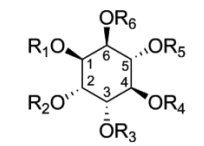

Mebu = 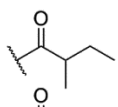

Tig = 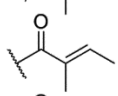

TigOH = 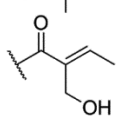

	R_1	R_2	R_3	R_4	R_5	R_6
1	Mebu	H	Tig	TigOH	TigOH	H
2	Tig	H	Mebu	TigOH	TigOH	H
3	Mebu	H	Mebu	TigOH	TigOH	H
4	H	Mebu	TigOH	H	TigOH	Tig
5	H	Mebu	TigOH	H	TigOH	Mebu
6	H	H	Tig	TigOH	TigOH	Tig

Figure 10. Structures of compounds **1**–**6** from *Chisocheton paniculatus*.

Compound **1** was isolated as a pale yellow oil. Its molecular formula, $C_{26}H_{38}O_{12}$, was determined by HRESIMS and NMR spectroscopic data analysis. The IR spectrum exhibited the presence of hydroxy (3446 cm^{-1}), ester (1718 cm^{-1}), and

olefinic (1649 cm^{-1}) functional groups in the molecule. Characteristic signals of three olefinic methine protons [δ_H 7.02, 6.91, 6.86], six methyl groups [δ_H 1.00 (3H, t, J = 7.5 Hz), 1.27 (3H, d, J = 7.1 Hz), 1.78 (6H), 1.88 (3H, d, J = 7.2 Hz), and 1.92 (3H, d, J = 7.2 Hz)], and ten oxygenated methine and/or methylene protons (δ_H 4.14–5.72) was detected in the ^{1}H NMR spectrum of **1** (Table 2). The ^{13}C NMR (Table 3) and HSQC spectra of **1** showed the presence of four carbonyl carbons [δ_C 177.2 (C-1′), 168.7 (C-1″), 167.7 (C-1‴), 168.1 (C-1⁗)], six olefinic carbons (δ_C 129.1–143.8), six oxygenated methine carbons [δ_C 74.7 (C-1), 74.5 (C-5), 73.3 (C-3), 71.4 (C-4), 68.4 (C-6), 68.2 (C-2)], two oxygenated methylene carbons [δ_C 56.2 (C-5⁗), 56.1 (C-5‴)], and eight sp^3 carbons (δ_C 11.9–42.4).

Table 2. ^{1}H (500 MHz) NMR data for **1**–**6** in CD_3OD (δ in ppm and J values in (Hz) in parentheses)

Position	**1**	**2**	**3**	**4**	**5**	**6**
1	5.27 dd (3.9, 4.0)	5.31 dd (3.7, 3.7)	5.25 dd (3.8, 3.9)	4.11[a]	4.06 dd (3.0, 3.4)	4.19 br.s
2	4.14 dd (3.7, 3.9)	4.11 dd (2.9, 3.7)	4.07 dd (3.5, 3.5)	5.41[a]	5.39 dd (3.4, 2.9)	4.19 br.s
3	5.17 dd (3.7, 10.5)	5.18 dd (2.9, 10.5)	5.17 dd (2.9, 10.5)	5.41[a]	5.40 dd (2.9, 9.6)	5.41 dt (7.5, 2.5)
4	5.72 dd (10.5, 10.2)	5.69 dd (10.5, 10.2)	5.68 dd (10.5, 10.0)	4.11[a]	4.08 dd (9.6, 9.9)	5.76 m
5	5.46 dd (10.2, 10.0)	5.47 dd (10.2, 10.0)	5.44 dd (9.8, 10.0)	5.64 dd (10.0, 10.4)	5.60 dd (9.9, 10.1)	5.76 m
6	4.30[a]	4.32[a]	4.32[a]	5.15 dd (2.9, 10.4)	5.14 dd (3.0, 10.1)	5.41 dt (7.5, 2.5)
	Mebu-1	Mebu-3	Mebu-1	Mebu-2	Mebu-2	Tig-3
2′	2.55 m	2.40 m	2.55 m	2.51 m	2.50 m	-
3′	1.78 m 1.57 m	1.60 m 1.41 m	1.77 m 1.58 m	1.74 m 1.56 m	1.72 m 1.56 m	6.88 q (7.3)
4′	1.00 t (7.5)	0.82 t (7.4)	0.99 t (7.4)	0.98 t (7.5)	0.97 t (7.5)	1.78 d (7.3)
5′	1.27 d (7.1)	1.09 d (6.9)	1.27 d (7.1)	1.22 d (7.0)	1.22 d (7.0)	1.79 s
	Tig-3	Tig-1	Mebu-3	Tig-6	Mebu-6	Tig-6
2″	-	-	2.40 m	-	2.40 m	-
3″	6.86 m	7.03[a]	1.58 m 1.42 m	6.88 m	1.60 m 1.43 m	6.88 q (7.3)
4″	1.78[a]	1.90 d (7.2)	0.82 t (7.4)	1.78[a]	0.83 t (7.4)	1.78 d (7.3)
5″	1.78[a]	1.93[a]	1.09 d (7.0)	1.78[a]	1.10 d (7.0)	1.79 s
	TigOH-4	TigOH-4	TigOH-4	TigOH-3	TigOH-3	TigOH-4
3‴	6.91 q (7.2)	7.03[a]	6.94 q (7.2)	7.06 q (7.2)	7.06[a]	6.91 q (7.2)

Position	1	2	3	4	5	6
4‴	1.88 d (7.2)	1.91 d (7.2)	1.92 d (7.3)	1.95 d (7.2)	1.95 d (7.3)	1.87 d (7.2)
5‴	4.24 s	4.25 s	4.25 s	4.37[a], 4.33[a]	4.37[a], 4.33[a]	4.24 s
	TigOH-5	TigOH-5	TigOH-5	TigOH-5	TigOH-5	TigOH-5
3⁗	7.02 q (7.2)	6.95 q (7.2)	7.01 q (7.3)	7.02 q (7.2)	7.06[a]	6.95 q (7.2)
4⁗	1.92 d (7.2)	1.93[a]	1.89 d (7.3)	1.93 d (7.2)	1.93 d (7.3)	1.87 d (7.2)
5⁗	4.33 d (12.0), 4.30 d (12.0)	4.33 d (11.9) 4.30 d (11.9)	4.33 d (12.0) 4.29 d (12.0)	4.37[a], 4.33[a]	4.37[a], 4.33[a]	4.24 s

[a] Overlapping signals.

The complete structure of **1** was established by correlation spectroscopy (COSY), heteronuclear single quantum coherence (HSQC), and heteronuclear multiple bond correlation (HMBC) data (Figure 10). The presence of six oxygenated methine carbons (δ_C 68.2–74.7) as well as the lack of the anomeric signal in the ^{13}C NMR spectrum, indicated the presence of an inositol moiety in **1**. This result was confirmed by the closed spin system [C(1)H–C(2)H–C(3)H–C(4)H-C(5)H–C(6)H–C(1)H] in the COSY spectrum. The coupling patterns of six oxygenated methine protons in **1** included three axial/equatorial and/or equatorial/equatorial couplings with small *J* values of 3.7, 3.9, and 4.0 Hz as well as three *trans*-diaxial couplings with large *J* values of 10.0, 10.2, and 10.5 Hz. In addition, the nuclear overhauser effect spectroscopy (NOESY) spectrum (Figure 11) revealed the presence of the key correlations of H-3 (δ_H 5.17) to H-5 (δ_H 5.46) and of H-4 (δ_H 5.72) to H-6 (δ_H 4.30). Based on this evidence, a *chiro*-form was determined for the inositol moiety of **1** (Fortuna et al., 2011; Wu et al., 2015).

Table 3. ^{13}C (125 MHz) NMR data for **1**–**6** in CD_3OD

Position	**1**	**2**	**3**	**4**	**5**	**6**
1	74.7	74.9	74.7	68.6	68.6	71.3
2	68.2	68.4	68.2	71.9	71.9	71.3
3	73.3	72.7	72.6	73.3	73.0	73.2
4	71.4	71.3	71.3	70.9	71.1	71.8
5	74.5	74.7	74.7	73.6	73.5	71.8
6	68.4	68.5	68.3	73.1	72.7	73.2
	Mebu-1	Mebu-3	Mebu-1	Mebu-2	Mebu-2	Tig-3
1′	177.2	177.7	177.2	176.6	176.6	168.8
2′	42.4	42.1	42.4	42.5	42.5	129.2
3′	27.6	27.7	27.6	27.8	27.8	139.8
4′	11.9	11.8	11.9	12.0	12.0	14.4
5′	17.2	16.5	17.2	17.2	17.2	12.0
	Tig-3	Tig-1	Mebu-3	Tig-6	Mebu-6	Tig-6
1″	168.7	168.3	177.7	168.8	177.7	168.8
2″	129.1	129.3	42.1	129.1	42.2	129.2
3″	139.9	139.8	27.7	139.9	27.7	139.8
4″	14.4	14.5	11.8	14.4	11.8	14.4
5″	12.0	12.3	16.5	12.1	16.6	12.0
	TigOH-4	TigOH-4	TigOH-4	TigOH-3	TigOH-3	TigOH-4
1‴	167.7	167.6	167.6	167.6	167.6	167.7
2‴	133.2	133.1	133.2	133.4	133.4	133.2
3‴	143.6	143.9	143.9	143.7	143.7	143.6
4‴	14.4	14.4	14.4	14.4	14.3	14.4
5‴	56.1	56.1	56.1	56.2	56.2	56.1
	TigOH-5	TigOH-5	TigOH-5	TigOH-5	TigOH-5	TigOH-5
1⁗	168.1	168.1	168.1	167.9	167.8	167.7
2⁗	133.2	133.1	133.2	133.5	133.5	133.2
3⁗	143.8	143.9	143.9	143.2	143.5	143.6
4⁗	14.4	14.4	14.4	14.4	14.3	14.4
5⁗	56.2	56.2	56.2	56.2	56.2	56.1

The cross-peaks of H_3-4′ (δ_H 1.00)/H_3-5′ (δ_H 1.27) to C-2′ (δ_C 42.4)/C-3′ (δ_C 27.6) and of H_3-5′ to C-1′ (δ_C 177.2) in the HMBC spectrum, along with the linear spin system [(C-4′)H_3–(C-3′)H_2–(C-2′)H–(C-5′)H_3] in the COSY spectrum (Figure 11) were observed, which confirmed the presence of a 2-methylbutyroyloxy moiety in **1**. Similarly, a (*E*)-2-methylbut-2-enoyloxy (trivial name: tigloyloxy) and two (*E*)-2-(hydroxymethyl)but-2-enoyloxy (trivial name: 5-hydroxytigloyloxy) moieties in **1** were concluded from analysis of the HMBC, COSY, and NOESY spectra (Figures 11 and 12). The 2-methylbutyroyloxy, tigloyloxy and two 5-hydroxytigloyloxy moieties were located at C-1, C-3, C-4 and C-5, based on the HMBC correlations from the oxygenated methine protons

of the inositol moiety to the carbonyl carbons of the ester groups [H-1/C-1′, H-3/C-1″, H-4/C-1‴, and H-5/C-1⁗]. Thus, compound **1** was assigned as 4,5-di-*O*-5-hydroxytigloyl-1-*O*-2-methylbutyroyl-3-*O*-tigloyl-*chiro*-inositol.

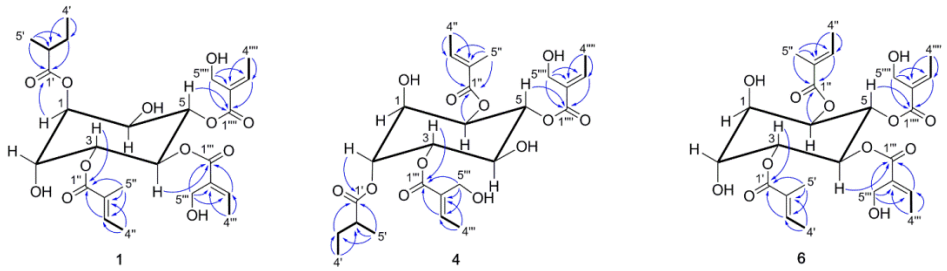

Figure 11. Key HMBC ($^{1}H \rightarrow ^{13}C$, arrows) and COSY (bold lines) correlations of compounds **1**, **4**, and **6**.

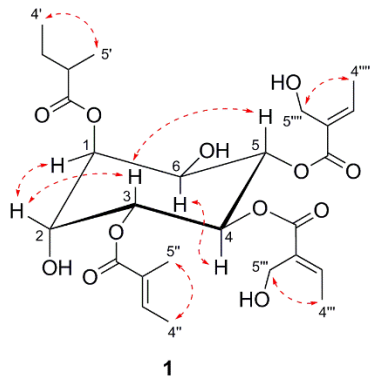

Figure 12. Key NOESY correlations (dashed arrows) of compound **1**.

Compound **2** was obtained as a pale yellow oil. The HRESIMS and NMR spectroscopy data suggested this isolate to have the same molecular formula and substituent groups present as those of **1**. Compound **2** possesses a 1,3,4,5-tetra-substituted inositol ring as in **1** based on the downfield chemical shifts of H-1 (δ_H 5.31), H-3 (δ_H 5.18), H-4 (δ_H 5.69), H-5 (δ_H 5.47). The HMBC correlations from H-4 to C-1‴ (δ_C 167.6) and from H-5 to C-1⁗ (δ_C 168.1) established the connection from the two 5-hydroxytigloyloxy moieties to C-4 and C-5, respectively.

Furthermore, the position of the tigloyloxy and 2-methylbutyroyloxy moieties was determined at C-1 and C-3 based on the HMBC correlations of H-1 to C-1″ (δ_C 168.3) and of H-3 to C-1′ (δ_C 177.7). Thus, compound **2** was elucidated as 4,5-di-*O*-5-hydroxytigloyl-3-*O*-2-methylbutyroyl-1-*O*-tigloyl-*chiro*-inositol.

Compound **3** was obtained as a pale yellow oil. This compound possessed the molecular formula $C_{26}H_{40}O_{12}$ (implying seven degrees of unsaturation) as determined by using the HRESIMS data at *m/z* 567.2418 $[M + Na]^+$.

The ^1H and ^{13}C NMR spectroscopic data (Tables 2 and 3) were similar to those of **2**, except for the presence of signals for an additional 2-methylbutyroyloxy group [δ_C/δ_H: 177.2 (C), 42.4/2.55 (CH), 27.6/1.77 and 1.58 (CH_2), 11.9/0.99 (CH_3), 17.2/1.27 (CH_3)] in **3**, instead of a tigloyloxy group in **2**. The HMBC correlation from H-1 (δ_H 5.25) to the carbonyl carbon at δ_C 177.2 (C-1′) demonstrated that this group is attached at C-1. The downfield chemical shifts of H-3 (δ_H 5.17), H-4 (δ_H 5.68), and H-5 (δ_H 5.44) as well as their HMBC correlations to the carbonyl carbons at δ_C 177.7, 167.6, and 168.1 indicated that the remaining 2-methylbutyroyloxy group and the two 5-hydroxytigloyloxy groups in **3** were placed at the same positions as in **2**. Consequently, compound **3** was proposed as 4,5-di-*O*-5-hydroxytigloyl-1,3-di-*O*-2-methylbutyroyl-*chiro*-inositol.

Compound **4**, obtained as a pale yellow oil, possessed the molecular formula $C_{26}H_{38}O_{12}$ based on the HRESIMS quasimolecular peak at *m/z* 581.1987 $[M+K]^+$ (calcd for $C_{26}H_{38}O_{12}K$, 581.2000). This isolate possesses a close structural resemblance to **1** and **2**, with a *chiro*-inositol skeleton linking to four ester moieties, except for the substituent pattern of the inositol ring, which was deduced from analysis of the NMR and HRESIMS data. The downfield chemical shifts of H-2, H-3 (δ_H 5.41), H-5 (δ_H 5.64), H-6 (δ_H 5.15) and their HMBC correlations to the corresponding carbonyl carbons in the ester groups indicated the presence of substitution at carbons C-2, C-3, C-5, and C-6 in **4**. Additionally, the 2-methylbutyroyloxy and tigloyloxy residues were linked to C-2 and C-6 via the cross-peaks from H-2 to C-1′ (δ_C 176.6), and from H-6 to C-1″ (δ_C 168.8). In the same manner, the presence of the two 5-hydroxytigloyloxy residues at C-3 and C-5 in **4** was deduced from the HMBC cross-peaks H-3/C-1‴ (δ_C 167.6) and H-5/C-1⁗ (δ_C 167.9). Thus, the structure of **4** was established as 3,5-di-*O*-5-hydroxytigloyl-2-*O*-2-methylbutyroyl-6-*O*-tigloyl-*chiro*-inositol.

Compound **5** was isolated as a pale yellow oil, and its molecular formula $C_{26}H_{40}O_{12}$ was determined by its ^{13}C NMR and HRESIMS data, requiring seven degrees of unsaturation. Except for signals showing the replacement of a tigloyloxy group by a 2-methylbutyroyloxy group in **5**, the ^1H and ^{13}C NMR spectroscopic data of **5** were very similar to those of **4**. Moreover, the additional 2-methylbutyroyloxy group at C-6 (δ_C 72.7) was verified by an HMBC correlation between H-6 (δ_H 5.14) and C-1″ (δ_C 177.7). Hence, compound **5** was assigned as 3,5-di-*O*-5-hydroxytigloyl-2,6-di-*O*-2-methylbutyroyl-*chiro*-inositol.

Compound **6**, isolated as a pale yellow oil, gave a molecular formula of $C_{26}H_{36}O_{12}$ on the basis of the HRESIMS sodiated molecular ion at *m/z* 563.2088 $[M+Na]^+$ (calcd for $C_{26}H_{36}O_{12}Na$, 563.2104). Surprisingly, the ^{13}C NMR spectrum of **6** showed only 13 carbon signals which suggested **6** to have a symmetrical structure (Mo et al., 2017). Three pairs of signals at δ_C/δ_H 71.3/4.19,

71.8/5.76, and 73.2/5.41 were observed in the ^{1}H, ^{13}C and HSQC NMR spectra, corresponding to six oxygenated methine groups in **6**. In addition, the signal at δ_H 5.41 (H-3, H-6) exhibited COSY cross-peaks with signals at δ_H 4.19 (H-1, H-2) and 5.76 (H-4, H-5). Thus, compound **6** was assigned for an inositol derivative. A di-axial relationship between H-3 and H-4 and between H-5 and H-6 was confirmed by the large $J_{3,4}$, $J_{5,6}$ values (7.5 Hz). The observed equatorial orientation was identified for both H-1 and H-2 due to the small $J_{1,6}$, $J_{2,3}$ values (2.5 Hz). Therefore, compound **6** was suggested to possess a *chiro*-inositol form in its structure. The ^{1}H and ^{13}C NMR data revealed this compound to have two tigloyloxy and two 5-hydroxytigloyloxy moieties, which was established from the HMBC spectrum. Furthermore, the HMBC correlations of H-3 and H-6 (δ_H 5.41) to carbonyl carbons at δ_C 168.8 (C-1′, C-1″) allowed two tigloyloxy units to be located at C-3 and C-6. The positions of two 5-hydroxytigloyloxy units were found to be identical to those of **1**–**3** on the basis of the downfield protons H-4 and H-5 (δ_H 5.76), and their HMBC correlations to two carbonyl carbonyl carbons at δ_C 167.7 (C-1‴, C-1⁗). Hence, the compound **6** was elucidated as 4,5-di-*O*-5-hydroxytigloyl-3,6-di-*O*-tigloyl-*chiro*-inositol.

6.1.1.2. Cytotoxic activity (I)

For the first screening of cytotoxic activity, the isolated compounds **1**–**6** were evaluated against the SK-LU-1 cell line. The results showed that all new *chiro*-inositol derivatives displayed very weak cytotoxicity against the tested cell lines (the IC_{50} values were above 100 µg/mL) (Table 4).

Table 4. Cytotoxic activity of **1**–**6** against human lung carcinoma (the SK-LU-1 cell line)

Concentration (µg/mL)	Compound						
	1	**2**	**3**	**4**	**5**	**6**	Ellipticine
100	30.0	30.8	38.5	20.8	22.5	33.7	101.8
20	17.9	15.4	19.2	7.9	5.9	21.1	90.9
4	14.6	11.2	15.2	2.6	1.5	14.9	46.5
0.8	2.8	4.8	10.7	-3.2	-1.8	7.5	21.3
IC_{50}	>100	>100	>100	>100	>100	>100	0.38 ± 0.04

IC_{50}: The half-maximal inhibitory concentration. Ellipticine was used as a positive control. Values represent mean ± SD of three parallel measurements.

6.1.1.3. Anti-inflammatory activity (I)

In order to screen their cytotoxicity and inhibition of NO production in LPS-stimulated RAW 264.7 cells by a Griess assay, the isolated compounds **1**–**6** were examined initially at a concentration of 100 µg/mL. None of them showed cytotoxicity (cell viability > 85%). The results of inhibition of NO production are summarized in Table 5. Compound **4** showed the most potent NO pro-

duction inhibitory activity, with an IC_{50} value of 7.1 μM, among the isolated compounds. Compounds **1**, **3**, and **6** displayed moderate inhibition of NO production, with IC_{50} values of 20.3, 62.9 and 56.7 μM, respectively. Compounds **2** and **5** exhibited very weak inhibitory activity, with IC_{50} values of 123.7 and 95.6 μM, respectively. Based on the present results, compound **4** could be a promising candidate for further studies (such as *in vivo* anti-inflammatory activity or other biological activity studies).

Table 5. Inhibition of NO-production of the compounds **1**–**6**

Compound	100 (μg/mL)	20 (μg/mL)	4 (μg/mL)	0.8 (μg/mL)	IC_{50} (μg/mL)	IC_{50} (μM)
1	62.3	54.9	44.8	33.5	11.0 ± 1.9	20.3 ± 3.5
2	54.3	40.6	36.7	32.0	67.0 ± 5.7	123.7 ± 10.5
3	56.4	46.5	38.5	29.3	24.3 ± 1.9	62.9 ± 4.9
4	67.7	60.2	51.6	40.0	3.9 ± 0.4	7.1 ± 0.7
5	59.0	39.7	27.5	20.4	52.0 ± 1.9	95.6 ± 3.5
6	63.2	45.6	36.4	28.4	30.6 ± 2.5	56.7 ± 4.6
L-NMMA	84.9	80.4	34.7	12.9	7.4 ± 0.6	30.0 ± 2.4

IC_{50}: The half-maximal inhibitory concentration L-NMMA was used as a positive control for inhibition of NO-production activity; and ellipticine was used as a positive control for cytotoxicity evaluation. Values represent mean ± SD of three parallel measurements. $p<0.05$ indicates significant differences when compared to a positive control.

6.1.2. *Alphonsea tonkinensis* (II)

6.1.2.1. Chemical structure elucidation (II)

Eight pure compounds (**7**–**14**) comprising six alkaloids were isolated from the stems and leaves of *A. tonkinensis* (Figure 13) by using combined chromatographic separation techniques. By means of 1D and 2D NMR spectroscopy and by comparisons to the reported data in the literature, the structures of these compounds were identified as liriodenine (**7**) (Kristanti et al., 2015), *N-trans*-feruloyltyramin (**8**) (Kanada et al., 2012), corydaldine (**9**) (Atan et al., 2011), 8-oxopseudopalmatine (**10**) (Costa et al., 2010), 3-hydroxy-7,8-dehydro-*β*-ionone (**11**) (Sannai et al., 1984), pseudopalmatine (**12**) (Stubba et al., 2015), pseudocolumbamine (**13**) (Moulis et al., 1977), and stigmasterol (**14**) (Forgo & Kövér, 2004). To the best of our knowledge, compounds **9** and **11** were isolated from the genus *Alphonsea* for the first time. ^{1}H NMR and ^{13}C NMR data of these compounds are listed below.

Liriodenine (**7**): pale yellow solid; ^{1}H NMR (500 MHz, DMSO-d_6): 7.59 (1H, s, H-3), 8.08 (1H, d, J = 4.5 Hz, H-4), 8.82 (1H, d, J = 4.5 Hz, H-5), 8.37 (1H, d, J = 8.0 Hz, H-8), 7.66 (1H, t, J = 8.0 Hz, H-9), 7.90 (1H, t, J = 8.0 Hz, H-10), 8.64 (1H, d, J = 8.0 Hz, H-11), 6.52 (2H, s, -O-CH_2-O-); ^{13}C NMR (125 MHz, DMSO-d_6): 148.8 (C-1), 152.0 (C-2), 103.5 (C-3), 143.9 (C-3a), 124.8

(C4), 143.9 (C-5), 135.8 (C-6a), 180.5 (C-7), 130.6 (C-7a), 127.9 (C-8), 128.6 (C-9), 134.3 (C-10), 127.1 (C-11), 132.5 (C-11a), 106.1 (C-11b), 122.5 (C-11c), 103.3 (O-CH_2-O).

N-trans-Feruloyltyramin (**8**): colourless oil; ^{1}H NMR (500 MHz, CD_3OD): 6.42 (1H, d, *J* = 15.5 Hz, H-2), 7.45 (1H, d, *J* = 15.5 Hz, H-3), 7.13 (1H, d, *J* = 1.5 Hz, H-5), 6.82 (1H, d, *J* = 8.0 Hz, H-8), 7.04 (1H, dd, *J* = 8.0, 2.0 Hz, H-9), 3.49 (2H, t, *J* = 7.0 Hz, H-1′), 2.78 (2H, t, *J* = 7.0 Hz, H-2′), 7.08 (2H, d, *J* = 8.5 Hz, H-4′, H-8′), 6.74 (2H, d, *J* = 8.5 Hz, H-5′, H-7′), 3.90 (3H, s, 6-OCH_3); ^{13}C NMR (125 MHz, CD_3OD): 169.2 (C-1), 118.8 (C-2), 142.0 (C-3), 128.3 (C-4), 111.6 (C-5), 149.3 (C-6), 149.9 (C-7), 116.5 (C-8), 123.2 (C-9), 42.5 (C-1′), 35.8 (C-2′), 131.3 (C-3′), 130.7 (C-4′), 116.3 (C-5′), 156.9 (C-6′), 116.3 (C-7′), 130.7 (C-8′), 56.4 (OCH_3-6).

Corydaldine (**9**): white powder; ^{1}H NMR (500 MHz, CD_3OD): 2.93 (2H, t, *J* = 7.0 Hz, H-4), 3.50 (2H, t, *J* = 7.0 Hz, H-3), 3.91 (3H, s, 6-OCH_3), 3.87 (3H, s, 7-OCH_3), 6.89 (1H, s, H-5), 7.50 (1H, s, H-8); ^{13}C NMR (125 MHz, CD_3OD): 28.6 (C-4), 41.1 (C-3), 56.5 (C-6, C-7), 111.4 (C-8), 114.4 (C-5), 122.0 (C-9), 135.1 (C-10), 149.5 (C-7), 154.2 (C-6), 169.0 (C-1).

8-Oxopseudopalmatine (**10**): Amorphous yellow powder; ^{1}H NMR (500 MHz, CD_3OD): 7.43 (1H, s, H-1), 6.93 (1H, s, H-4), 2.98 (2H, t, *J* = 6.0 Hz, H-5), 4.33 (2H, t, *J* = 6.0 Hz, H-6), 7.72 (1H, s, H-9), 7.20 (1H, s, H-12), 7.72 (1H, s, H-12a), 7.19 (1H, s, H-13), 3.96 (3H, s, OCH_3-2), 3.97 (3H, OCH_3-3), 3.92 (3H, s, OCH_3-10), 4.00 (3H, s, OCH_3-11); ^{13}C NMR (125 MHz, CD_3OD): 109.7 (C-1), 150.0 (C-2), 152.0 (C-3), 112.1 (C-4), 138.0 (C-4a), 30.7 (C-5), 41.3 (C-6), 163.5 (C-8), 119.0 (C-8a), 108.2 (C-9), 151.0 (C-10), 155.5 (C-11), 107.7 (C-12), 108.2 (C-12a), 103.5 (C-13), 129.5 (C-13a), 123.0 (C-13b), 56.9 (OCH_3-2), 56.5 (OCH_3-3), 56.6 (OCH_3-10), 56.6 (OCH_3-11).

3-Hydroxy-7,8-dehydro-*β*-ionone (**11**): reddish-brown oil; ^{1}H-NM (500 MHz, CD_3OD): 1.16 (3H, s), 1.21 (3H, s), 1.44 (1H, t, *J* = 12.0 Hz), 1.85 (1H, m), 2.00 (3H, s), 2.10 (1H, m), 2.40 (3H, s), 2.48 (1H, ddd, *J* = 1.5, 5.5, 17.0 Hz), 3.94 (1H, m); ^{13}C NMR (125 MHz, CD_3OD): 22.9, 28.9, 30.6, 32.8, 37.2, 42.3, 47.0, 64.7, 91.4, 94.7, 123.2, 148.8, 186.3.

Pseudopalmatine (**12**): amorphous yellow powder; ^{1}H NMR (500 MHz, DMSO-d_6): 7.68 (1H, s, H-1), 7.09 (1H, s, H-4), 3.24 (2H, t, *J* = 6.0 Hz, H-5), 4.80 (2H, t, *J* = 6.0 Hz, H-6), 9.49 (1H, s, H-8), 7.70 (1H, s, H-9), 7.63 (1H, s, H-12), 8.79 (1H, s, H-13), 3.95 (3H, s, OCH_3-2), 3.87 (3H, s, OCH_3-3), 4.02 (3H, s, OCH_3-10), 4.09 (3H, s, OCH_3-11); ^{13}C NMR (125 MHz, DMSO-d_6): 109.1 (C-1), 148.8 (C-2), 151.7 (C-3), 111.5 (C-4), 128.5 (C-4a), 25.9 (C-5), 54.5 (C-6), 145.2 (C-8), 121.9 (C-8a), 106.5 (C-9), 152.2 (C-10), 157.5 (C-11), 105.1 (C-12), 136.5 (C-12a), 117.7 (C-13), 138.2 (C-13a), 118.8 (C-13b), 56.1 (OCH_3-10 and OCH_3-2), 56.1 (OCH_3-3), 56.4 (OCH_3-11).

Pseudocolumbamine (**13**): amorphous yellow powder; ^{1}H NMR (500 MHz, CD_3OD): 7.56 (1H, s, H-1), 7.03 (1H, s, H-4), 3.26 (2H, t, *J* = 6.5 Hz, H-5), 4.83 (2H, H-6), 9.32 (1H, s, H-8), 7.62 (1H, s, H-9), 7.61 (1H, H-12), 8.50 (1H, s, H-13), 3.99 (3H, s, OCH_3-3), 4.08 (3H, s, OCH_3-10), 4.15 (3H, s, OCH_3-11);

^{13}C NMR (125 MHz, CD_3OD): 113.2 (C-1), 148.2 (C-2), 152.5 (C-3), 112.1 (C-4), 128.6 (C-4a), 27.9 (C-5), 56.7 (C-6), 146.1 (C-8), 124.1 (C-8a), 107.2 (C-9), 154.6 (C-10), 160.0 (C-11), 106.3 (C-12), 139.0 (C-12a), 119.1 (C-13), 140.7 (C-13a), 120.8 (C-13b), 56.6 (OCH_3-3), 57.0 (OCH_3-10), 57.5 (OCH_3-11).

Stigmasterol (**14**): white powder; ^{1}H NMR (500 MHz, $CDCl_3$): 5.35 (1H, brd, J = 4.5 Hz, H-6), 5.15 (dd, J = 15.5, 3.5 Hz, H-22), 5.03 (1H, dd, J = 15.5; 9.0 Hz, H-23), 3.52 (m, H-3), 0.70 (1H, s, H_3-18), 1.01 (1H, s, H_3-19), 0.82 (3H, d, J = 7.0 Hz, H_3-27), 0.85 (3H, d, J = 7.0 Hz, H_3-26), 0.93 (3H, d, J = 6.5 Hz, H_3-21) 0.85 (3H, t, J = 7.5 Hz, H_3-29).

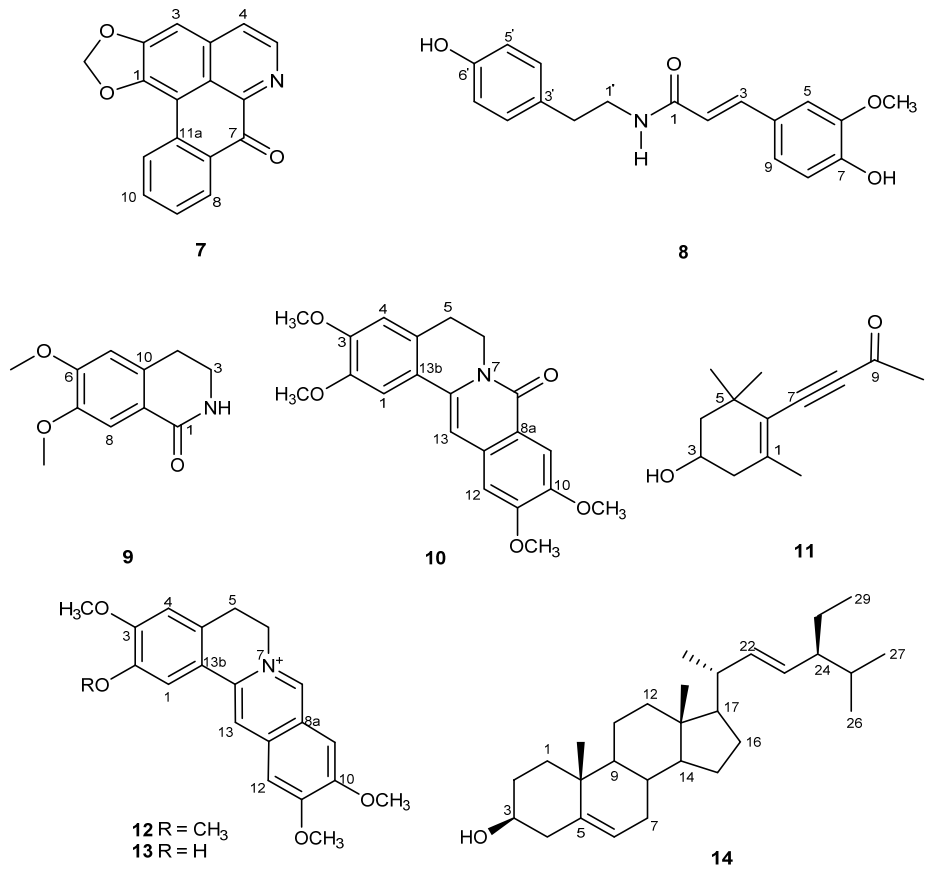

Figure 13. Structures of the compounds **7**–**14** isolated from *Alphonsea tonkinensis.*

6.1.2.2. Anti-inflammatory activity (II)

Anti-inflammatory activity of all isolates was evaluated based on the NO production inhibitory effects by using a Griess assay. To determine IC_{50} values, the dose-dependent response of compounds **7**–**14** was carried out. As shown in Table 6, compound **11** exhibited the potent NO production inhibitory activity against LPS stimulated RAW 264.7 cells, with an IC_{50} value of 20.4 μM. Significantly, its IC_{50} value was markedly less than that of positive control L-NMMA. On the other hand, the remaining compounds did not display any effect on inhibition of NO-production activity. To our best knowledge, this is the first report of compound **11** inhibiting the NO production. In addition, this promising result suggested that the compound **11** could be used for further investigations.

6.1.2.3. Cytotoxic activity (II)

Lung carcinoma is the leading cause and hepatocellular carcinoma is the third most cause of cancer deaths worldwide (Forner et al., 2012; Pratap et al., 2018). In the current work, we studied the cytotoxicity activity of phytochemicals against these cancers. It should be emphasized, however, that this is a preliminary study, and further long-term studies will be needed to reveal a true therapeutic potential of these compounds. For this purpose, the obtained compounds **8**–**14** were tested for their cytotoxic activity towards HepG2 cell line and the SK-LU-1 cell line. The amount of compound **7** was no longer sufficient for testing activity. The result indicated that compound **8**, **9**, **12**, **13**, **14** did not exhibit any inhibitions against the tested cell lines. While compound **10** and **11** possessed an inhibitory effect against the two tested cancer cell lines, with IC_{50} values ranging from 54.4 and 69.6 μM, as shown in Table 6. Notably, compound **10** was isolated from *Stephanla suberosa* for the first time in 1985 (Patra et al., 1987). Yet, this compound has not been reported the cytotoxic activity against HepG2 and SK-LU-1. Interestingly, a comparison of the cytotoxicity of compound **10** and that of compound **12** and **13** obviously revealed that the presence of carbonyl functional group (in **10**) may support a significant effect on cytotoxic activity. To the best of our knowledge, cytotoxic activity of compound **10** and **11** has not been reported yet.

Table 6. Inhibition of NO-production and cytotoxic activity of the compounds **7**–**14**

Compound	IC_{50} (μM) ± SD		
	Inhibition of NO-production activity	Cytotoxicity	
		HepG2	SK-LU-1
Liriodenine (**7**)	>100	N.T	N.T
N-trans-Feruloyltyramin (**8**)	>100	>100	>100
Corydaldine (**9**)	>100	>100	>100
8-Oxopseudopalmatine (**10**)	>100	56.6 ± 1.5*	69.6 ± 1.3*
3-Hydroxy-7,8-dehydro-*β*-ionone (**11**)	20.4 ± 0.4*	56.2 ± 0.5*	54.0 ± 0.8*
Pseudopalmatine (**12**)	>100	>100	>100
Pseudocolumbamine (**13**)	>100	>100	>100
Stigmasterol (**14**)	>100	>100	>100
L-NMMA	25.0 ± 0.8		
Ellipticine		1.5 ± 0.1	1.5 ± 0.1

IC_{50}: The half-maximal inhibitory concentration; HepG2: human hepatocellular carcinoma cell lines; and SK-LU-1: human lung carcinoma cell lines. N.T: the compounds were not tested. L-NMMA was used as a positive control for inhibition of NO-production activity; and ellipticine was used as a positive control for cytotoxicity evaluation. Values represent mean ± SD of three parallel measurements. *p< 0.05 indicates significant differences when compared to a positive control.

6.1.2.4. Acetylcholinesterase inhibitory activity (III)

The extracts and compounds isolated from *A. tonkinensis* were evaluated for AChE inhibitory activity using an Ellman's colorimetric method, with galanthamine as a positive control. The results are summarized in Table 7. Regarding with the extracts, the MeOH portion (the sub-fraction of an alkaloid extract) showed the most potent AChE inhibitory effects, followed by the total MeOH extract, CH_2Cl_2 extract, aqueous phase (pH 9) and aqueous phase, with corresponding IC_{50} inhibition values for 14.6, 22.7, 32.8, 84.4 and 90.2 μg/mL, respectively. In relation to compounds, pseudopalmatine and pseudocolumbamine exhibited potent AChE inhibition with IC_{50} values of 8.6 μM and 18.9 μM, respectively.

Table 7. The anti-acetylcholinesterase (AChE) activity of extracts and compounds from the *Alphonsea tonkinensis*.

Sample	IC_{50} (μg/mL)	IC_{50} (μM)
MeOH extract	22.7 ± 0.6	
EA extract	>100	
Aqueous phase pH 9	84.4 ± 0.7	
CH_2Cl_2 extract	32.9 ± 0.3	
n-Hexane portion	>100	
EC extract	>100	
MeOH portion	14.6 ± 0.3	
Aqueous phase	90.2 ± 1.5	
Pseudopalmatine (**12**)	3.0 ± 0.0	8.6 ± 0.1
Pseudocolumbamine (**13**)	6.4 ± 0.1	18.9 ± 0.3
N-trans-Feruloyltyramine (**8**)		>100
Corydaldine (**9**)		>100
3-Hydroxy-7,8-dehydro-*β*-ionone (**11**)		>100
Stigmasterol (**14**)		>100
Liriodenine (**7**)		N.T
8-Oxopseudopalmatine (**10**)		N.T
Galanthamine	0.3 ± 0.0	1.0 ± 0.1

N.T: the compounds were not tested. Galanthamine was used as a positive control for the anti-AChE activity. Values represent mean ± SD of three parallel measurements.

Le et al. reported that there were 10% of samples of the methanolic extracts from 30 medicinal plants in Viet Nam showing anti-AChE effect with an IC_{50} value less than 50 μg/mL (Le et al., 2018). Similar findings (i.e., the same proportion of plants investigated in India) were indicated in the study of Maya Mathew and Sarada Subramanian (Mathew & Subramanian, 2014). In our study, the total dry MeOH extract revealing a strong anti-AChE activity, with an IC_{50} value of 22.7 μg/mL, was a promising source for further investigation.

It is generally known that alkaloids have become the most successful drug candidates for AD drug development due to their nitrogen-containing structures (Konrath et al., 2013; Orhan & Senol, 2013). Interestingly, TLC analysis in our study displayed that total dry MeOH extract of *A. tonkinensis* contained a Dragendorff's reagent-positive substances. A conventional alkaloid extraction method was applied. As expected, we obtained six alkaloids. Furthermore, two alkaloid compounds pseudocolumbamine and pseudopalmatine along with

the MeOH portion (the sub-fraction of an alkaloid extract, containing these two isolates) and total dry MeOH extract showed the potent anti-AChE effect. They are potential candidates in drug discovery for AD.

6.1.2.5. Antioxidant activity (III)

The extracts and compounds isolated from *A. tonkinensis* along with quercetin, as a positive control, were assessed antioxidant capacity by using a DPPH assay. An IC_{50} value was calculated to specify the concentration providing 50% inhibition of radicals. As shown in Table 8, the dry aqueous phase (pH 9) extract exhibited the best antioxidant efficiency, with an IC_{50} value of 24.5 µg/mL and the next was that of the dry MeOH portion extract with an IC_{50} value of 72.1 µg/mL. Among of pure compounds, *N-trans*-feruloyltyramine possessed a significant antioxidant activity with an IC_{50} value of 61.3 µM.

Table 8. The antioxidant activity of extracts and compounds of *Alphonsea tonkinensis*.

Sample	IC_{50} (µg/mL)	IC_{50} (µM)
MeOH extract	>200	
EA extract	>200	
Aqueous phase pH 9	24.5 ± 1.0	
CH_2Cl_2 extract	>200	
n-Hexane portion	>200	
EC extract	>200	
MeOH portion	72.1 ± 0.7	
Aqueous phase	>200	
N-trans-Feruloyltyramin (**8**)	19.2 ± 1.0	61.3 ± 3.2
Corydaldine (**9**)		>100
3-Hydroxy-7,8-dehydro-*β*-ionone (**11**)		>100
Pseudopalmatine (**12**)		>100
Pseudocolumbamine (**13**)		>100
Stigmasterol (**14**)		>100
Liriodenine (**7**)		N.T
8-Oxopseudopalmatine (**10**)		N.T
Quercetin	6.5 ± 0.1	21.4 ± 0.3

N.T: the compounds were not tested

It is well known that DPPH is the preferred method for evaluating antioxidant capacity *in vitro*, because this assay is rapid, accurate, valid, economic, simple and requires a UV-vis spectrophotometer to perform (de Torre et al., 2019). In the present study, the findings suggest that antioxidant active constituents are most likely polar. This is confirmed that the dry aqueous phase (pH 9) extract and the dry MeOH portion extract had significant DPPH radical scavenging activity. In addition, *N-trans*-feruloyltyramine showed considerable antioxidant capacity *in vitro*. The result is also in a good agreement with previous data reported by Wen Jie Li (Li et al., 2012).

6.1.3. *Zephyranthes ajax* (IV)

6.1.3.1. Chemical structure elucidation (IV)

After using an extraction and chromatographic technique for the powdered bulbs of *Z. ajax*, a new flavanol derivative: (2*R*,3*R*)-3-acetoxy-7-hydroxy-3′,4′-methylenedioxyflavan (**15**), and seven known compounds: 7-hydroxyflavan (**16**) (Moodley, 2004), 7,4′-dihydroxyflavan (**17**) (Meksuriyen & Cordell, 1988), 7,4′-dihydroxy-8-methylflavan (**18**) (Ioset et al., 2001), 7,3′-dihydroxy-4′-methoxyflavan (**19**) (Sun et al., 2016), 5,4′-dihydroxy-7-methoxy-6-methyl-flavan (**20**) (Zheng et al., 2004), 7-hydroxy-3′,4′-methylenedioxyflavanone (**21**) (Ali et al., 2017) and haemanthamine (**22**) (Bastida et al., 1987; Bohno et al., 2007) were obtained (Figure 14). To the best of our knowledge, compound **16**, **17**, **18**, **20** and **21** were isolated from the genus *Zephyranthes* for the first time. ^{1}H NMR and ^{13}C NMR data of these compounds are listed below.

7-Hydroxyflavan (**16**): pale yellow powder; ^{1}H NMR (500 MHz, CD_3OD): 5.01 (1H, dd, *J* = 10.0, 2.5 Hz, H-2), 1.99 (1H, m, H-3a), 2.17 (1H, m, H-3b), 2.66 (1H, dt, *J* = 16.0, 4.5 Hz, H-4a), 2.87 (1H, m, H-4b), 6.88 (1H, d, *J* = 8.5 Hz, H-5), 6.35 (1H, dd, *J* = 8.5, 2.5 Hz, H-6), 6.31 (1H, d, *J* = 2.5 Hz, H-8), 7.41 (2H, dd, *J* = 7.5, 1.5 Hz, H-2′ and H-6′), 7.37 (2H, t, *J* = 7.5 Hz, H-3′ and H-5′), 7.30 (1H, tt, *J* = 7.5, 1.5 Hz, H-4′); ^{13}C NMR (125 MHz, CD_3OD): 79.0 (C-2), 31.5 (C-3), 25.2 (C-4), 131.0 (C-5), 109.2 (C-6), 157.6 (C-7), 104.1 (C-8), 157.0 (C-9), 114.3 (C-10), 143.4 (C-1′), 127.0 (C-2′ and C-6′), 129.4 (C-3′ and C-5′), 128.6 (C-4′).

7,4′-Dihydroxyflavan (**17**): pale yellow powder; ^{1}H NMR (500 MHz, CD_3OD): 4.92 (1H, dd, *J* = 10.0, 1.5 Hz, H-2), 1.99 (1H, m, H-3a), 2.13 (1H, m, H-3b), 2.68 (1H, dt, *J* = 16.0, 5.0 Hz, H-4a), 2.85 (1H, m, H-4b), 6.88 (1H, d, *J* = 8.5 Hz, H-5), 6.33 (1H, dd, *J* = 8.5, 2.5 Hz, H-6), 6.27 (1H, d, *J* = 2.5 Hz, H-8), 7.24 (1H, d, *J* = 8.5 Hz, H-2′ and H-6′), 6.80 (1H, d, *J* = 8.5 Hz, H-3′ and H-5′).

7,4′-Dihydroxy-8-methylflavan (**18**): white powder; ^{1}H NMR (500 MHz, CD_3OD): 4.95 (1H, dd, *J* = 10.0, 2.0 Hz, H-2), 1.95 (1H, m, H-3a), 2.15 (1H, m, H-3b), 2.68 (1H, m, H-4a), 2.88 (1H, m, H-4b), 6.71 (1H, d, *J* = 8.0 Hz, H-5), 6.34 (1H, d, *J* = 8.0 Hz, H-6), 7.27 (1H, d, *J* = 9.0 Hz, H-2′ and H-6′), 6.80 (1H,

d, *J* = 9.0 Hz, H-3′ and H-5′), 2.05 (3H, s, -CH_3); ^{13}C NMR (125 MHz, CD_3OD): 78.7 (C-2), 31.4 (C-3), 25.8 (C-4), 127.3 (C-5), 108.3 (C-6), 155.1 (C-7), 112.7 (C-8), 155.0 (C-9), 114.1 (C-10), 134.8 (C-1′), 128.2 (C-2′ and C-6′), 116.1 (C-3′ and C-5′), 157.9 (C-4′), 8.5 (-CH_3).

7,3′-Dihydroxy-4′-methoxyflavan (**19**): ivory-yellow powder; ^{1}H NMR (500 MHz, CD_3OD): 4.91 (1H, dd, *J* = 10.0, 2.5 Hz, H-2), 1.97 (1H, m, H-3a), 2.14 (1H, m, H-3b), 2.67 (1H, dt, *J* = 15.5, 4.5 Hz, H-4a), 2.86 (1H, m, H-4b), 6.88 (1H, overlapped, H-5), 6.33 (1H, dd, *J* = 8.0, 2.5 Hz, H-6), 6.28 (1H, d, *J* = 2.5 Hz, H-8), 6.89 (1H, d, *J* = 2.0 Hz, H-2′), 6.92 (1H, d, *J* = 8.5 Hz, H-5′), 6.86 (1H, dd, *J* = 8.5, 2.0 Hz, H-6′), 3.87 (3H, s, -OCH_3); ^{13}C NMR (125 MHz, CD_3OD): 78.8 (C-2), 31.3 (C-3), 25.3 (C-4), 130.9 (C-5), 109.1 (C-6), 157.6 (C-7), 104.1 (C-8), 157.1 (C-9), 114.3 (C-10), 136.4 (C-1′), 112.6 (C-2′), 147.6 (C-3′), 148.6 (C-4′), 114.2 (C-5′), 118.5 (C-6′), 56.5 (-OCH_3),; HRESIMS *m/z* 295.0941 $[M + Na]^+$ (calcd for $C_{16}H_{16}O_4Na$, 295.0946).

5,4′-Dihydroxy-7-methoxy-6-methylflavan (**20**): white powder; ^{1}H NMR (500 MHz, CD_3OD): 4.84 (1H, overlapped, H-2), 1.88 (1H, m, H-3a), 2.15 (1H, m, H-3b), 2.61 (1H, m, H-4a), 2.69 (1H, m, H-4b), 6.06 (1H, s, H-8), 7.26 (1H, d, *J* = 8.5 Hz, H-2′ and H-6′), 6.80 (1H, d, *J* = 8.5 Hz, H-3′ and H-5′), 3.75 (3H, s, -OCH_3), 1.99 (3H, s, -CH_3); ^{13}C NMR (125 MHz, CD_3OD): 78.5 (C-2), 30.7 (C-3), 20.5 (C-4), 155.0 (C-5), 105.0 (C-6), 157.1 (C-7), 92.1 (C-8), 155.5 (C-9), 103.3 (C-10), 134.7 (C-1′), 128.2 (C-2′ and C-6′), 116.1 (C-3′ and C-5′), 157.9 (C-4′), 55.7 (-OCH_3), 8.0 (-CH_3).

7-hydroxy-3′,4′-methylenedioxyflavanone (**21**): pale yellow powder; ^{1}H NMR (500 MHz, CD_3OD): 5.43 (1H, dd, *J* = 13.0, 3.0 Hz, H-2), 2.74 (1H, dd, *J* = 17.0, 3.0 Hz, H-3a), 3.04 (1H, dd, *J* = 17.0, 13.0 Hz, H-3b), 7.75 (1H, d, *J* = 9.0 Hz, H-5), 6.52 (1H, dd, *J* = 9.0, 2.5 Hz, H-6), 6.39 (1H, d, *J* = 2.5 Hz, H-8), 7.05 (1H, d, *J* = 1.5 Hz, H-2′), 6.86 (1H, d, *J* = 8.0 Hz, H-5′), 6.98 (1H, dd, *J* = 8.0, 1.5 Hz, H-6′), 5.99 (2H, s, -OCH_2O-); ^{13}C NMR (125 MHz, CD_3OD): 80.9 (C-2), 45.1 (C-3), 193.1 (C-4), 129.8 (C-5), 111.9 (C-6), 167.1 (C-7), 103.9 (C-8), 165.4 (C-9), 114.9 (C-10), 134.5 (C-1′), 107.9 (C-2′), 149.4 (C-3′), 149.4 (C-4′), 109.1 (C-5′), 121.2 (C-6′), 102.6 (-OCH_2O-); HRESIMS *m/z* 283.0606 $[M - H]^-$ (calcd for $C_{16}H_{11}O_5$, 283.0606).

Haemanthamine (**22**): colorless crystal; ^{1}H NMR (500 MHz, $CDCl_3$): 6.41 (1H, d, *J* = 10.5 Hz, H-1), 6.35 (1H, dd, *J* = 10.5, 5.0 Hz, H-2), 3.86 (1H, m, H-3), 2.11 (1H, ddd, *J* = 13.5, 13.5, 4.0 Hz, H-4), 2.01 (1H, dd, *J* = 13.5, 4.5 Hz, H-4), 4.32 (1H, d, *J* = 16.5 Hz, H-6); 3.68 (1H, d, *J* = 16.5 Hz, H-6), 6.47 (1H, s, H-7), 6.82 (1H, s, H-10), 3.97 (1H, brd, *J* = 4.0 Hz, H-11), 3.35 (1H, dd, *J* = 13.5, 6.5 Hz, H-12), 3.22 (1H, dd, *J* = 13.5, 3.5 Hz, H-12), 5.88 (1H, d, *J* = 4.5 Hz, -OCH_2O-), 3.35 (1H, s, -OCH_3); ^{13}C NMR (125 MHz, $CDCl_3$): 127.4 (C-1), 126.9 (C-2), 72.8 (C-3), 28.3 (C-4), 62.7 (C-5), 63.6 (C-6), 132.0 (C-6a), 106.9 (C-7), 146.2 (C-8), 146.5 (C-9), 103.3 (C-10), 135.4 (C-10a), 50.1 (C-10b), 80.2 (C-11), 61.4 (C-12), 100.8 (-OCH_2O-), 56.7 (-OCH_3).

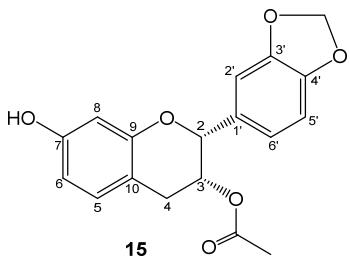

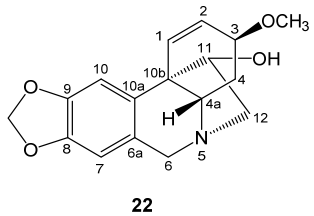

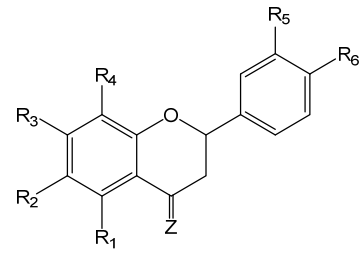

	R_1	R_2	R_3	R_4	R_5	R_6	Z
16	H	H	OH	H	H	H	H_2
17	H	H	OH	H	H	OH	H_2
18	H	H	OH	CH_3	H	OH	H_2
19	H	H	OH	H	OH	OCH_3	H_2
20	OH	CH_3	OCH_3	H	H	OH	H_2
21	H	H	OH	H	$O-CH_2-O$		O

Figure 14. Structures of **15**–**22** isolated from *Zephyranthes ajax*.

Compound **15** was isolated as a colourless powder. The HRESIMS showed a sodiated molecular ion peak at *m/z* 329.1021 $[M + H]^+$, corresponding to the molecular formula $C_{18}H_{16}O_6$, implying eleven degrees of unsaturation. The characteristic signals corresponding to two sets of ABX patterns at δ_H 6.90 (d, J = 8.5 Hz, H-5), 6.40 (dd, J = 8.5, 2.5 Hz, H-6), 6.37 (d, J = 2.5 Hz, H-8) and δ_H 6.98 (d, J = 1.0 Hz, H-2′), 6.82 (d, J = 8.0 Hz, H-5′), 6.95 (dd, J = 8.0, 1.0 Hz, H-6′), belonging to two 1,3,4-trisubstituted benzene rings were observed in the ^{1}H NMR spectrum of **15**. Furthermore, the ^{1}H NMR spectrum of **15** showed the signals of a dioxygenated methylene group at δ_H 5.97 (s), two oxygenated methine groups at δ_H 5.11 (s, H-2), 5.37 (m, H-3) and an acetoxy group at δ_H 1.89 (s). The anisotropic effect of two aromatic rings causes the acetoxy methyl protons to resonate at higher field. This result is in accordance with previous studies on 3-acetoxyflavanol derivatives (Li et al., 2007; Meng et al., 2010). The ^{13}C NMR, DEPT and HSQC spectra of **15** indicated the presence of 18 signals including a carbonyl carbon (δ_C 171.9), twelve aromatic carbons (δ_C 158.0, 156.2, 149.0, 148.7, 133.7, 131.3, 121.0, 110.8, 110.0, 108.8, 108.1, 104.0), a dioxygenated methylene carbon (δ_C 102.4), two oxygenated methine carbons (δ_C 78.4, 70.2), a methylene carbon (δ_C 31.1) and a methyl carbon (δ_C 20.8) (Table 9). Based on this evidence, compound **15** was deduced to be a flavanol derivative. The planar structure of **15** was determined by detailed HMBC analysis (Figure 15). Notably, the HMBC correlations of H-3 (δ_H 5.37) to carbonyl carbon (δ_C 171.9) established the connection from acetoxy group to C-3. This was confirmed by the strong downfield shifts of C-3 (δ_C 70.2), H-3 (δ_H 5.37) compared to those of (2*R*,3*R*)-3,7-dihydroxy-3,4-methylenedioxyflavan (δ_C 67.1, δ_H 4.21) (Jitsuno et al., 2009). The CD spectrum of **15**

revealed the presence of a negative Cotton effect at λ 288 nm (^1L_b band) which correspond to *P*-helicity of heterocyclic C ring. Thus, the absolute configuration of C-2 was established as *R* form (Slade et al., 2005). In additional, the *cis* relationship between H-2 and H-3 was deduced from analysis of the small vicinal coupling constant values ($J_{H\text{-}2/H\text{-}3}$ = 0 Hz, $J_{H\text{-}3/H\text{-}4a}$ = 2.0 Hz, $J_{H\text{-}3/H\text{-}4b}$ = 4.0 Hz) (Vdovin et al., 1997). Thus, compound **15** was assigned as (2*R*,3*R*)-3-acetoxy-7-hydroxy-3′,4′-methylenedioxyflavan.

Table 9. ^1H (500 MHz) and ^{13}C (125 MHz) NMR data of **15** in methanol-d_4 [δ (ppm), *J* (Hz)].

Position	δ_C	δ_H
2	78.4	5.11 s
3	70.2	5.37 m
4	31.1	2.81 dd (17.0, 2.0) (H-4a) 3.25 dd (17.0, 4.0) (H-4b)
5	131.3	6.90 d (8.5)
6	110.0	6.40 dd (8.5, 2.5)
7	158.0	–
8	104.0	6.37 d (2.5)
9	156.2	–
10	110.8	–
1′	133.7	–
2′	108.1	6.98 d (1.0)
3′	149.0	–
4′	148.7	–
5′	108.8	6.82 d (8.0)
6′	121.0	6.95 dd (8.0, 1.0)
-OAc	171.9	–
	20.8	1.89 s
-OCH_2O-	102.4	5.97 s

Assignments were done by HSQC, HMBC experiments.

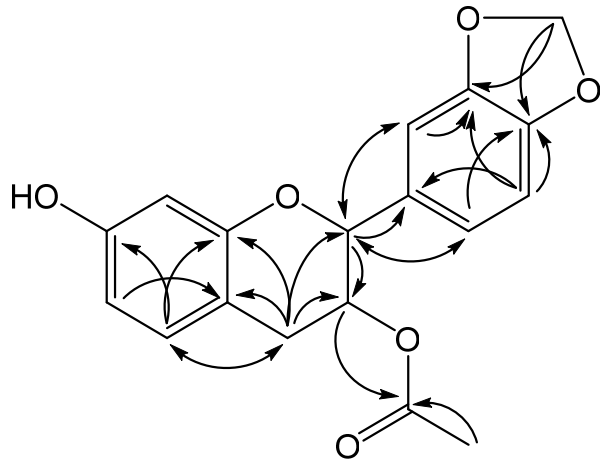

Figure 15. Key HMBC ($^{1}H \rightarrow ^{13}C$, arrows) correlations of **15**.

6.1.3.2. Cytotoxic activity (IV)

As mentioned above, lung carcinoma and hepatocellular carcinoma are two of the most common causes of cancer deaths worldwide (Forner et al., 2012; Pratap et al., 2018). Thus, all isolates from *Z. ajax* were initially tested against the HepG2 cell line and the SK-LU-1 cell line for the first screening of cytotoxic activity. The result was indicated in Table 10. Compounds **15**–**21** did not reveal any *in vitro* activity toward the tested cell lines. In contrast, compound **22** showed potent cytotoxicity against the HepG2 and SK-LU-1 cell lines, with IC_{50} values of 9.7 and 5.4 μM, respectively. Interestingly, to our best knowledge, this is the first study ever reporting the cytotoxic activity against the SK-LU-1 cancer cell line of **22.** These results encouraged us to further examine cytotoxicity of **22** against the KB cell line, the SW480 cell line and the AGS cell line. As anticipated, this compound exhibited a strong inhibition towards the KB, SW480 and AGS cell lines, with IC_{50} values of 11.3, 4.4 and 6.5 μM, respectively. The obtained results agreed well with the previous studies (Nair et al., 2012; Havelek et al., 2017).

Table 10. Cytotoxicity of the compounds **15**–**22** isolated from *Zephyranthes ajax* and ellipticine (as a positive control).

Compound	IC_{50} (μM) ± SD				
	HepG2	SK-LU-1	KB	SW480	AGS
(2*R*,3*R*)-3-Acetoxy-7-hydroxy-3′,4′-methylenedioxyflavan (**15**)	>100	>100	N.T	N.T	N.T
7-Hydroxyflavan (**16**)	>100	>100	N.T	N.T	N.T
7,4′-Dihydroxyflavan (**17**)	>100	>100	N.T	N.T	N.T
7,4′-Dihydroxy-8-methylflavan (**18**)	>100	>100	N.T	N.T	N.T
7,3′-Dihydroxy-4′-methoxyflavan (**19**)	>100	>100	N.T	N.T	N.T
5,4′-Dihydroxy-7-methoxy-6-methylflavan (**20**)	>100	>100	N.T	N.T	N.T
7-Hydroxy-3′,4′-methylenedioxyflavanone (**21**)	>100	>100	N.T	N.T	N.T
Haemanthamine (**22**)	9.7 ± 0.7	5.4 ± 0.2	11.3 ± 0.9	4.4 ± 0.1	6.5 ± 0.7
Ellipticine	1.5 ± 0.1	1.6 ± 0.1	1.5 ± 0.1	1.5 ± 0.1	0.7 ± 0.1

N.T. the compounds were not tested

Havelek et al. reported that compound **22** (haemanthamine – HAE) is a promising anticancer agent because it can not only induce apoptosis accelerating the caspases activation but also stimulate DNA damage checkpoint kinase Chk1 and the $p16^{INK4a}$ cyclin-dependent kinase inhibitor (Havelek et al., 2014). In addition, it is able to produce a sandwich-like structure between the two 25S rRNA residues (U2875 and C2821). As a result, HAE treatment leads to restraint of ribosome biogenesis, activation of nucleolar stress response and stabilization of p53 in cancer cells, thus killing of cancer cells (Pellegrino et al., 2018).

Greatly, basing on extraction, chromatographic methods and crystallization techniques, we found out and obtained a rather large amount of HAE. This compound has been proven to have a potent cytotoxic activity, but poorly-water solubility. Hence, HAE was selected to develop novel HAE-loaded amphiphilic NFs to overcome these formulation challenges (Nguyen et al., 2019).

6.2. Nanoformulation of electrospun amphiphilic nanofibers and self-assembled liposomes for the delivery of plant-origin haemanthamine

6.2.1. Size, shape and morphology of amphiphilic nanofibers (V)

The plant-origin active ingredient (HAE) used in the present nanoformulations was isolated from *Z. ajax*. The representative SEM images of HAE powder particles and the individual amphiphilic NFs of HAE as a solid nanofibrous template for self-assembled liposomes are displayed in Figure 16. HAE in a pre-milled powder form consisted of large irregular particles with a particle size ranging from some tenths of micrometers to several hundred micrometers (Figure 16A). Visually, the performance of an ES process and the formation of NFs were not weakened by the combination of HAE and soybean PC with the ES carrier polymer PVP. The NFs generated from the ES solutions of HAE, soybean PC and PVP exhibited a smooth surface and uniform fiber diameter with no evidence of beads as defects (Figure 16B,C). The external pore size of the present amphiphilic nanofibrous templates ranged from a few micrometers to ten micrometers. The nanofibrous solid templates revealed the topography with a non-woven and loosely packed platform.

The present results agree well with those reported in the literature (Yu et al., 2011). Yu et al. (2011) proposed in their pioneer work that ES is a feasible method for generating amphiphilic NFs intended for the solid templates for self-assembled liposomes (Yu et al., 2011). They did not incorporate, however, any active ingredient(s) in the NFs. In our study, we applied the same ratio of PC and PVP (1:2 w/w) for HAE-loaded NFs as Yu and co-workers in their bulk NFs. The mean fiber diameter of electrospun amphiphilic NFs loaded with HAE

was 392 ± 66 nm (n = 100), and the fiber size ranged from 197 nm to 534 nm with the individual NFs (Figure 16). Yu et al. (2011) reported that the average fiber diameter of the corresponding amphiphilic bulk NFs (without any active ingredient) ranged from 580 nm to 1250 nm. Notably, this study indicated that the average diameter of NFs fabricated from pure PVP (910 ± 110 nm) reduced significantly owing to the increasing PC content up to 33.3%. The amphiphilic NFs had the lowest diameter (580 ± 90 nm) with 33.3% *w*/*w* of PC, for the reason that there was a reverse increase in the average diameter of NFs (1010 ± 110 nm) as the PC content was increased to 50% (*w*/*w*). It is evident that the presence of PC (a zwitterionic surfactant) alters the surface tension and viscosity of the PVP solution, thus modifying the morphology and diameter of the NFs (Yu et al., 2011). Taking advantage of the technical pioneer formulation of Yu and co-workers, we succeeded to fabricate corresponding amphiphilic NFs and self-assembled liposomes for plant-origin HAE isolated from *Z. ajax*.

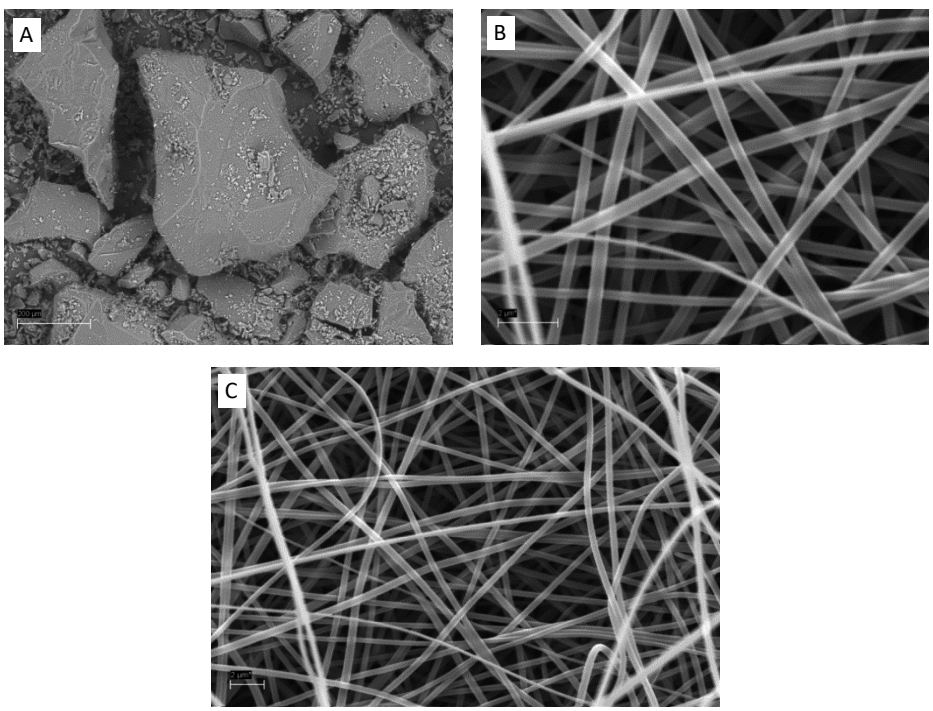

Figure 16. The scanning electron microscopy (SEM) images of an isolated and milled haemanthamine (HAE) powder (**A**) and the amphiphilic electrospun nanofibers (NFs) (**B**,**C**) used as a solid template for the self-assembled liposomes. Scale bar 200 μm (**A**) and 2.0 μm (**B**,**C**).

PVP is an established pharmaceutical excipient which is soluble both in water and ethanol, and thus it is a good carrier polymer in a solvent-based ES and for fabricating polymeric NFs. A homogeneous PVP solution for ES was prepared effortlessly using ethanol as solvent. When adding to PVP solutions, PC induces evidently electrostatic hydrophobic interactions with PVP (Yu et al., 2011) which modify the conformation of a PVP chain and PVP–PVP molecular interactions. As a result, these molecular-level interactions lead to decrease in entanglements and viscosity (Yu et al., 2011; Kogermann et al., 2013; Shi et al., 2014).

Compared to Yu and coworkers' research work (Yu et al., 2011), our study comprises some significant differences such as active ingredient (HAE *vs* none), organic solvent, the grade of PVP (in our study K90), polymer concentration and air humidity. These variables may be the major reasons that the diameter of amphiphilic NFs in our study was much smaller than that of the bulk NFs introduced by Yu and coworkers (Figure 16). According to the literature, the changes in the above mentioned factors most likely affect (decrease) the viscosity of the ES solution and modify solvent evaporation, thus contributing to a decrease in a fiber diameter (Z. Li & Wang, 2013; Hu et al., 2014).

6.2.2. Formation of self-assembled liposomes (V)

After exposing an amphiphilic nanofibrous template to the drop of purified water, optical micrographs were taken at regular intervals to monitor the formation of the self-assembled liposomes in water. As seen in Figure 17, the liposomes were spontaneously formed (self-assembled) in water within a few seconds, thus verifying the appropriate performance of the present delivery system. While PVP dissolves in water, the soybean PC releases from the amphiphilic nanofibrous PVP matrix (solid template) in contact with water, and this results in the instant formation of the individual or co-aggregated vesicles. Yu et al. (2011) reported that PC molecules tend to co-aggregate in water after they were released from the PVP nanofibrous matrix, and the location of original NFs in the matrix template influences the formation of liposomes. These are also in line with our current findings. In addition, our results suggest that the present molecular self-assembly strategy is applicable in the nanoformulation of a plant-origin alkaloid (HAE).

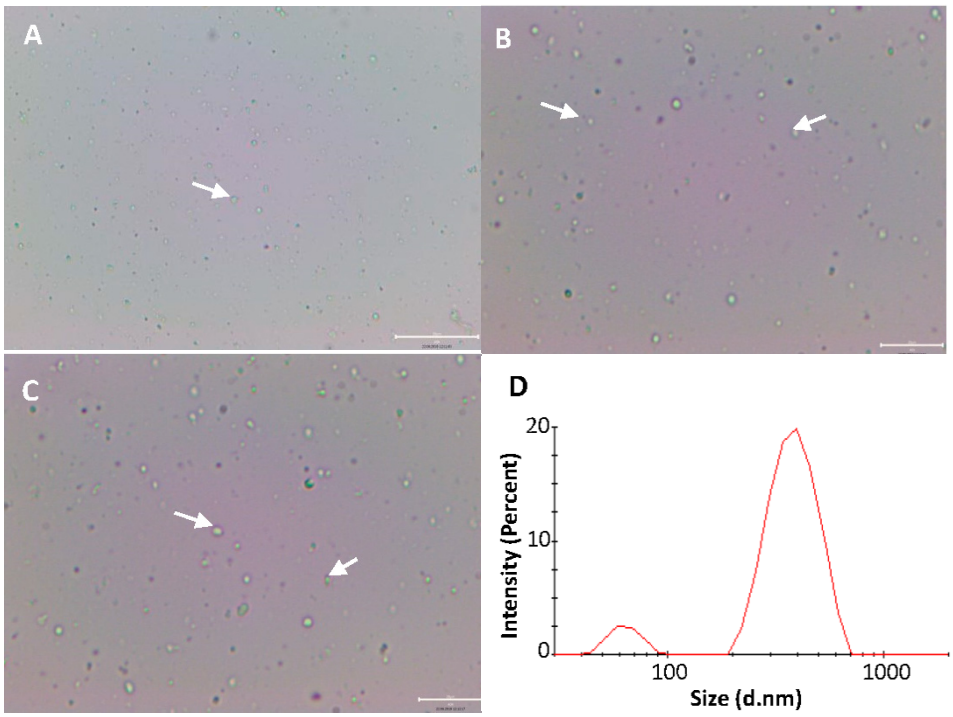

Figure 17. The optical microscopy images (**A**–**C**) and the PCS size and size distribution (**D**) of the self-assembled liposomes in purified water. The liposomes consisting of soybean PC and haemanthamine (HAE) are spontaneously dispersed from the electrospun amphiphilic nanofibrous template. Due to the limited magnification (50×) of an optical microscope, only the liposomes composed of large vesicles can be seen. Some selected clusters of liposomes are indicated by white arrows. Scale bar 20 µm with 20× (**A**), and 40× (**B**,**C**).

6.2.3. Particle size of self-assembled liposomes (V)

PCS was conducted to verify the molecular self-assembly process by analyzing the size and size distribution of the soybean PC and HAE containing liposomes. Due to their nanoscale size, optical microscopy was not possible to be applied for determining the vesicle size. As shown in Figure 17D, the liposomes were spherical in shape and presented a bi-modal size distribution with two distinct peaks at 63 ± 70 nm (10.3%) and 401 ± 64 nm (89.7%). The polydispersity index (PDI) was 0.474. This reveals that *in-situ* formation of liposomes occurred as expected. Yu and coworkers (2011) reported that the average vesicle size and PDI for the self-assembled liposomes ranged from 64 nm to 369 nm and from 0.182 to 0.299, respectively (Yu et al., 2011). They investigated the hydrodynamic diameter and size distribution of self-assembled liposomes by static and dynamic light scattering. The formation of active HAE-loaded self-assembled liposomes from the nanofiber-based solid templates is in

line with the results reported by Yu et al. (2011) on the corresponding non-active containing bulk liposomes.

6.2.4. Physical solid-state properties (V)

XRPD, FTIR spectroscopy and DSC were used to verify potential process-induced solid-state transformations and molecular interactions of HAE and carrier polymer in the ES of amphiphilic NFs. The XRPD pattern of HAE (as a pure material) presented numerous distinct crystalline reflections (Figure 18A). The characteristic XRPD peaks of HAE were shown at 12.2, 12.6, 13.8, 16.1, 17.6, 19.6, 20.2, 21.1, 22.6, 23.8 and 27.8°2θ. No reflection characteristics to crystalline nature, however, were revealed on the XRPD pattern for the HAE-loaded electrospun NFs. As shown in Figure 18A, two broad amorphous halos can be seen in the XRPD pattern of the amphiphilic NFs (most likely contributed by PVP), thus suggesting an amorphous solid-state structure of the present NFs. The solid-state transformation of HAE could be attributed to the enhanced rate of a solvent evaporation during the ES process that could prevent any recrystallization of the API (Laidmäe et al., 2021). It is also well known that the dissolution of a high-energetic amorphous form in water is better (improved) than that of a highly-ordered crystalline form of a corresponding compound. In our study, however, the small concentration of HAE in the NFs (approximately 4.5% *w*/*w*) made the final interpretation of the present XRPD results on the solid state of HAE in the NFs challenging. According to Yu et al. (2011), the electrospun amphiphilic bulk NFs of soybean PC and PVP were amorphous, but they also found that increasing the amount of PC in these NFs lead to the phase separation of PC from the PVP matrix template. Our results are in line with the findings reported by Yu et al. (2011), and support the molecular self-assemble strategy selected for the present nanoformulation of HAE (Yu et al., 2011; Nguyen et al., 2019).

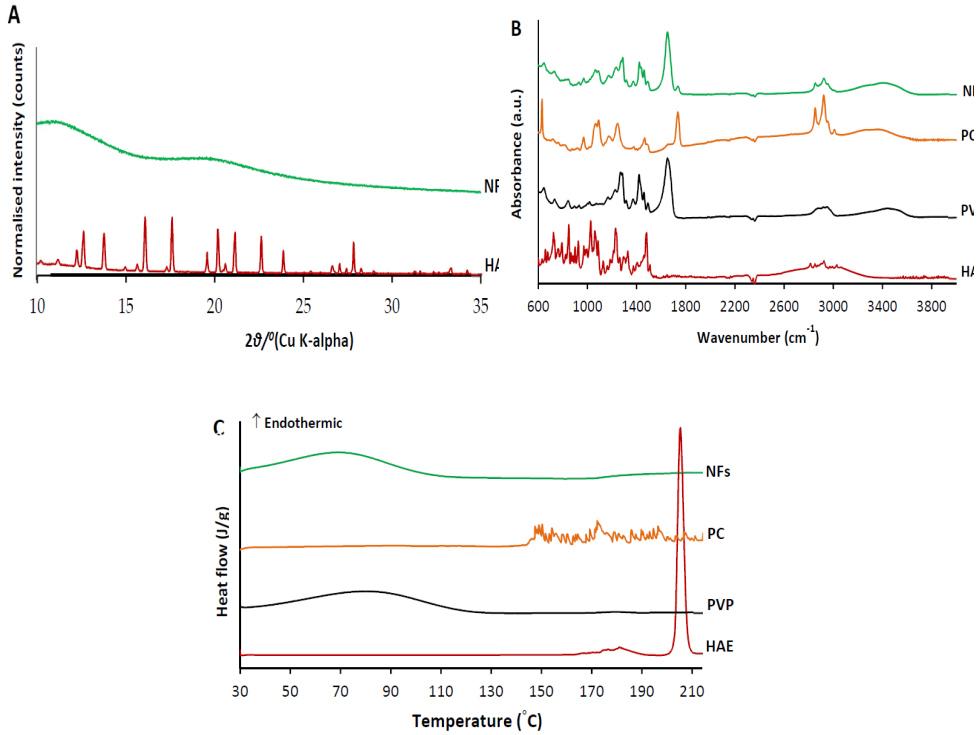

Figure 18. The XRPD patterns (**A**), FTIR spectra (**B**) and DSC thermographs (**C**) of haemanthamine (HAE) (as a powder form) and HAE-loaded amphiphilic electrospun NFs.

The FTIR spectra of electrospun amphiphilic NFs loaded with HAE and pure materials (HAE, PC, PVP in a powder form) are presented in Figure 18B. The distinct peaks in the region of C–H aromatic and aliphatic vibrations ranging from 3051 to 2810 cm^{-1} were detected in the FTIR spectrum of HAE (Figure 18B). The peaks of the N–H, C–N and C–O groups of HAE were shown at 1475, 1225 and 1053 cm^{-1}. The FTIR spectrum of soybean PC shows four bands with corresponding distinct peaks at 2945, 2916, 2847 and 1450 cm^{-1}. This finding is also in a good agreement with Yu et al. (2011), suggesting the presence of antisymmetric CH_3 stretching, antisymmetric CH_2, symmetric CH_2 and CH_2 scissoring, respectively. The characteristic band with a single peak at 961 cm^{-1} corresponds to the N^+ $(CH_3)_3$ stretching vibration (Figure 18B). The two distinct peaks at 1232 and 1056 cm^{-1} are in the region of the antisymmetric and symmetric PO_2^- stretching vibrations (Tantipolphan et al., 2007). The FTIR spectrum for PVP shows distinct peaks at 2900, 1643 and 1261 cm^{-1}, representing antisymmetric CH_3 stretching, C=O amide stretching and C–N stretching vibration, respectively (Figure 18B) (Nguyen et al., 2019). Compared to the spectra of pure materials, there

were only small changes in the FTIR spectra of the HAE-loaded amphiphilic NFs (Figure 18B). The FTIR spectrum for the HAE-loaded NFs exhibited the weak absorbance bands characteristics to HAE and excipients (soybean PC, PVP), thus suggesting the absence of molecular interaction between the three materials used in a solvent-based ES. However, the distinction of the characteristic peaks of the active agent was challengeable due to the low drug loading in the NFs.

The DSC thermographs of HAE-loaded amphiphilic electrospun NFs and pure materials as a powder form are presented in Figure 18C. As shown in the DSC thermograms, a broad endotherm from 50 °C to 120 °C (due to dehydration) and multiple small endothermal events (peaks) ranging from 140 °C to 210 °C were observed for PVP K90 and soybean PC, respectively. The presence of unsaturated bonds and the heat-induced movement of polar moieties leading to a phase transition from a gel state to a liquid crystal state were recorded by these multiple fluctuating endothermal peaks for PC (Koynova & Caffrey, 1998; Maiti et al., 2007). A single sharp melting endotherm at 205.4 °C was displayed in the DSC thermogram of HAE. This is also in agreement with the characteristic melting point of HAE (206 °C) reported in the literature (*Haemanthamine – Antineoplastic Agents*, n.d.; retrieved May 30, 2022, from https://pharmacycode.com/Haemanthamine.html). In the DSC thermogram of HAE-loaded amphiphilic NFs, however, the characteristic peak for the melting point of HAE was not observed after the broad endothermal event of PVP ranging from 40 °C to 110 °C (Figure 18C). Therefore, this finding suggests that HAE is most likely in an amorphous form in the NFs. It is complicated, however, to fully validate the state of HAE in the NFs, since HAE could be dissolved in the melt of the excipients due to PVP and PC melting at lower temperatures. In addition, there are no signs of chemical decomposition of HAE as well as significant interactions or incompatibilities between HAE and excipients. However, more research work is needed on the storage stability of the present nanoformulations.

6.2.5. *In-vitro* drug release (V)

The *in-vitro* dissolution of HAE as a powder form and loaded in the amphiphilic electrospun NFs were investigated using an in-house dialysis method. HAE is poorly soluble in water which limits the use of it as a therapeutic drug substance. As shown in Figure 19, approximately 50% of HAE (as a powder form) was dissolved within the first 2 h and over 80% of HAE was dissolved within the next 16 h (after 18 h the dissolution reached the plateau).

The theoretical amount of HAE in the solid NFs sample applied in the dissolution test was 0.89 mg (respective to 100% in the dissolution study). Figure 19 shows the three distinct phases in the release of HAE from the amphiphilic electrospun NFs and self-assembled liposomes. Within the first 2-hour phase, more than half of the content of HAE was released, and in the subsequent 2-hour phase approximately 80% of HAE was released from the

NFs. The initial burst release was, most likely, owing to the physical solid state of HAE in the nanofibrous templates and the surface or near-surface distribution of HAE in the NFs. In the last phase, the release of HAE was completed within 30 hours. A steady-state release pattern in the third phase could be attributed to the drug release from the self-assembled liposomes. Our previous XRPD findings indicated the presence of amorphous HAE in the electrospun NFs, thus suggesting enhanced dissolution of HAE, and supporting the present amphiphilic nanofiber-based strategy selected.

According to Yu et al. (2011), hydrophobic repulsion from the solvent is the primary reason for the phenomen where the hydrated PC molecules are concentrated within the framework of the swelling NFs as the amphiphilic NFs are exposed to water. As hydrated PC molecules form co-aggregates, the self-assembled liposomes are generated with entrapping water within them. In the final stage, the self-assembled liposomes are released in the dissolution medium (Yu et al., 2011). Thus, it was of interest to compare the dissolution properties of HAE and the present amphiphilic nanofibrous templates loaded with the active agent. Accounting for this rationale, our dissolution study was investigated (as shown in Figure 19). The *in-vitro* drug release of HAE from the present amphiphilic NFs and liposomes exhibited the initial burst release, and approximately 80% of HAE released within the first four hours. Yet, to reach an understanding of the self-assembly of liposomes in the aqueous media and actual release of the active agent from the formed liposomes, more research is needed (Nguyen et al., 2019).

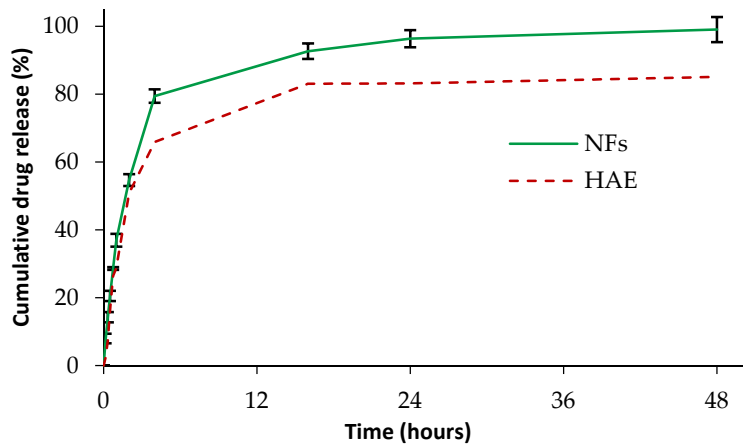

Figure 19. The *in vitro* dissolution profiles of haemanthamine (HAE) (as a powder form; a dotted red curve) and HAE-loaded amphiphilic electrospun NFs (a continuous green curve) (n = 3).

7. SUMMARY AND CONCLUSIONS

In summary, the present study provides new knowledge on phytochemical constituents and bioactivity of *C. paniculatus*, *A. tonkinensis* and *Z. ajax* known in traditional medicine of Vietnam. Special attention was paid on HAE which was discovered and obtained from *Z. ajax*, and subsequently used as a plant-origin API for formulating amphiphilic NFs and liposomes as a novel nanotechnology-based DDSs. Following detailed conclusions can be drawn:

1. From the selected medicinal plants, total twenty two compounds were isolated and characterized, including seven new compounds. Six of them include six new *chiro*-inositol derivatives from the leaves of *C. paniculatus* (4,5-di-*O*-5-hydroxytigloyl-1-*O*-2-methylbutyroyl-3-*O*-tigloyl-*chiro*-inositol; 4,5-di-*O*-5-hydroxytigloyl-3-*O*-2-methyl-butyroyl-1-*O*-tigloyl-*chiro*-inositol; 4,5-di-*O*-5-hydroxytigloyl-1,3-di-*O*-2-methylbutyroyl-*chiro*-inositol; 3,5-di-*O*-5-hydroxy-tigloyl-2-*O*-2-methylbutyroyl-6-*O*-tigloyl-*chiro*-inositol; 3,5-di-*O*-5-hydroxytigloyl-2,6-di-*O*-2-methylbutyroyl-*chiro*-inositol; 4,5-di-*O*-5-hydroxy-tigloyl-3,6-di-*O*-tigloyl-*chiro*-inositol), one new flavanol derivative from the rhizomes of *Z. ajax* [(2*R*,3*R*)-3-acetoxy-7-hydroxy-3′,4′-methylenedioxyflavan], and fifteen known compounds (seven compounds from *Z. ajax*: 7-hydroxyflavan, 7,4′-dihydroxyflavan, 7,4′-dihydroxy-8-methylflavan, 7,3′-dihydroxy-4′-methoxyflavan, 5,4′-dihydroxy-7-methoxy-6-methylflavan, 7-hydroxy-3′,4′-methylenedioxyflavanone and HAE, and eight compounds from *A. tonkinensis*: liriodenine, *N*-*trans*-feruloyltyramin, corydaldine, 8-oxopseudopalmatine, 3-hydroxy-7,8-dehydro-*β*-ionone, pseudopalmatine, pseudocolumbamine, and stigmasterol). All known compounds were the first phytochemical investigation of these species.
2. Regarding bioactivities, compound 3,5-di-*O*-5-hydroxytigloyl-2-*O*-2-methylbutyroyl-6-*O*-tigloyl-*chiro*-inositol (from *C. paniculatus*) and 3-hydroxy-7,8-dehydro-*β*-ionone (from *A. tonkinensis*) showed a potent inhibitory activity for NO production. Total MeOH extract, MeOH portion (extracted from CH_2Cl_2 extract), pseudocolumbamine and pseudopalmatine (from *A. tonkinensis*) revealed a potential anti-AChE activity. Compound HAE (from *Z. ajax*) exhibited potent cytotoxic activity against the HepG2, the SK-LU-1, the KB, the SW480 and the AGS cell line.
3. Electrospun HAE-loaded amphiphilic nanofibers intended for a solid template for self-assembled liposomes were successfully prepared. PVP is an appropriate carrier polymer in generating electrospun polymeric NFs loaded with HAE (a crinine-type alkaloid of plant origin). The ratio of 1:2 (w/w) for PC and PVP enables to formulate desired amphiphilic NFs intended for a stabilizing platform (template) of self-assembled liposomes of HAE. The preparation of NFs with suitable materials and ES parameters plays a fundamental role in ES such DDS. The amphiphilic NFs loaded with plant-origin API was reported for the first time.

4. The nanofibrous solid templates showed a non-woven and loosely packed platform with a nanoscale size ranging from 197 nm to 534 nm. The *in-vitro* drug release of HAE from the amphiphilic NFs and liposomes showed the initial burst release, and approximately 80% of HAE released within the first four hours. An improved dissolution of poorly water-soluble HAE suggests that the present amphiphilic nanofiber-based strategy for delivering self-assembled liposomes is applicable for such plant-origin alkaloids. The performance of the present DDS was verified by spontaneously forming (self-assembled) liposomes in water within a few seconds.

REFERENCES

Abu-Diak, O. A., Andrews, G. P., & Jones, D. S. (2012). Hydrophobic Polymers of Pharmaceutical Significance. In J. Siepmann, R. A. Siegel, & M. J. Rathbone (Eds.), *Fundamentals and Applications of Controlled Release Drug Delivery* (pp. 47–73). Springer US. https://doi.org/10.1007/9781-4614-0881-9_3

Acevedo, F., Hermosilla, J., Sanhueza, C., Mora-Lagos, B., Fuentes, I., Rubilar, M., Concheiro, A., & Alvarez-Lorenzo, C. (2018). Gallic acid loaded PEO-core/zein-shell nanofibers for chemopreventive action on gallbladder cancer cells. *European Journal of Pharmaceutical Sciences*, *119*, 49–61. https://doi.org/10.1016/j.ejps.2018.04.009

Acosta, J., Wang, W., & Feldser, D. M. (2018). Off and back-on again: A tumor suppressor's tale. *Oncogene*, *37*(23), 3058–3069. https://doi.org/10.1038/s41388-018-0186-3

Agarwal, S., Wendorff, J. H., & Greiner, A. (2009). Progress in the Field of Electrospinning for Tissue Engineering Applications. *Advanced Materials*, *21*(32–33), 3343–3351. https://doi.org/10.1002/adma.200803092

Ali, R., Rahim, A., & Islam, A. (2017). Synthesis and Antimicrobial Activity of 7-Hydroxy-3',4'-Methylenedioxy- and 7-Benzyloxy-3',4'-Methylenedioxy Flavanones. *Journal of Scientific Research*, *9*(3), 297–306. https://doi.org/10.3329/jsr.v9i3.31229

Alves, R. R., & Rosa, I. M. (2007). Biodiversity, traditional medicine and public health: Where do they meet? *Journal of Ethnobiology and Ethnomedicine*, *3*, 14. https://doi.org/10.1186/1746-4269-3-14

Ansari, S. H., Islam, F., & Sameem, Mohd. (2012). Influence of nanotechnology on herbal drugs: A Review. *Journal of Advanced Pharmaceutical Technology & Research*, *3*(3), 142–146. https://doi.org/10.4103/2231-4040.101006

Aragues, R., Sander, C., & Oliva, B. (2008). Predicting cancer involvement of genes from heterogeneous data. *BMC Bioinformatics*, *9*(1), 172. https://doi.org/10.1186/1471-2105-9-172

Atan, M. S., Dzulkefly, K. A., Aspollah, S. M., Anuar, K., & Vijay, S. (2011). Isolation and antibacterial activity of alkaloids from *Phaeanthus opthalmicus*. *Asian Journal of Chemistry*, *23*(9), 3824–3826.

Atanasov, A. G., Waltenberger, B., Pferschy-Wenzig, E.-M., Linder, T., Wawrosch, C., Uhrin, P., Temml, V., Wang, L., Schwaiger, S., Heiss, E. H., Rollinger, J. M., Schuster, D., Breuss, J. M., Bochkov, V., Mihovilovic, M. D., Kopp, B., Bauer, R., Dirsch, V. M., & Stuppner, H. (2015). Discovery and resupply of pharmacologically active plant-derived natural products: A review. *Biotechnology Advances*, *33*(8), 1582–1614. https://doi.org/10.1016/j.biotechadv.2015.08.001

Atanasov, A. G., Zotchev, S. B., Dirsch, V. M., & Supuran, C. T. (2021). Natural products in drug discovery: Advances and opportunities. *Nature Reviews Drug Discovery*, *20*(3), 200–216. https://doi.org/10.1038/s41573-020-00114-z

Bakri, Y. M., Talip, M. A., & Azziz, S. S. S. A. (2017). A Mini Review on *Alphonsea* sp. (Annonaceae): Traditional uses, Biological Activities and Phytochemistry. –. *Journal of Applied Pharmaceutical Science*, *7*(10), 200–203.

Baliyan, S., Mukherjee, R., Priyadarshini, A., Vibhuti, A., Gupta, A., Pandey, R. P., & Chang, C.-M. (2022). Determination of Antioxidants by DPPH Radical Scavenging Activity and Quantitative Phytochemical Analysis of *Ficus religiosa*. *Molecules*, *27*(4), 1326. https://doi.org/10.3390/molecules27041326

Bastida, J., Viladomat, F., Llabres, J. M., Codina, C., Feliz, M., & Rubiralta, M. (1987). Alkaloids from *Narcissus confusus*. *Phytochemistry*, *26*(5), 1519–1524. https://doi.org/10.1016/S0031-9422(00)81849-X

Begum, R., Farooqi, Z. H., Naseem, K., Ali, F., Batool, M., Xiao, J., & Irfan, A. (2018). Applications of UV/Vis Spectroscopy in Characterization and Catalytic Activity of Noble Metal Nanoparticles Fabricated in Responsive Polymer Microgels: A Review. *Critical Reviews in Analytical Chemistry*, *48*(6), 503–516. https://doi.org/10.1080/10408347.2018.1451299

Bhatia, S. (2016). Natural Polymers vs Synthetic Polymer. In S. Bhatia (Ed.), *Natural Polymer Drug Delivery Systems: Nanoparticles, Plants, and Algae* (pp. 95–118). Springer International Publishing. https://doi.org/10.1007/978-3-319-41129-3_3

Bhattacharyya, N. K., & Kataky, J. (2014). *Isolation of Meliacins from Chisocheton Paniculatus Hiern, their Chemical Transformations to New Limonoids and Screening for Antifungal Activity*. 12.

Bhattarai, R. S., Bachu, R. D., Boddu, S. H. S., & Bhaduri, S. (2019). Biomedical Applications of Electrospun Nanofibers: Drug and Nanoparticle Delivery. *Pharmaceutics*, *11*(1), 5. https://doi.org/10.3390/pharmaceutics11010005

Bohno, M., Sugie, K., Imase, H., Yusof, Y. B., Oishi, T., & Chida, N. (2007). Total synthesis of Amaryllidaceae alkaloids, (+)-vittatine and (+)-haemanthamine, starting from d-glucose. *Tetrahedron*, *63*(30), 6977–6989. https://doi.org/10.1016/j.tet.2007.05.041

Bonifácio, B. V., da Silva, P. B., Ramos, M. A. dos S., Negri, K. M. S., Bauab, T. M., & Chorilli, M. (2013). Nanotechnology-based drug delivery systems and herbal medicines: A review. *International Journal of Nanomedicine*, *9*, 1–15. https://doi.org/10.2147/IJN.S52634

Bordoloi, M., Saikia, B., Mathur, R. K., & Goswami, B. N. (1993). A meliacin from *Chisocheton paniculatus*. *Phytochemistry*, *34*(2), 583–584. https://doi.org/10.1016/0031-9422(93)80054-V

Braghirolli, D. I., Steffens, D., & Pranke, P. (2014). Electrospinning for regenerative medicine: A review of the main topics. *Drug Discovery Today*, *19*(6), 743–753. https://doi.org/10.1016/j.drudis.2014.03.024

Briggs, R., Kennelly, S. P., & O'Neill, D. (2016). Drug treatments in Alzheimer's disease. *Clinical Medicine*, *16*(3), 247–253. https://doi.org/10.7861/clinmedicine.16-3-247

Bucar, F., Wube, A., & Schmid, M. (2013). Natural product isolation – how to get from biological material to pure compounds. *Natural Product Reports*, *30*(4), 525–545. https://doi.org/10.1039/C3NP20106F

Buxani, N., Mehta, D., Gupta, M., & Mehta, B. (2014). Natural Products: Source of Potential Drugs. *African Journal of Basic & Applied Sciences*, *6*. https://doi.org/10.5829/idosi.ajbas.2014.6.6.21983

Campiglio, C. E., Contessi Negrini, N., Farè, S., & Draghi, L. (2019). Cross-Linking Strategies for Electrospun Gelatin Scaffolds. *Materials (Basel, Switzerland)*, *12*(15), E2476. https://doi.org/10.3390/ma12152476

Chakraborty, S., Liao, I.-C., Adler, A., & Leong, K. W. (2009). Electrohydrodynamics: A facile technique to fabricate drug delivery systems. *Advanced Drug Delivery Reviews*, *61*(12), 1043–1054. https://doi.org/10.1016/j.addr.2009.07.013

Chatterjee, A., Nayak, L., Das, B., Patra, A., Dhara, K. P., Mukherjee, K., & Banerji, J. (1989). Chemistry of phyto constituents of *chisocheton paniculatus* hiern meliaceae.

Indian Journal of Chemistry Section B Organic Chemistry Including Medicinal Chemistry, *28*(3), 231–236.

Chauhan, A. (2014). Powder XRD Technique and its Applications in Science and Technology. *Journal of Analytical & Bioanalytical Techniques*, *5*(6). https://doi.org/10.4172/2155-9872.1000212

Clardy, J., & Walsh, C. (2004). Lessons from natural molecules. *Nature*, *432*(7019), 829–837. https://doi.org/10.1038/nature03194

Connolly, J. D., Labbé, C., Rycroft, D. S., & Taylor, D. A. H. (1979). Tetranortriterpenoids and related compounds. Part 22. New apotirucailol derivatives and tetranortriterpenoids from the wood and seeds of *chisocheton paniculatus* (meliaceae). *Journal of the Chemical Society, Perkin Transactions 1*, *0*, 2959–2964. https://doi.org/10.1039/P19790002959

Cordell, G. A. (2011a). Sustainable Medicines and Global Health Care. *Planta Medica*, *77*(11), 1129–1138. https://doi.org/10.1055/s-0030-1270731

Cordell, G. A. (2011b). Phytochemistry and traditional medicine – A revolution in process. *Phytochemistry Letters*, *4*(4), 391–398. https://doi.org/10.1016/j.phytol.2011.05.005

Costa, E. V., Pinheiro, M. L. B., Barison, A., Campos, F. R., Salvador, M. J., Maia, B. H. L. N. S., Cabral, E. C., & Eberlin, M. N. (2010). Alkaloids from the Bark of *Guatteria hispida* and Their Evaluation as Antioxidant and Antimicrobial Agents. *Journal of Natural Products*, *73*(6), 1180–1183. https://doi.org/10.1021/np100013r

Cragg, G. M., & Newman, D. J. (2013). Natural products: A continuing source of novel drug leads. *Biochimica et Biophysica Acta (BBA) – General Subjects*, *1830*(6), 3670–3695. https://doi.org/10.1016/j.bbagen.2013.02.008

Cragg, G. M., Schepartz, S. A., Suffness, M., & Grever, M. R. (1993). The Taxol Supply Crisis. New NCI Policies for Handling the Large-Scale Production of Novel Natural Product Anticancer and Anti-HIV Agents. *Journal of Natural Products*, *56*(10), 1657–1668. https://doi.org/10.1021/np50100a001

Danaei, M., Dehghankhold, M., Ataei, S., Hasanzadeh Davarani, F., Javanmard, R., Dokhani, A., Khorasani, S., & Mozafari, M. R. (2018). Impact of Particle Size and Polydispersity Index on the Clinical Applications of Lipidic Nanocarrier Systems. *Pharmaceutics*, *10*(2), 57. https://doi.org/10.3390/pharmaceutics10020057

David, B., Wolfender, J.-L., & Dias, D. A. (2015). The pharmaceutical industry and natural products: Historical status and new trends. *Phytochemistry Reviews*, *14*(2), 299–315. https://doi.org/10.1007/s11101-014-9367-z

de Oliveira Júnior, R. G., Christiane Adrielly, A. F., da Silva Almeida, J. R. G., Grougnet, R., Thiéry, V., & Picot, L. (2018). Sensitization of tumor cells to chemotherapy by natural products: A systematic review of preclinical data and molecular mechanisms. *Fitoterapia*, *129*, 383–400. https://doi.org/10.1016/j.fitote.2018.02.025

de Torre, M. P., Cavero, R. Y., Calvo, M. I., & Vizmanos, J. L. (2019). A Simple and a Reliable Method to Quantify Antioxidant Activity In Vivo. *Antioxidants*, *8*(5), 142. https://doi.org/10.3390/antiox8050142

Dehelean, C. A., Marcovici, I., Soica, C., Mioc, M., Coricovac, D., Iurciuc, S., Cretu, O. M., & Pinzaru, I. (2021). Plant-Derived Anticancer Compounds as New Perspectives in Drug Discovery and Alternative Therapy. *Molecules*, *26*(4), 1109. https://doi.org/10.3390/molecules26041109

Ding, Y., Qu, D., Zhang, K.-M., Cang, X.-X., Kou, Z.-N., Xiao, W., & Zhu, J.-B. (2017). Phytochemical and biological investigations of Amaryllidaceae alkaloids: A

review. *Journal of Asian Natural Products Research*, *19*(1), 53–100. https://doi.org/10.1080/10286020.2016.1198332

Efferth, T., Davey, M., Olbrich, A., Rücker, G., Gebhart, E., & Davey, R. (2002). Activity of Drugs from Traditional Chinese Medicine toward Sensitive and MDR1- or MRP1-Overexpressing Multidrug-Resistant Human CCRF-CEM Leukemia Cells. *Blood Cells, Molecules, and Diseases*, *28*(2), 160–168. https://doi.org/10.1006/bcmd.2002.0492

Egbuna, C., Ifemeje, J., Kryeziu, T., Mukherjee, M., Shah, H., Narasimha Rao, G., Gido, L., & Tijjani, H. (2018). *INTRODUCTION TO PHYTOCHEMISTRY* (pp. 1–29). https://doi.org/10.13140/RG.2.2.18812.23687

El-Aassar, M. R., Ibrahim, O. M., & Al-Oanzi, Z. H. (2021). Biotechnological Applications of Polymeric Nanofiber Platforms Loaded with Diverse Bioactive Materials. *Polymers*, *13*(21), 3734. https://doi.org/10.3390/polym13213734

Elashnikov, R., Slepička, P., Rimpelova, S., Ulbrich, P., Švorčík, V., & Lyutakov, O. (2017). Temperature-responsive PLLA/PNIPAM nanofibers for switchable release. *Materials Science and Engineering: C*, *72*, 293–300. https://doi.org/10.1016/j.msec.2016.11.028

Elyashberg, M. (2015). Identification and structure elucidation by NMR spectroscopy. *TrAC Trends in Analytical Chemistry*, *69*, 88–97. https://doi.org/10.1016/j.trac.2015.02.014

Ertas, Y. N., Abedi Dorcheh, K., Akbari, A., & Jabbari, E. (2021). Nanoparticles for Targeted Drug Delivery to Cancer Stem Cells: A Review of Recent Advances. *Nanomaterials*, *11*(7), 1755. https://doi.org/10.3390/nano11071755

Fadil, F., Affandi, N. D. N., Misnon, M. I., Bonnia, N. N., Harun, A. M., & Alam, M. K. (2021). Review on Electrospun Nanofiber-Applied Products. *Polymers*, *13*(13), 2087. https://doi.org/10.3390/polym13132087

Falzon, C. C., & Balabanova, A. (2017). Phytotherapy: An Introduction to Herbal Medicine. *Primary Care: Clinics in Office Practice*, *44*(2), 217–227. https://doi.org/10.1016/j.pop.2017.02.001

Farooq, S., Mehmood, Z., Qais, F. A., Khan, M. S., & Ahmad, I. (2019). Chapter 22 – Nanoparticles in Ayurvedic Medicine: Potential and Prospects. In M. S. Ahmad Khan, I. Ahmad, & D. Chattopadhyay (Eds.), *New Look to Phytomedicine* (pp. 581–596). Academic Press. https://doi.org/10.1016/B978-0-12-814619-4.00023-9

Forgo, P., & Kövér, K. E. (2004). Gradient enhanced selective experiments in the 1H NMR chemical shift assignment of the skeleton and side-chain resonances of stigmasterol, a phytosterol derivative. *Steroids*, *69*(1), 43–50. https://doi.org/10.1016/j.steroids.2003.09.012

Forner, A., Llovet, J. M., & Bruix, J. (2012). Hepatocellular carcinoma. *The Lancet*, *379*(9822), 1245–1255. https://doi.org/10.1016/S0140-6736(11)61347-0

Fortuna, A. M., Juárez, Z. N., Bach, H., Nematallah, A., Av-Gay, Y., Sánchez-Arreola, E., Catalán, C. A. N., Turbay, S., & Hernández, L. R. (2011). Antimicrobial activities of sesquiterpene lactones and inositol derivatives from *Hymenoxys robusta*. *Phytochemistry*, *72*(18), 2413–2418. https://doi.org/10.1016/j.phytochem.2011.09.001

Fu, Y., & Kao, W. J. (2010). Drug release kinetics and transport mechanisms of non-degradable and degradable polymeric delivery systems. *Expert Opinion on Drug Delivery*, *7*(4), 429–444. https://doi.org/10.1517/17425241003602259

Garg, A., Garg, S., Kumar, M., Kumar, S., Shukla, A. K., & Kaushik, S. P. C. (2018). Applications of natural polymers in mucoadhesive drug delivery: An overview. *Advance Pharmaceutical Journal*, *3*(2), 38–42. https://doi.org/10.31024/apj.2018.3.2.1

Geetha, R. G., & Ramachandran, S. (2021). Recent Advances in the Anti-Inflammatory Activity of Plant-Derived Alkaloid Rhynchophylline in Neurological and Cardiovascular Diseases. *Pharmaceutics*, *13*(8), 1170. https://doi.org/10.3390/pharmaceutics13081170

Greenwell, M., & Rahman, P. K. S. M. (2015). Medicinal Plants: Their Use in Anti-cancer Treatment. *International Journal of Pharmaceutical Sciences and Research*, *6*(10), 4103–4112. https://doi.org/10.13040/IJPSR.0975-8232.6(10).4103-12

Gunasekaran, T., Haile, T., Nigusse, T., & Dhanaraju, M. D. (2014). Nanotechnology: An effective tool for enhancing bioavailability and bioactivity of phytomedicine. *Asian Pacific Journal of Tropical Biomedicine*, *4*, S1–S7. https://doi.org/10.12980/APJTB.4.2014C980

Haemanthamine – Antineoplastic Agents. (n.d.). Retrieved May 30, 2022, from https://pharmacycode.com/Haemanthamine.html

Havelek, R., Muthna, D., Tomsik, P., Kralovec, K., Seifrtova, M., Cahlikova, L., Hostalkova, A., Safratova, M., Perwein, M., Cermakova, E., & Rezacova, M. (2017). Anticancer potential of Amaryllidaceae alkaloids evaluated by screening with a panel of human cells, real-time cellular analysis and Ehrlich tumor-bearing mice. *Chemico-Biological Interactions*, *275*, 121–132. https://doi.org/10.1016/j.cbi.2017.07.018

Havelek, R., Seifrtova, M., Kralovec, K., Bruckova, L., Cahlikova, L., Dalecka, M., Vavrova, J., Rezacova, M., Opletal, L., & Bilkova, Z. (2014). The effect of Amaryllidaceae alkaloids haemanthamine and haemanthidine on cell cycle progression and apoptosis in p53-negative human leukemic Jurkat cells. *Phytomedicine*, *21*(4), 479–490. https://doi.org/10.1016/j.phymed.2013.09.005

Ho, P. H. (2003). An Illustrated Flora of Vietnam. *Youth Publishing House*, *Ho Chi Minh City, Vietnam,* Vol. 3, 496-503.

Hoai, N. T., Duc, H. V., Raal, A., & Morita, H. (2018). A New Limonoid from *Chisocheton paniculatus* Fruit Collected in Vietnam and Its NO Production Inhibitory Activity. *Natural Product Communications*, *13*(10), 1934578X1801301005. ttps://doi.org/10.1177/1934578X1801301005

Hu, X., Liu, S., Zhou, G., Huang, Y., Xie, Z., & Jing, X. (2014). Electrospinning of polymeric nanofibers for drug delivery applications. *Journal of Controlled Release*, *185*, 12–21. https://doi.org/10.1016/j.jconrel.2014.04.018

Ioset, J.-R., Marston, A., Gupta, M. P., & Hostettmann, K. (2001). A methylflavan with free radical scavenging properties from *Pancratium littorale*. *Fitoterapia*, *72*(1), 35–39. https://doi.org/10.1016/S0367-326X(00)00250-1

Jitsuno, M., Yokosuka, A., Sakagami, H., & Mimaki, Y. (2009). Chemical Constituents of the Bulbs of *Habranthus brachyandrus* and Their Cytotoxic Activities. *Chemical and Pharmaceutical Bulletin*, *57*(10), 1153–1157. https://doi.org/10.1248/cpb.57.1153

Kai, D., Liow, S. S., & Loh, X. J. (2014). Biodegradable polymers for electrospinning: Towards biomedical applications. *Materials Science and Engineering: C*, *45*, 659–670. https://doi.org/10.1016/j.msec.2014.04.051

Kajdič, S., Planinšek, O., Gašperlin, M., & Kocbek, P. (2019). Electrospun nanofibers for customized drug-delivery systems. *Journal of Drug Delivery Science and Technology*, *51*, 672–681. https://doi.org/10.1016/j.jddst.2019.03.038

Kalaydina, R.-V., Bajwa, K., Qorri, B., Decarlo, A., & Szewczuk, M. R. (2018). Recent advances in "smart" delivery systems for extended drug release in

cancer therapy. *International Journal of Nanomedicine*, *13*, 4727–4745. https://doi.org/10.2147/IJN.S168053

Kanada, R. M., Simionato, J. I., Arruda, R. F. de, Santin, S. M. de O., Souza, M. C. de, & Silva, C. C. da. (2012). N-trans-feruloyltyramine and flavonol glycosides from the leaves of *Solanum sordidum*. *Revista Brasileira de Farmacognosia*, *22*(3), 502–506. https://doi.org/10.1590/S0102-695X2012005000029

Katoch D, & Singh B. (2015). Phytochemistry and Pharmacology of Genus *Zephyranthes*. *Medicinal & Aromatic Plants*, *04*(04). https://doi.org/10.4172/2167-0412.1000212

Kempski, H., Austin, N., Roe, A., Chatters, S., & Jayasinghe, S. N. (2008). Pilot study to investigate the possibility of cytogenetic and physiological changes in bio-electrosprayed human lymphocyte cells. *Regenerative Medicine*, *3*(3), 343–349. https://doi.org/10.2217/17460751.3.3.343

Keshvardoostchokami, M., Majidi, S. S., Huo, P., Ramachandran, R., Chen, M., & Liu, B. (2021). Electrospun Nanofibers of Natural and Synthetic Polymers as Artificial Extracellular Matrix for Tissue Engineering. *Nanomaterials*, *11*(1), 21. https://doi.org/10.3390/nano11010021

Khan, H., Ullah, H., Aschner, M., Cheang, W. S. & Akkol, E. K. (2019). Neuroprotective Effects of Quercetin in Alzheimer's Disease. *Biomolecules*, *10*(1). https://doi.org/10.3390/biom10010059

Khan, S., Barve, K. H., & Kumar, M. S. (2020). Recent Advancements in Pathogenesis, Diagnostics and Treatment of Alzheimer's Disease. *Current Neuropharmacology*, *18*(11), 1106–1125. https://doi.org/10.2174/1570159X18666200528142429

Koehn, F. E., & Carter, G. T. (2005). The evolving role of natural products in drug discovery. *Nature Reviews Drug Discovery*, *4*(3), 206–220. https://doi.org/10.1038/nrd1657

Kogermann, K., Penkina, A., Predbannikova, K., Jeeger, K., Veski, P., Rantanen, J., & Naelapää, K. (2013). Dissolution testing of amorphous solid dispersions. *International Journal of Pharmaceutics*, *444*(1), 40–46. https://doi.org/10.1016/j.ijpharm.2013.01.042

Kong, L. Y. (2010). Chemical Constituents Study on Three Species of Medicinal Plants. *Planta Medica*, *76*(5), S43. https://doi.org/10.1055/s-0030-1251758

Konrath, E. L., Passos, C. dos S., Klein, L. C., & Henriques, A. T. (2013). Alkaloids as a source of potential anticholinesterase inhibitors for the treatment of Alzheimer's disease. *The Journal of Pharmacy and Pharmacology*, *65*(12), 1701–1725. https://doi.org/10.1111/jphp.12090

Koynova, R., & Caffrey, M. (1998). Phases and phase transitions of the phosphatidylcholines. *Biochimica et Biophysica Acta (BBA) – Reviews on Biomembranes*, *1376*(1), 91–145. https://doi.org/10.1016/S0304-4157(98)00006-9

Kristanti, A. N., Aminah, N. S., & Tanjung, M. (2015). Phenolic compounds from the stem bark of *Saccopetalumhors fiedii* Benn. *Der Pharmacia Letrtre*, *7*(3), 149–152.

Kuang, G., Zhang, Z., Liu, S., Zhou, D., Lu, X., Jing, X., & Huang, Y. (2018). Biphasic drug release from electrospun polyblend nanofibers for optimized local cancer treatment. *Biomaterials Science*, *6*(2), 324–331. https://doi.org/10.1039/C7BM01018D

Lachance, H., Wetzel, S., Kumar, K., & Waldmann, H. (2012). Charting, Navigating, and Populating Natural Product Chemical Space for Drug Discovery. *Journal of Medicinal Chemistry*, *55*(13), 5989–6001. https://doi.org/10.1021/jm300288g

Laidmäe, I., Meos, A., Kjærvik, I. A., Ingebrigtsen, S. G., Škalko-Basnet, N., Kirsimäe, K., Romann, T., Joost, U., Kisand, V., & Kogermann, K. (2021). Electrospun

Amphiphilic Nanofibers as Templates for In Situ Preparation of Chloramphenicol-Loaded Liposomes. *Pharmaceutics*, *13*(11), 1742. https://doi.org/10.3390/pharmaceutics13111742

Le, T. B. H., Nguyen, T. T. H., Tran, T. T., & Nguyen, T. H. (2018). Screening of acetylcholinesterase inhibitory activity of some medicinal herbs in Central Vietnam. *Journal of Medicinal Materials*, *507*, 20–25.

Leite, P. M., Camargos, L. M., & Castilho, R. O. (2021). Recent progess in phytotherapy: A Brazilian perspective. *European Journal of Integrative Medicine*, *41*, 101270. https://doi.org/10.1016/j.eujim.2020.101270

Li, D. L., Li, X.-M., Peng, Z.-Y., & Wang, B.-G. (2007). Flavanol Derivatives from *Rhizophora stylosa* and Their DPPH Radical Scavenging Activity. *Molecules*, *12*(5), 1163–1169. https://doi.org/10.3390/12051163

Li, W. J., Cheng, X. L., Liu, J., Lin, R. C., Wang, G. L., Du, S. S., & Liu, Z. L. (2012). Phenolic Compounds and Antioxidant Activities of *Liriope muscari*. *Molecules*, *17*(2), 1797–1808. https://doi.org/10.3390/molecules17021797

Li, Z., & Wang, C. (2013). Effects of Working Parameters on Electrospinning. In Z. Li & C. Wang (Eds.), *One-Dimensional nanostructures: Electrospinning Technique and Unique Nanofibers* (pp. 15–28). Springer. https://doi.org/10.1007/978-3-642-36427-3_2

López, S., Bastida, J., Viladomat, F., & Codina, C. (2002). Solid-phase extraction and reversed-phase high-performance liquid chromatography of the five major alkaloids in *Narcissus confusus*. *Phytochemical Analysis*, *13*(6), 311–315. https://doi.org/10.1002/pca.660

Magalhães, V., Rios, R. M., Silva, F. G. C. P., & Dias, A. C. P. (2020). Comparative Study on the Inhibition of Acetylcholinesterase Activity by *Hyptis marrubioides*, *Hyptis pectinata*, and *Hyptis suaveolens* Methanolic Extracts. *Proceedings*, *70*(1), 81. https://doi.org/10.3390/foods_2020-07628

Maghsoudi, S., Taghavi Shahraki, B., Rabiee, N., Fatahi, Y., Dinarvand, R., Tavakolizadeh, M., Ahmadi, S., Rabiee, M., Bagherzadeh, M., Pourjavadi, A., Farhadnejad, H., Tahriri, M., Webster, T. J., & Tayebi, L. (2020). Burgeoning Polymer Nano Blends for Improved Controlled Drug Release: A Review. *International Journal of Nanomedicine*, *15*, 4363–4392. https://doi.org/10.2147/IJN.S252237

Maiti, K., Mukherjee, K., Gantait, A., Saha, B. P., & Mukherjee, P. K. (2007). Curcumin–phospholipid complex: Preparation, therapeutic evaluation and pharmacokinetic study in rats. *International Journal of Pharmaceutics*, *330*(1), 155–163. https://doi.org/10.1016/j.ijpharm.2006.09.025

Mathew, M., & Subramanian, S. (2014). In Vitro Screening for Anti-Cholinesterase and Antioxidant Activity of Methanolic Extracts of Ayurvedic Medicinal Plants Used for Cognitive Disorders. *PLOS ONE*, *9*(1), e86804. https://doi.org/10.1371/journal.pone.0086804

Mattiuzzi, C., & Lippi, G. (2019). Current Cancer Epidemiology. *Journal of Epidemiology and Global Health*, *9*(4), 217–222. https://doi.org/10.2991/jegh.k.191008.001

Medzhitov, R. (2008). Origin and physiological roles of inflammation. *Nature*, *454*(7203), 428–435. https://doi.org/10.1038/nature07201

Meksuriyen, D. & Cordell, G. A. (1988). Traditional medicinal plants of Thailand XIII. Flavonoid derivatives from *Dracaena loureiri* (Agavaceae). *ScienceAsia*. *14*, 3-24

Mele, E. (2016). Electrospinning of natural polymers for advanced wound care: Towards responsive and adaptive dressings. *Journal of Materials Chemistry B*, *4*(28), 4801–4812. https://doi.org/10.1039/C6TB00804F

Meng, D., Wu, J., & Zhao, W. (2010). Glycosides from *Breynia fruticosa* and *Breynia rostrata*. *Phytochemistry*, *71*(2), 325–331. https://doi.org/10.1016/j.phytochem.-2009. 10.002

Min, H.-Y., Kim, M. S., Jang, D. S., Park, E.-J., Seo, E.-K., & Lee, S. K. (2009). Suppression of lipopolysaccharide-stimulated inducible nitric oxide synthase (iNOS) expression by a novel humulene derivative in macrophage cells. *International Immunopharmacology*, *9*(7), 844–849. https://doi.org/10.1016/j.intimp.2009.03.005

Mo, E. J., Ahn, J. H., Jo, Y. H., Kim, S. B., Hwang, B. Y., & Lee, M. K. (2017). Inositol Derivatives and Phenolic Compounds from the Roots of *Taraxacum coreanum*. *Molecules*, *22*(8), 1349. https://doi.org/10.3390/molecules22081349

Mokhtarzadeh, A., Alibakhshi, A., Hashemi, M., Hejazi, M., Hosseini, V., de la Guardia, M., & Ramezani, M. (2017). Biodegradable nano-polymers as delivery vehicles for therapeutic small non-coding ribonucleic acids. *Journal of Controlled Release*, *245*, 116–126. https://doi.org/10.1016/j.jconrel.2016.11.017

Monks, A., Scudiero, D., Skehan, P., Shoemaker, R., Paull, K., Vistica, D., Hose, C., Langley, J., Cronise, P., Vaigro-Wolff, A., Gray-Goodrich, M., Campbell, H., Mayo, J., & Boyd, M. (1991). Feasibility of a High-Flux Anticancer Drug Screen Using a Diverse Panel of Cultured Human Tumor Cell Lines. *JNCI: Journal of the National Cancer Institute*, *83*(11), 757–766. https://doi.org/10.1093/jnci/83.11.757

Moodley, N. (2004). The chemical investigation of the Amaryllidaceae and Hyacinthaceae. *Doctor of Philosophy in the School of Pure and Applied Chemistry*, University of KwaZulu-Natal, Durban, South Africa 41–42

Moulis, C., Gleye, J., & Stanislas, E. (1977). Alcaloïdes de l' Isopyrum thalictroïdes – Bases quaternaires des feuilles – Isolement et identification de quatre pseudoprotoberberines. *Phytochemistry*, *16*(8), 1283–1287. https://doi.org/10.1016/S0031-9422(00)94375-9

Mount, C., & Downton, C. (2006). Alzheimer disease: Progress or profit? *Nature Medicine*, *12*(7), 780–784. https://doi.org/10.1038/nm0706-780

Munj, H. R., Lannutti, J. J., & Tomasko, D. L. (2017). Understanding drug release from PCL/gelatin electrospun blends. *Journal of Biomaterials Applications*, *31*(6), 933–949. https://doi.org/10.1177/0885328216673555

Murray, A. P., Faraoni, M. B., Castro, M. J., Alza, N. P., & Cavallaro, V. (2013). Natural AChE Inhibitors from Plants and their Contribution to Alzheimer's Disease Therapy. *Current Neuropharmacology*, *11*(4), 388–413.

Murray, C. J. L., Aravkin, A. Y., Zheng, P., Abbafati, C., Abbas, K. M., Abbasi-Kangevari, M., Abd-Allah, F., Abdelalim, A., Abdollahi, M., Abdollahpour, I., Abegaz, K. H., Abolhassani, H., Aboyans, V., Abreu, L. G., Abrigo, M. R. M., Abualhasan, A., Abu-Raddad, L. J., Abushouk, A. I., Adabi, M., … Lim, S. S. (2020). Global burden of 87 risk factors in 204 countries and territories, 1990–2019: A systematic analysis for the Global Burden of Disease Study 2019. *The Lancet*, *396*(10258), 1223–1249. https://doi.org/10.1016/S0140-6736(20)30752-2

Mushtaq, S., Abbasi, B. H., Uzair, B., & Abbasi, R. (2018). Natural products as reservoirs of novel therapeutic agents. *EXCLI Journal*, *17*, 420–451. https://doi.org/10.17179/excli2018-1174

Nair, J. J., Bastida, J., Viladomat, F., & van Staden, J. (2012). Cytotoxic Agents of the Crinane Series of Amaryllidaceae Alkaloids. *Natural Product Communications*, *7*(12), 1934578X1200701234. https://doi.org/10.1177/1934578X1200701234

Newman, D. J., & Cragg, G. M. (2020). Natural Products as Sources of New Drugs over the Nearly Four Decades from 01/1981 to 09/2019. *Journal of Natural Products*, *83*(3), 770–803. https://doi.org/10.1021/acs.jnatprod.9b01285

Nguyen, H. T., Tran, L. T. T., Ho, D. V., Phan, K. V., Raal, A., & Morita, H. (2019). Three new inositol derivatives from *Chisocheton paniculatus*. *Tetrahedron Letters*, *60*(28), 1841–1844. https://doi.org/10.1016/j.tetlet.2019.06.015

Nguyen, K. V., Nguyen, T. O. T., Ho, D. V., Heinämäki, J., Raal, A., & Nguyen, H. T. (2021). In Vitro Acetylcholinesterase Inhibitory and Antioxidant Activity of *Alphonsea tonkinensis* A.DC. *Natural Product Communications*, *16*(9), 1934578X211042134. https://doi.org/10.1177/1934578X211042134

Nguyen, K. V., Ho, D., Le, A. T., Heinämäki, J., Raal, A., & Nguyen, H. T. (2020). Secondary metabolites from *Alphonsea tonkinensis* A.DC. showing inhibition of nitric oxide production and cytotoxic activity. *Journal of Pharmacy & Pharmacognosy Research*, *9*, 24–32.

Nguyen, K. V., Laidmäe, I., Kogermann, K., Lust, A., Meos, A., Ho, D. V., Raal, A., Heinämäki, J., & Nguyen, H. T. (2019). Preformulation Study of Electrospun Haemanthamine-Loaded Amphiphilic Nanofibers Intended for a Solid Template for Self-Assembled Liposomes. *Pharmaceutics*, *11*(10), 499. https://doi.org/10.3390/pharmaceutics11100499

Nguyen, L. T., Kaptchuk, T. J., Davis, R. B., Nguyen, G., Pham, V., Tringale, S. M., Loh, Y. L., & Gardiner, P. (2016). The Use of Traditional Vietnamese Medicine Among Vietnamese Immigrants Attending an Urban Community Health Center in the United States. *Journal of Alternative and Complementary Medicine*, *22*(2), 145–153.

Ngwuluka, N. C., Ochekpe, N. A., & Aruoma, O. I. (2014). Naturapolyceutics: The Science of Utilizing Natural Polymers for Drug Delivery. *Polymers*, *6*(5), 1312–1332. https://doi.org/10.3390/polym6051312

Nikmaram, N., Roohinejad, S., Hashemi, S., Koubaa, M., Barba, F. J., Abbaspourrad, A., & Greiner, R. (2017). Emulsion-based systems for fabrication of electrospun nanofibers: Food, pharmaceutical and biomedical applications. *RSC Advances*, *7*(46), 28951–28964. https://doi.org/10.1039/C7RA00179G

Orhan, I. E., & Senol, F. S. (2013). Alkaloids and Inhibitory Effects Against Enzymes Linked to Neurodegenerative Diseases (Physostigmine, Galanthamine, Huperzine, etc.). In K. G. Ramawat & J.-M. Mérillon (Eds.), *Natural Products: Phytochemistry, Botany and Metabolism of Alkaloids, Phenolics and Terpenes* (pp. 1525–1539). Springer. https://doi.org/10.1007/978-3-642-22144-6_23

Ovais, M., Zia, N., Ahmad, I., Khalil, A. T., Raza, A., Ayaz, M., Sadiq, A., Ullah, F., & Shinwari, Z. K. (2018). Phyto-Therapeutic and Nanomedicinal Approaches to Cure Alzheimer's Disease: Present Status and Future Opportunities. *Frontiers in Aging Neuroscience*, *10*, 284. https://doi.org/10.3389/fnagi.2018.00284

Paaver, U., Heinämäki, J., Laidmäe, I., Lust, A., Kozlova, J., Sillaste, E., Kirsimäe, K., Veski, P., & Kogermann, K. (2015). Electrospun nanofibers as a potential controlled-release solid dispersion system for poorly water-soluble drugs. *International Journal of Pharmaceutics*, *479*(1), 252–260. https://doi.org/10.1016/j.ijpharm.2014.12.024

Papkov, D., Delpouve, N., Delbreilh, L., Araujo, S., Stockdale, T., Mamedov, S., Maleckis, K., Zou, Y., Andalib, M. N., Dargent, E., Dravid, V. P., Holt, M. V., Pellerin, C., & Dzenis, Y. A. (2019). Quantifying Polymer Chain Orientation in Strong and Tough Nanofibers with Low Crystallinity: Toward Next Generation

Nanostructured Superfibers. *ACS Nano*, *13*(5), 4893–4927. https://doi.org/10.1021/acsnano.8b08725

Patra, J. K., Das, G., Fraceto, L. F., Campos, E. V. R., Rodriguez-Torres, M. del P., Acosta-Torres, L. S., Diaz-Torres, L. A., Grillo, R., Swamy, M. K., Sharma, S., Habtemariam, S., & Shin, H.-S. (2018). Nano based drug delivery systems: Recent developments and future prospects. *Journal of Nanobiotechnology*, *16*(1), 71. https://doi.org/10.1186/s12951-018-0392-8

Pellegrino, S., Meyer, M., Zorbas, C., Bouchta, S. A., Saraf, K., Pelly, S. C., Yusupova, G., Evidente, A., Mathieu, V., Kornienko, A., Lafontaine, D. L. J., & Yusupov, M. (2018). The Amaryllidaceae Alkaloid Haemanthamine Binds the Eukaryotic Ribosome to Repress Cancer Cell Growth. *Structure*, *26*(3), 416–425.e4. https://doi.org/10.1016/j.str.2018.01.009

Pepeu, G., & Giovannini, M. G. (2010). Cholinesterase inhibitors and memory. *Chemico-Biological Interactions*, *187*(1), 403–408. https://doi.org/10.1016/j.cbi.2009.11.018

Pishva, S. P., Elaheh Mousavi, E., Mousavi, Z., Jaafari, M. R., Dehpour, A. R., & Rezayat Sorkhabadi, S. M. (2018). The effect of berberine nanomicelles on hepatic cirrhosis in bile duct-ligated rats. *Nanomedicine Journal*, *5*(4), 199–209. https://doi.org/10.22038/nmj.2018.05.00003

Piwowarski, J. P., Kiss, A. K., & Kozłowska-Wojciechowska, M. (2011). Anti-hyaluronidase and anti-elastase activity screening of tannin-rich plant materials used in traditional Polish medicine for external treatment of diseases with inflammatory background. *Journal of Ethnopharmacology*, *137*(1), 937–941. https://doi.org/10.1016/j.jep.2011.05.039

Potrč, T., Baumgartner, S., Roškar, R., Planinšek, O., Lavrič, Z., Kristl, J., & Kocbek, P. (2015). Electrospun polycaprolactone nanofibers as a potential oromucosal delivery system for poorly water-soluble drugs. *European Journal of Pharmaceutical Sciences*, *75*, 101–113. https://doi.org/10.1016/j.ejps.2015.04.004

Pratap, P., Raza, S. T., Abbas, S., & Mahdi, F. (2018). MicroRNA-associated carcinogenesis in lung carcinoma. *Journal of Cancer Research and Therapeutics*, *14*(2), 249–254. https://doi.org/10.4103/0973-1482.187283

Renault, J.-H. (2015). Modern Separation Techniques for the Isolation of Natural Products. *Planta Medica*, *81*(17), 1569. https://doi.org/10.1055/s-0035-1558218

Reneker, D. H., & Yarin, A. L. (2008). Electrospinning jets and polymer nanofibers. *Polymer*, *49*(10), 2387–2425. https://doi.org/10.1016/j.polymer.2008.02.002

Roodbar Shojaei, T., Hajalilou, A., Tabatabaei, M., Mobli, H., & Aghbashlo, M. (2019). Characterization and Evaluation of Nanofiber Materials. In A. Barhoum, M. Bechelany, & A. S. H. Makhlouf (Eds.), *Handbook of Nanofibers* (pp. 491–522). Springer International Publishing. https://doi.org/10.1007/978-3-319-53655-2_15

Sahoo, S., Ang, L. T., Goh, J. C.-H., & Toh, S.-L. (2010). Growth factor delivery through electrospun nanofibers in scaffolds for tissue engineering applications. *Journal of Biomedical Materials Research – Part A*, *93*(4), 1539–1550. Scopus. https://doi.org/10.1002/jbm.a.32645

Saikia, B., Kataky, J. C. S., Mathur, R. K., & Baruah, J. N. (1978). New meliacins from the fruits of *chisocheton paniculatus*. *Indian Journal of Chemistry Section B Organic Chemistry Including Medicinal Chemistry*, *16*(11), 1042–1044.

Sannai, A., Fujimori, T., Uegaki, R., & Akaki, T. (1984). Isolation of 3-hydroxy-7, 8-dihydro-beta-ionone from *Lycium chinense* M. *Agricultural and Biological Chemistry (Japan)*. https://scholar.google.com/scholar_lookup?title=Isolation+of+3-hydroxy-7%2C+8-dihydro-beta-

ionone+from+Lycium+chinense+M.&author=Sannai%2C+A.+%28Fuji+Flavor+Co.+Ltd.%2C+Hamura%2C+Tokyo+%28Japan%29%29&publication_year=1984

Sayed, S. M. A., Siems, K., Schmitz-Linneweber, C., Luyten, W., & Saul, N. (2021). Enhanced Healthspan in *Caenorhabditis elegans* Treated With Extracts From the Traditional Chinese Medicine Plants Cuscuta chinensis Lam. And *Eucommia ulmoides* Oliv. *Frontiers in Pharmacology*, *12*. https://www.frontiersin.org/article/10.3389/fphar.2021.604435

Schoolaert, E., Steyaert, I., Vancoillie, G., Geltmeyer, J., Lava, K., Hoogenboom, R., & Clerck, K. D. (2016). Blend electrospinning of dye-functionalized chitosan and poly(ε-caprolactone): Towards biocompatible pH-sensors. *Journal of Materials Chemistry B*, *4*(26), 4507–4516. https://doi.org/10.1039/C6TB00639F

Shahriar, S. M. S., Mondal, J., Hasan, M. N., Revuri, V., Lee, D. Y., & Lee, Y.-K. (2019). Electrospinning Nanofibers for Therapeutics Delivery. *Nanomaterials (Basel, Switzerland)*, *9*(4), E532. https://doi.org/10.3390/nano9040532

Sharma, M., Sharma, R., & Jain, D. K. (2016). Nanotechnology Based Approaches for Enhancing Oral Bioavailability of Poorly Water Soluble Antihypertensive Drugs. *Scientifica*, *2016*, e8525679. https://doi.org/10.1155/2016/8525679

Sharma, R., Singh, H., Joshi, M., Sharma, A., Garg, T., Goyal, A., & Rath, G. (2014). Recent Advances in Polymeric Electrospun Nanofibers for Drug Delivery. *Critical Reviews™ in Therapeutic Drug Carrier Systems*, *31*(3). https://doi.org/10.1615/CritRevTherDrugCarrierSyst.2014008193

Shi, N.-Q., Yao, J., & Wang, X.-L. (2014). Effect of polymers and media type on extending the dissolution of amorphous pioglitazone and inhibiting the recrystallization from a supersaturated state. *Drug Development and Industrial Pharmacy*, *40*(8), 1112–1122. https://doi.org/10.3109/03639045.2013.809536

Shilpi, J. A., Saha, S., Chong, S.-L., Nahar, L., Sarker, S. D., & Awang, K. (2016). Advances in Chemistry and Bioactivity of the Genus *Chisocheton* Blume. *Chemistry & Biodiversity*, *13*(5), 483–503. https://doi.org/10.1002/cbdv.201400373

Singh, N., Baby, D., Rajguru, J. P., Patil, P. B., Thakkannavar, S. S., & Pujari, V. B. (2019). Inflammation and Cancer. *Annals of African Medicine*, *18*(3), 121–126. https://doi.org/10.4103/aam.aam_56_18

Širc, J., Hobzová, R., Kostina, N., Munzarová, M., Juklíčková, M., Lhotka, M., Kubinová, Š., Zajícová, A., & Michálek, J. (2012). Morphological Characterization of Nanofibers: Methods and Application in Practice. *Journal of Nanomaterials*, *2012*, e327369. https://doi.org/10.1155/2012/327369

Slade, D., Ferreira, D., & Marais, J. P. J. (2005). Circular dichroism, a powerful tool for the assessment of absolute configuration of flavonoids. *Phytochemistry*, *66*(18), 2177–2215. https://doi.org/10.1016/j.phytochem.2005.02.002

Stubba, D., Lahm, G., Geffe, M., Runyon, J. W., Arduengo III, A. J., & Opatz, T. (2015). Xylochemistry – Making Natural Products Entirely from Wood. *Angewandte Chemie International Edition*, *54*(47), 14187–14189. https://doi.org/10.1002/anie.201508500

Sun, Q., Li, F.-F., Wang, D., Wu, J., Yao, G.-D., Li, X., Li, L.-Z., Liu, Q.-B., Huang, X.-X., & Song, S.-J. (2016). Flavans with cytotoxic activity from the stem and root bark of *Daphne giraldii*. *RSC Advances*, *6*(61), 55919–55929. https://doi.org/10.1039/C6RA08537G

Supriatno, Nurlelasari, Herlina, T., Harneti, D., Maharani, R., Hidayat, A. T., Mayanti, T., Supratman, U., Azmi, M. N., & Shiono, Y. (2018). A new limonoid from stem

bark of *Chisocheton pentandrus* (Meliaceae). *Natural Product Research*, *32*(21), 2610–2616. https://doi.org/10.1080/14786419.2018.1428600

Swartz, M. (2010). HPLC Detectors: A Brief Review. *Journal of Liquid Chromatography & Related Technologies*, *33*(9–12), 1130–1150. https://doi.org/10.1080/10826076.2010.484356

Tantipolphan, R., Rades, T., McQuillan, A. J., & Medlicott, N. J. (2007). Adsorption of bovine serum albumin (BSA) onto lecithin studied by attenuated total reflectance Fourier transform infrared (ATR-FTIR) spectroscopy. *International Journal of Pharmaceutics*, *337*(1), 40–47. https://doi.org/10.1016/j.ijpharm.2006.12.021

Tanzi, R. E. (2021). FDA Approval of Aduhelm Paves a New Path for Alzheimer's Disease. *ACS Chemical Neuroscience*, *12*(15), 2714–2715. https://doi.org/10.1021/acschemneuro.1c00394

Teja, P. K., Mithiya, J., Kate, A. S., Bairwa, K., & Chauthe, S. K. (2022). Herbal nanomedicines: Recent advancements, challenges, opportunities and regulatory overview. *Phytomedicine*, *96*, 153890. https://doi.org/10.1016/j.phymed.2021.153890

T. Mader, K., Peeters, M., L. Detiger, S. E., N. Helder, M., H. Smit, T., Maitre, C. L. L., & Sammon, C. (2016). Investigation of intervertebral disc degeneration using multivariate FTIR spectroscopic imaging. *Faraday Discussions*, *187*(0), 393–414. https://doi.org/10.1039/C5FD00160A

Toth, M. J., Matthews, D. E., Tracy, R. P., & Previs, M. J. (2005). Age-related differences in skeletal muscle protein synthesis: Relation to markers of immune activation. *American Journal of Physiology-Endocrinology and Metabolism*, *288*(5), E883–E891. https://doi.org/10.1152/ajpendo.00353.2004

Vaidya, P., Grove, T., Edgar, K. J., & Goldstein, A. S. (2015). Surface grafting of chitosan shell, polycaprolactone core fiber meshes to confer bioactivity. *Journal of Bioactive and Compatible Polymers*, *30*(3), 258–274. https://doi.org/10.1177/0883911515571147

Vdovin, A. D., Kuliev, Z. A., & Abdullaev, N. D. (1997). ^{1}H and ^{13}C NMR spectroscopy in the study of flavan-3-ols, proanthocyanidins, and their derivatives III.13C nuclear magnetic resonance spectroscopy of flavan-3-ols and proanthocyanidins. *Chemistry of Natural Compounds*, *33*(4), 417–437. https://doi.org/10.1007/BF02282359

Vishal, V., Sharma Ganesh N., Gaur Mukesh, & Bairwa Ranjan. (2014). A review on some plants having anti-inflammatory activity. *The Journal of Phytopharmacology*, *3*(3), 214–221.

Vogelstein, B., & Kinzler, K. W. (2004). Cancer genes and the pathways they control. *Nature Medicine*, *10*(8), 789–799. https://doi.org/10.1038/nm1087

Wang, B., Wu, L., Chen, J., Dong, L., Chen, C., Wen, Z., Hu, J., Fleming, I., & Wang, D. W. (2021). Metabolism pathways of arachidonic acids: Mechanisms and potential therapeutic targets. *Signal Transduction and Targeted Therapy*, *6*(1), 1–30. https://doi.org/10.1038/s41392-020-00443-w

Wang, H., Naghavi, M., Allen, C., Barber, R. M., Bhutta, Z. A., Carter, A., Casey, D. C., Charlson, F. J., Chen, A. Z., Coates, M. M., Coggeshall, M., Dandona, L., Dicker, D. J., Erskine, H. E., Ferrari, A. J., Fitzmaurice, C., Foreman, K., Forouzanfar, M. H., Fraser, M. S., … Murray, C. J. L. (2016). Global, regional, and national life expectancy, all-cause mortality, and cause-specific mortality for 249 causes of death, 1980–2015: A systematic analysis for the Global Burden of Disease Study 2015. *The Lancet*, *388*(10053), 1459–1544. https://doi.org/10.1016/S0140-6736(16)31012-1

Wang, R., Zhou, M., Ma, H., Qiao, Y., & Li, Q. (2021). The Role of Chronic Inflammation in Various Diseases and Anti-inflammatory Therapies Containing Natural Products. *ChemMedChem*, *16*(10), 1576–1592. https://doi.org/10.1002/cmdc.202000996

White, K. P. (2009). What psychologists should know about homeopathy, nutrition, and botanical medicine. *Professional Psychology: Research and Practice*, *40*(6), 633–640. https://doi.org/10.1037/a0016051

WHO, 2022. Cancer [WWW Document]. URL https://www.who.int/news-room/fact-sheets/detail/cancer (accessed 30.05.2022)

Woerdenbag, H. J., Nguyen, T. M., Vu, D. V., Tran, H., Nguyen, D. T., Tran, T. V., De Smet, P. A., & Brouwers, J. R. (2012). Vietnamese traditional medicine from a pharmacist's perspective. *Expert Review of Clinical Pharmacology*, *5*(4), 459–477. https://doi.org/10.1586/ecp.12.34

Wongrakpanich, S., Wongrakpanich, A., Melhado, K., & Rangaswami, J. (2018). A Comprehensive Review of Non-Steroidal Anti-Inflammatory Drug Use in The Elderly. *Aging and Disease*, *9*(1), 143. https://doi.org/10.14336/AD.2017.0306

Wu, J., Tang, C., Yao, S., Zhang, L., Ke, C., Feng, L., Lin, G., & Ye, Y. (2015). Anti-inflammatory Inositol Derivatives from the Whole Plant of Inula cappa. *Journal of Natural Products*, *78*(10), 2332–2338. https://doi.org/10.1021/acs.jnatprod.5b00135

Xie, X., Tao, Q., Zou, Y., Zhang, F., Guo, M., Wang, Y., Wang, H., Zhou, Q., & Yu, S. (2011). PLGA Nanoparticles Improve the Oral Bioavailability of Curcumin in Rats: Characterizations and Mechanisms. *Journal of Agricultural and Food Chemistry*, *59*(17), 9280–9289. https://doi.org/10.1021/jf202135j

Xue, J., Wu, T., Dai, Y., & Xia, Y. (2019). Electrospinning and Electrospun Nanofibers: Methods, Materials, and Applications. *Chemical Reviews*, *119*(8), 5298–5415. https://doi.org/10.1021/acs.chemrev.8b00593

Yach, D., Leeder, S. R., Bell, J., & Kistnasamy, B. (2005). Global Chronic Diseases. *Science*, *307*(5708), 317–317. https://doi.org/10.1126/science.1108656

Yadav, R. D., Kataky, J. C. S., & Mathur, R. K. (1999). New protolimonoids and limonoids: Part I-Isolation, structure elucidation of new protolimonoids and limonoid from the root wood of *Chisocheton paniculatus Hiern* (Meliaceae). 5.

Yaffe, M. B. (2019). Why geneticists stole cancer research even though cancer is primarily a signaling disease. *Science Signaling*, *12*(565), eaaw3483. https://doi.org/10.1126/scisignal.aaw3483

Yang, M.-H., Wang, J.-S., Luo, J.-G., Wang, X.-B., & Kong, L.-Y. (2011). Chisopanins A-K, 11 new protolimonoids from *Chisocheton paniculatus* and their anti-inflammatory activities. *Bioorganic & Medicinal Chemistry*, *19*(4), 1409–1417. https://doi.org/10.1016/j.bmc.2011.01.007

Yang, M.-H., Wang, J.-S., Luo, J.-G., Wang, X.-B., & Kong, L.-Y. (2012). Four new triterpenoids from *Chisocheton paniculatus* and their anti-inflammatory activities. *Canadian Journal of Chemistry*, *90*(2), 199–204. https://doi.org/10.1139/v11-147

Yeon, E. T., Lee, J. W., Lee, C., Jin, Q., Jang, H., Lee, D., Ahn, J. S., Hong, J. T., Kim, Y., Lee, M. K., & Hwang, B. Y. (2015). Neo-Clerodane Diterpenoids from *Scutellaria barbata* and Their Inhibitory Effects on LPS-Induced Nitric Oxide Production. *Journal of Natural Products*, *78*(9), 2292–2296. https://doi.org/10.1021/acs.jnatprod.5b00126

Yeung, Y. T., Aziz, F., Guerrero-Castilla, A., & Arguelles, S. (2018). Signaling Pathways in Inflammation and Anti-inflammatory Therapies. *Current Pharmaceutical Design*, *24*(14), 1449–1484. https://doi.org/10.2174/1381612824666180327165604

Yu, D.-G., Branford-White, C., Williams, G. R., Bligh, S. W. A., White, K., Zhu, L.-M., & Chatterton, N. P. (2011). Self-assembled liposomes from amphiphilic electrospun nanofibers. *Soft Matter*, *7*(18), 8239–8247. https://doi.org/10.1039/C1SM05961K

Yuan, H., Ma, Q., Ye, L., & Piao, G. (2016). The Traditional Medicine and Modern Medicine from Natural Products. *Molecules*, *21*(5), 559. https://doi.org/10.3390/molecules21050559

Yuan, R., Hou, Y., Sun, W., Yu, J., Liu, X., Niu, Y., Lu, J.-J., & Chen, X. (2017). Natural products to prevent drug resistance in cancer chemotherapy: A review: Natural products prevent drug resistance. *Annals of the New York Academy of Sciences*, *1401*(1), 19–27. https://doi.org/10.1111/nyas.13387

Zhang, F., He, X.-F., Wu, W.-B., Chen, W.-S., & Yue, J.-M. (2012). New apotirucallane-type triterpenoids from *Chisocheton paniculatus*. *Natural Products and Bioprospecting*, *2*(6), 235–239. https://doi.org/10.1007/s13659-012-0065-5

Zhang, L., Yan, J., Liu, X., Ye, Z., Yang, X., Meyboom, R., Chan, K., Shaw, D., & Duez, P. (2012). Pharmacovigilance practice and risk control of Traditional Chinese Medicine drugs in China: Current status and future perspective. *Journal of Ethnopharmacology*, *140*(3), 519–525. https://doi.org/10.1016/j.jep.2012.01.058

Zhang, R. X., Li, J., Zhang, T., Amini, M. A., He, C., Lu, B., Ahmed, T., Lip, H., Rauth, A. M., & Wu, X. Y. (2018). Importance of integrating nanotechnology with pharmacology and physiology for innovative drug delivery and therapy – an illustration with firsthand examples. *Acta Pharmacologica Sinica*, *39*(5), 825–844. https://doi.org/10.1038/aps.2018.33

Zheng, Q.-A., Li, H.-Z., Zhang, Y.-J., & Yang, C.-R. (2004). Flavonoids from the Resin of *Dracaena cochinchinensis*. *Helvetica Chimica Acta*, *87*(5), 1167–1171. https://doi.org/10.1002/hlca.200490106

Zhu, M., Li, Y., Zhou, J., Wang, T., Li, X., Zhang, J., Qiao, Y., Han, J., Xu, Z., & Lou, H. (2022). Pinguisane Sesquiterpenoids from the Chinese Liverwort *Trocholejeunea sandvicensis* and Their Anti-Inflammatory Activity. *Journal of Natural Products*, *85*(1), 205–214. https://doi.org/10.1021/acs.jnatprod.1c00964

Zieneldien, T., Kim, J., & Cao, C. (2022). The Multifaceted Role of Neuroprotective Plants in Alzheimer's Disease Treatment. *Geriatrics (Basel, Switzerland)*, *7*(2), 24. https://doi.org/10.3390/geriatrics7020024

Zupancic, S., Kocbek, P., Baumgartner, S., & Kristl, J. (2015). Contribution of Nanotechnology to Improved Treatment of Periodontal Disease. *Current Pharmaceutical Design*, *21*(22), 3257–3271.

SUMMARY IN ESTONIAN

Vietnami ravimtaimedest isoleeritud ekstraktide ja toimeainete keemiline koostis ja bioaktiivsus ning nende nanotehnoloogial põhinevad ravimkandursüsteemid

Sissejuhatus

Juba eelajaloolistest aegadest saadik kasutusel olnud ravimtaimed on osutunud väga edukaks toimeainete allikaks uute ravimite avastamisel (Atanasov et al., 2015). Ravimtaimed pakuvad inimkonnale tohutut hulka looduslikke ühendeid, mida tuleb jätkuvalt uurida (Cragg & Newman, 2013). Taimset päritolu ravimid võivad aga kaasa tuua ka negatiivseid aspekte: toimeainete vähest lahustuvust, piiratud lahustumiskiirust, pärsitud imendumist organismis, sihtmärgistatud ravimkandursüsteemide piiratust, kõrget metaboliseerumistaset ja kiiret eritumisprotsessi, mis tingib madala biosaadavuse ja vähenenud terapeutilise toime. Need näitajad piiravad oluliselt fütopreparaatide kasulikkust kliinilises praktikas (Júnior et al., 2018).

Nanotehnoloogia on arenev teadusvaldkond, mis on leidnud mitmekülgset rakendust ka meditsiinis, eriti ravimkandursüsteemide (DDS) väljatöötamisel. Nanoskaala DDSid pakuvad uudset ja perspektiivikat alternatiivi tavapärastele ravimvormidele, olles mõeldud potentsiaalsete uute taimse päritoluga toimeainete kohaletoimetamiseks vajalikku kohta organismis (Patra et al., 2018; Zhang et al., 2018). On tõestatud, et taimse päritoluga toimeainete nanotehnoloogiapõhised DDS-d suurendavad toimeaine suukaudset biosaadavust mitu kuni isegi sada korda (Teja et al., 2022). Seetõttu võib eeldada, et taimsete toimeainete kombineerimine farmatseutilise nanotehnoloogia võimalustega pakub uut perspektiivi ravimtaimede uurimisel ja ravi edendamisel (Teja et al., 2022).

Elektrospinnimine on mitmekülgne ja paljulubav meetod ühtlaste ja ülipeente fiibrite valmistamiseks (Xue et al., 2019). Elektrospinnitud nano- ja mikrofiibrid võimaldavad luua paindlikke DDSe ja saavutada mitmekülgset ravimi vabanemise kineetikat, parandades sellega mitmeid terapeutilisi vajadusi. Sellised DDSs kasutatavad polümeersed nano- ja mikrokiud võivad parandada näiteks toimeainete suukaudset biosaadavust ja terapeutilist toimet tänu ravimi vabanemiseks sobivale kohale, ajastusele ja kiirusele (Kajdič et al., 2019).

Eesmärgid

Käesoleval doktoritööl on kaks peamist eesmärki: 1) saada teadmisi Vietnami traditsioonilises meditsiinis kasutatavatest ravimtaimedest eraldatud ekstraktide ja neis sisalduvate ühendite keemilise koostise ja bioaktiivsuse kohta; 2) töötada analüüsitud taimsetest ekstraktidest isoleeritud toimeainete jaoks välja uudsed farmatseutilisel nanotehnoloogial põhinevad DDSd. Uuritavad ravimtaimed valiti välja nende bioaktiivsuse potentsiaali põhjal.

Eesmärkide saavutamiseks püstitati tööle neli spetsiifilist ülesannet:

1. Isoleerida huvipakkuvatest taimeekstraktidest individuaalsed ühendid ja identifitseerida nende keemiline struktuur (I-IV).
2. Hinnata taimeekstraktidest eraldatud ühendite bioaktiivsust (sh vähivastast tsütotoksilisust, põletikuvastast ja AChE-vastast toimet) (I-IV).
3. Disainida ja valmistada taimedest isoleeritud ühendite põhjal elektrospinnitud amfifiilsed nanofiibrid, mida saab kasutada isetekkeliste liposoomide valmistamiseks (V).
4. Hinnata ülalnimetatud nanopreparaatide füsikokeemilisi omadusi: lahustumist *in vitro* ja stabiilsust (V).

Materjalid ja meetodid

Taimne materjal: Taimseks materjaliks olid taimeliigid *Chisocheton paniculatus* Hiern, *Alphonsea tonkinensis* A.DC. ja *Zephyranthes ajax* Hort., mis valiti välja Vietnami põlisrahvaste etnomeditsiinile tuginedes ning identifitseeriti ja koguti Vietnami keskosast.

Isoleeritud toimeaine: Hemantamiin (alkaloid), valge kristalne pulber, mille puhtus on 95%, eraldatud taimest *Z. ajax* ja kasutatud elektrospinnitud nanofiibrite valmistamiseks.

Lahustid, muud materjalid ja reaktiivid: metanool (MeOH), n-heksaan, etüülatsetaat (EtOAc), atsetoon, diklorometaan, kloroform ($CHCl_3$), vesinikkloriidhape (HCl) ja vesi reaktiividele omase ja HPLC-puhtusega (Xilong, Hiina ja Sigma-Aldrich C.C., USA), mida kasutati taimse materjali ekstraheerimiseks ja toimeainete isoleerimiseks ekstraktidest. Amfifiilsete nanofiibrite valmistamisel kasutati lahustina etanooli (Merck GmbH, Saksamaa). Polüvinüülpürrolidoon (PVP) (Kollidon 90F K90) osteti ettevõttelt BASF SE (Saksamaa), ja sojaoa fosfatidüülkoliin (PC) (Lipoid S-100) saadi ettevõttest Lipoid GmbH (Saksamaa).

Toimeainete isoleerimine taimeekstraktidest ja nende keemiliste struktuuride tuvastamine: Erinevate ekstraheerimis- ja kromatograafiliste meetodite kombinatsioon, sealhulgas normaalfaasi kromatograafia, pöördfaasikromatograafia, suurus-eraldus-kromatograafia, ioonvahetuskromatograafia, kõrgefektiivne vedelik-kromatograafia või kristallisatsioonitehnikad ja erinevad keemilised meetodid võimaldas taimsest materjalist eraldada piisavalt puhtaid individuaalseid ühendeid. Isoleeritud toimeainete keemilised struktuurid määrati kindlaks spektroskoopiliste analüüsidega ja vajadusel kombineerides neid erinevate keemiliste meetoditega. Spekroskoopilised andmed salvestati ja säilitatakse Vietnami Teadus- ja Tehnoloogiaakadeemia keemiainstituudis.

Ekstraktide ja eraldatud ühendite bioaktiivsuse hindamine:
Tsütotoksilisuse test: Eraldatud sekundaarsete metaboliitide tsütotoksilist aktiivsust hinnati sulforodamiin B (SRB) testi abil. Rakkude elujõulisuse hindamine SRB testi abil põhineb raku valgusisalduse määramisel (Monks et al., 1991) inimese vähirakkude, sealhulgas inimese kopsukartsinoomi (rakuliin SK-LU-1)

kasvu suhtes ja/või inimese hepatotsellulaarse kartsinoomi (HepG2) ja/või inimese suu kartsinoomi (KB) ja/või inimese käärsoole kartsinoomi (SW480) ja/või inimese mao adenokartsinoomi (AGS) kasvu kaudu.

Põletikuvastane test: Meetod põhineb nitriti kontsentratsioonil, mis on lämmastikoksiidi (NO) olemasolu indikaator söötmes. Kontsentratsioon määrati Griessi reaktsiooni ja RAW 264.7 rakkude abil (Yeon et al., 2015; Nguyen et al., 2020).

AChE inhibeeriva aktiivsuse test: Test viidi läbi pisut modifitseeritud Ellmani meetodil järgi, kasutades AChE-d, atsetüültiokoliinkloriidi, DTNB-d, etüülparaoksooni, indoksüülatsetaati ja fosfaatpuhverdatud soolalahust (Magalhães et al., 2020).

Taimse päritoluga hemantamiini amfifiilsete nanofiibrite valmistamine ja iseloomustamine: Nanofiibrid valmistati lahustipõhisel elektrospinnimise meetodil. Hemantamiini keemilist struktuuri ja nanofiibrite geomeetrilisi omadusi, molekulaarseid interaktsioone ja füüsikalisi tahke faasi omadusi uuriti tuumamagnetresonantsspektroskoopia (NMR), skaneeriva elektronmikroskoopia (SEM), footonkorrelatsioonispektroskoopia (PCS), Fourier' teisendatud infrapuna spektroskoopia (FTIR), pulberröntgendifraktsiooni (XRPD) ja diferentsiaalse skaneeriva kalorimeetria (DSC) meetodeid kasutades. Toimeaine vabanemise uurimiseks *in vitro* kasutati dialüüsipõhist lahustumismeetodit.

Tulemused ja arutelu

Taimedest eraldatud ühendite keemilise struktuuri selgitamine, nende tsütotoksilisus ja bioloogiline aktiivsus:

Vietnamist kogutud taime *C. paniculatus* lehtedest eraldati kuus uut kiroinositooli derivaati (**1-6**): 4,5-di-*O*-5-hüdroksütigloüül-1-*O*-2-metüülbutüroüül-3-*O*-tigloüül-kiroinositool (**1**), 4,5-di-*O*-5-hüdroksütigloüül-3-*O*-2-metüülbutüroüül-1-*O*-tigloüül-kiroinositool (**2**), 4,5-di-*O*-5-hüdroksütigloüül-1,3-di-*O*-2-metüülbutüroüül-kiroinositool (**3**), 3,5-di-*O*-5-hüdroksütigloüül-2-*O*-2-metüülbutüroüül-6-*O*-tigloüül-kiroinositool (**4**), 3,5-di-*O*-5-hüdroksütigloüül-2,6-di-*O*-2-metüülbutüroüül-kiroinositool (**5**), ja 4,5-di-*O*-5-hüdroksütigloüül-3,6-di-*O*-tigloüül-kiroinositool (**6**).

Nende kuue ühendi keemilised struktuurid selgitati välja 1D- ja 2D-NMR ning kõrge eraldusvõimega elektronpihustusionisatsiooni massispektomeetria meetodil. Kõiki eraldatud ühendeid analüüsiti nende inhibeeriva toime osas lipopolüsahhariidide poolt indutseeritud lämmastikoksiidi (NO) tootmise suhtes RAW 264.7 makrofaagide rakuliinis. Ühend **4** näitas eraldatud ainete seas kõige tugevamat NO tootmist inhibeerivat toimet IC_{50} väärtusega 7,1 μM. Ühendid **1, 3** ja **6** inhibeerisid mõõdukat NO produktsiooni, nende IC_{50} väärtused olid vastavalt 20,3, 62,9 ja 56,7 μM. Ühendid **2** ja 5 avaldasid väga nõrka inhibeerivat aktiivsust, IC_{50} väärtused olid vastavalt 123,7 ja 95,6 μM. Tsütotoksilise toime suhtes hinnati eraldatud ühendeid **1–6** inimese kopsukartsinoomi (SK-LU-1) rakuliini suhtes. Tulemused näitasid, et kõigil uutel kiroinositooli derivaatidel oli uuritud rakuliinide suhtes väga nõrk tsütotoksilisus.

Taime *A. tonkinensis* varte ja lehtede fütokeemilise uuringu tulemuseks oli varasemalt tuntud ühendite liriodeniini (**7**) (Kristanti et al., 2015), N-trans-feruloüültüramiini (**8**) (Kanada et al., 2012), koridaldiini (**9**) (Atan et al., 2011), 8-oksopseudopalmatiini (**10**) (Costa et al., 2010), 3-hüdroksü-7,8-dehüdro-*β*-ionooni (**11**) (Sannai et al., 1984), pseudopalmatiini (**12**) (Stubba et al., 2015), pseudokolumbamiini (**13**) (Moulis et al., 1977) ja stigmasterooli (**14**) (Forgo & Kövér, 2004) eraldamine ja identifitseerimine. Meie parima teadmise kohaselt eraldati ühendid **9** ja **11** taimeperekonnast *Alphonsea* esimest korda.

Ühendite **7-14** põletikuvastast toimet hinnati NO tootmist inhibeeriva toime põhjal, kasutades Griessi testi. Ühendil **11** oli tugev NO tootmist inhibeeriv toime LPS-i poolt stimuleeritud BV2 rakkude suhtes IC_{50} väärtusega 20,4 µM. Märkimisväärne on avastus, et selle ühendi IC_{50} väärtus oli märksa väiksem kui positiivse kontrolli L-NMMA väärtus. Ülejäänud ühendid ei avaldanud NO-tootmise aktiivsuse pärssimisele mingit mõju. Meie andmetel oleme esimestena näidanud ühendi **11** mõju inhibeerida NO tootmist.

Saadud ühendeid **8–14** testiti nende tsütotoksilise toime suhtes inimese hepatotsellulaarse kartsinoomi (HepG2) ja inimese kopsukartsinoomi (SK-LU-1) rakuliini suhtes. Ühendi **7** kogus ei olnud kahjuks testimiseks piisav. Tulemused näitasid, et ühendid **8, 9, 12, 13** ja **14** ei inhibeerinud uuritud rakuliine. Kuid ühenditel **10** ja **11** ilmnes inhibeeriv toime mõlema kahe testitud vähirakuliini suhtes, kusjuures IC_{50} väärtused jäid vahemikku 54,4-69,6 µM. Huvitaval kombel näitas ühendi **10** ja ühendite **12** ja **13** tsütotoksilisuse võrdlus ilmselgelt, et karbonüülrühma olemasolu aine struktuuris (**10**) võib avaldada tsütotoksilisele aktiivsusele suurendavat mõju. Meie teada ei ole ühendite **10** ja **11** tsütotoksilist aktiivsust varasemalt kirjeldatud.

Taimest *A. tonkinensis* eraldatud ekstrakte ja ühendeid hinnati AChE inhibeeriva toime suhtes, kasutades Ellmani kolorimeetrilist meetodit, kusjuures positiivse kontrollina tarvitati galantamiini. Tulemused näitasid, et MeOH alafraktsioon (see ekstraheeriti omakorda CH_2Cl_2 ekstraktist MeOH abil) näitas kõige tugevamat AChE-inhibeerivat toimet IC_{50} inhibeerimisväärtusega 14,6 µg/ml, millele järgnesid MeOH ekstrakt IC_{50} väärtusega 22,7 µg/ml ja CH_2Cl_2 ekstrakt IC_{50} väärtusega 32,8 µg/ml. Pseudopalmatiin ja pseudokolumbamiin avaldasid tugevat AChE-inhibeerivat toimet IC_{50} väärtustega vastavalt 8,6 µM ja 18,9 µM.

Mis puutub kolmandasse ravimtaime, siis pärast taime *Z. ajax* lehtede ekstraheerimist ja ekstrakti koostisainete isoleerimist ja identifitseerimist leiti täiesti uus flavanooli derivaat (2*R*,3*R*)-3-atsetoksü-7-hüdroksü-3′,4′-metüleendioksüflavaan (**15**) ja seitse teadaolevat ühendit: 7-hüdroksüflavaan (**16**) (Moodley, 2004), 7,4′-dihüdroksüflavaan (**17**) (Meksuriyen & Cordell, 1988), 7,4′-dihüdroksü-8-metüülflavaan (**18**) (Ioset et al., 2001), 7,3′-dihüdroksü-4′-metoksüflavaan (**19**) (Sun et al., 2016), 5,4′-dihüdroksü-7-metoksü-6-metüülflavaan (**20**) (Zheng jt, 2004), 7-hüdroksü-3′,4′-metüleendioksüflavanoon (**21**) (Ali et al., 2017) ja hemantamiin (**22**) (Bastida et al., 1987; Bohno et al., 2007). Meie parimate teadmiste kohaselt eraldati ühendid **16, 17, 18, 20** ja **21** taimepere-

konnast *Zephyranthes* esimest korda. Lisaks näitas tsütotoksilisuse test, et ühendil **22** on tugev tsütotoksiline toime inimese hepatotsellulaarse kartsinoomi (HepG2), inimese kopsukartsinoomi (SK-LU-1), inimese suus esineva kartsinoomi (KB), inimese käärsoolekartsinoomi (SW480) ja inimese mao adenokartsinoom (AGS), mille IC_{50} väärtused on vahemikus 4,4-11,3 μM. See on esimene uuring, mis näitab ühendi **22** tsütotoksilisust SK-LU-1 vähirakuliini suhtes.

Elektrospinnitud amfifiilsete nanofiibrite ja isetekkeliste liposoomide nanoformulatsioon taimse päritoluga hemantamiini kohaletoimetamiseks:
Taimse päritoluga toimeainet hemantamiin, mis eraldati taimest *Z. ajax*, kasutati nanoformulatsioonide valmistamiseks. Elektrospinnimisel õnnestus saada sama PC ja PVP suhega (1:2 mass/mass) hemantamiini sisaldavad amfifiilsed nanofiibrid, mida saab kasutada tahke vaheproduktina isetekkeliste liposoomide valmistamiseks. Nanofiibridolid mittepõimunud ja lõdvalt pakitud kiududena. Hemantamiiniga laetud elektrospinnitud amfifiilsete nanofiibrite keskmine kiu läbimõõt oli 392±66 nm (n=100) ja kiu suurus oli üksikutel nanofiibritel vahemikus 197-534 nm. Tilga puhastatud vee lisamisel amfifiilsele nanofiibermatile moodustusid mõne sekundi jooksul spontaanselt liposoomid, tõestades seega välja töötatud nanosüsteemi asjakohast toimimist.

PCS tulemused näitavad, et liposoomid olid sfäärilise kujuga ja neil oli bimodaalne suurusjaotus kahe erineva piigiga 63±70 nm (10,3%) ja 401±64 nm (89,7%) juures. Polüdisperssuse indeks (PDI) oli 0,474. See näitab, et liposoomide *in situ* moodustumine toimus ootuspäraselt. Puhta hemantamiini XRPD-muster näitas arvukalt selgeid kristallilisi peegeldusi. Hemantamiini sisaldavate elektrospinnitud nanofiibrite XRPD-mustris ei ilmnenud kristallilisele vormile iseloomulikke peegeldusi. Amfifiilsete nanofiibrite XRPD-mustris on näha kahte laia amorfset halo (tõenäoliselt on sellele kaasa aidanud PVP), mis viitab praeguste fiibrite tahke faasi amorfsele struktuurile. Hemantamiini tahke faasi muundumine võib olla tingitud lahusti suurenenud aurustumiskiirusest elektrospinnimise protsessi ajal, mis võib takistada API ümberkristalliseerumist (Laidmäe et al., 2021). Hemantamiini *in vitro* lahustumist pulbri kujul ja amfifiilsete elektrospinnitud nanofiibritena uuriti dialüüsimeetodi abil. Esimese 2-tunnise faasi jooksul vabanes üle poole ja järgnevas 2-tunnises faasis vabanes ligikaudu 80% nanofiibritesse seotud hemantamiinist. Esialgne kiire vabanemine tulenes suure tõenäosusega hemantamiini tahke aine vormist, st olekust nanokiulistes mallides ja tema pinna- või pinnalähedasest jaotusest nanofiibrites, mis viitab hemantamiini paranenud lahustumisele ja toetab praegust amfifiilsetel nanofiibritel põhinevat strateegia. Välja töötatud hemantamiini sisaldavad amfifiilsed nanofiibrid on alternatiivne lähenemisviis liposomaalse ravimkandursüsteemi disainimiseks ja uuritud alkaloidi liposoomide stabiliseerimiseks.

Järeldused ja kokkuvõte

Kokkuvõttes pakub käesolev uuring uusi teaduslikke andmeid taimede *C. paniculatus, A. tonkinensis* ja *Z. ajax* fütokeemilise koostise ja bioaktiivsuse kohta. Erilist tähelepanu pöörati uurimuses hemantamiinile, mis avastati taimest *Z. ajax* ja kasutati taimse päritoluga amfifiilsete nanofiibrite ja liposoomide formuleerimiseks uudsete nanotehnoloogiapõhiste ravimkandursüsteemidena. Uurimusest saab teha järgmised järeldused:

1. Uuritud kolmest ravimtaimest eraldati ja iseloomustati kokku 22 koostisainet, sealhulgas seitset uut ühendit. Need uued ühendid hõlmavad kuut uut kiroinositooli derivaati taime *C. paniculatus* lehtedest (4,5-di-*O*-5-hüdroksütigloüül-1-*O*-2-metüülbutüroüül-3-*O*-tigloüül-kiroinositool; 4,5-di-*O*-5-hüdroksütigloüül-3-*O*-2-metüülbutüroüül-1-*O*-tigloüül-kiroinositool, 4,5-di-*O*-5-hüdroksütigloüül-1,3-di-*O*-2-metüülbutüroüül-kiro-inositool; 3,5-di-*O*-5-hüdroksü-tigloüül-2-*O*-2-metüülbutüroüül-6-*O*-tigloüül-kiro-inositool; 3,5-di-*O*-5-hüdroksütigloüül-2,6-di-*O*-2-metüülbutüroüül-kiroinositool; 4,5-di-*O*-5-hüdroksü-tigloüül-3,6-di-*O*-tigloüül-kiroinositool) ja ühte uut flavanooli derivaati taime *Z. ajax* risoomidest, aga ka (2*R*,3*R*)-3-atsetoksü-7-hüdroksü-3′,4′-metüleendioksüflavaani ja viitteist tuntud ühendit (seitse taimest *Z. ajax*: 7-hüdroksüflavaan, 7,4′-dihüdroksüflavaan, 7,4′-dihüdroksü-8-metüülflavaan, 7,3′-dihüdroksü-4′-metoksüflavaan, 5,4′-dihüdroksü-7-metoksü-6-metüülflavaan, 7-hüdroksü-3′,4′-metüleendioksüflavanoon ja hemantamiin, ning kaheksa taime *A. tonkinensis* vartest ja lehtedest: liriodeniin, N-trans-feruloüültüramiin, koridaldiin, 8-oksopseudopalmatiin, 3-hüdroksü-7,8-dehüdro-*β*-ionoon, pseudopalmatiin, pseudokolumbamiin ja stigmasterol). Kõik varem teadaolevad ühendid olid nendest taimeliikidest esimest korda eraldatud meie poolt.
2. Bioaktiivsusse puutuvalt näitasid ühendid 3,5-di-*O*-5-hüdroksütigloüül-2-*O*-2-metüülbutüroüül-6-*O*-tigloüül-kiroinositool (taimest *C. paniculatus*) ja 3-hüdroksü-7,8-dehüdro-*β*-ionoon (*A. tonkinensis*) tugevat NO moodustumist pärssivat toimet. MeOH koguekstrakt, MeOH osa (ekstraheeritud CH_2Cl_2 ekstraktist), pseudokolumbamiin ja pseudopalmatiin (*A. tonkinensis*) näitasid potentsiaalset AChE-vastast toimet. Hemantamiin (*Z. ajax*) avaldas tugevat tsütotoksilist toimet inimese vähirakuliinide HepG2, SK-LU-1, KB, SW480 ja AGS suhtes.
3. Õnnestus edukalt valmistada hemantamiini sisaldavad elektrospinnitud amfifiilsed nanofiibrid, mida saab kasutada tahke vaheproduktina isetekkeliste liposoomide valmistamiseks. PVP on sobiv kandepolümeer hemantamiiniga (taimse päritoluga kriiniini-tüüpi alkaloid) laetud elektrospinnitud polümeersete nanofiibrite genereerimiseks. PC ja PVP suhe 1:2 (mass/mass) võimaldab valmistada soovitud amfifiilseid nanofiibreid, mida saab kasutada hemantamiini isetekkeliste liposoomide stabiilse vaheproduktina. Sobivate materjalide ja elektrospinnimise parameetritega nanofiibrite valmistamine mängib sellises elektrospinnitud ravimkandursüsteemis olulist rolli. Tege-

mist on esmakordse taimset päritolu toimeainet sisaldava isetekkeliste liposoomide valmistamiseks mõeldud amfifiilsete nanofiibrite disainiga.

4. Nanofiibrid olid mittepõimunud ja lõdvalt pakitud kiududena, fiibrite läbimõõt oli vahemikus 197–534 nm. Hemantamiini *in vitro* vabanemine amfifiilsetest nanofiibritest ja liposoomidest näitas algset kiiret vabanemist ja ligikaudu 80% hemantamiinist vabanes esimese nelja tunni jooksul. Vees halvasti lahustuva hemantamiini paranenud lahustuvus viitab sellele, et praegune amfifiilsetel nanofiibritel põhinev strateegia isetekkeliste liposoomide valmistamiseks on rakendatav taimse päritoluga alkaloidide jaoks. Välja töötatud ravimkandursüsteemi toimivust kinnitas mõne sekundi jooksul spontaansete (isetekkeliste) liposoomide moodustumine vees.

ACKNOWLEDGEMENTS

The experiments for this study were performed at the Institute of Pharmacy, Faculty of Medicine, University of Tartu, Estonia, and Faculty of Pharmacy, Hue University of Medicine and Pharmacy, Vietnam during the years 2018–2021.

The Erasmus Plus, Edushare Funding Programme, the national research projects in Estonia IUT34-18 and PUT1088, the National Foundation for Science and Technology Development (NAFOSTED) of Vietnam, Hue University are acknowledged for research investigation and mobility funding.

Words cannot express my sincere gratitude to my supervisors, Professor Ain Raal, Professor Hoai Thi Nguyen, and Professor Jyrki Heinämäki for your invaluable advice, great support and continuous guidance during my academic research. I have been honestly fortunate and happy to have you as my supervisors. Your immense knowledge and your kindness have encouraged and inspired me during the journey.

I would like to extend my special thanks to my reviewers Associate Professor Külli Jaako and Associate Professor Uno Mäeorg for the time and effort with valuable advice and comments to improve the thesis.

I would like to express my deep gratitude to Associate Professor Ivo Laidmäe, Professor Karin Kogermann, Associate Professor Duc Viet Ho, Associate Professor Andres Meos and PhD Andres Lust for the treasured experimental guidance, help and shared ideas.

I am grateful to Anh Tuan Le and Nhan Trong Le for helping to collect medicinal plant materials.

I would like to extend my sincere thanks to Lecturers at the Institute of Pharmacy and Lecturers in University of Tartu who have given me precious lessons with kindness and dedication.

I would like to thank all my colleagues, friends at the Faculty of Pharmacy, Hue University of Medicine and Pharmacy and at the Institute of Pharmacy, Faculty of Medicine, University of Tartu, Estonia for their support and encouragement.

My gratitude extends to all the persons involved with my study in Estonia and Vietnam.

Finally, I would like to express my love and gratitude to my parents, my wife and my little sons who have massive understanding, encourangement and unconditional support. They constantly keep my motivation high all the time in my academic research and daily life.

PUBLICATIONS

CURRICULUM VITAE

Name	Khan Nguyen Viet
Date of birth	March 14, 1982
Address	Faculty of Pharmacy, Hue University of Medicine and Pharmacy, 06 Ngo Quyen street, Hue city 530000, Vietnam
Telephone	+84 931771514
E-mail	nvietkhan@gmail.com, nvkhan@huemed-univ.edu.vn

Education

2019–…	University of Tartu, Faculty of Medicine, Institute of Pharmacy, PhD studies in Pharmacy
2005–2007	Hue University of Education, Faculty of Chemistry (MSc in Analytical Chemistry)
2000–2004	Hue University of Education, Faculty of Chemistry (Bachelor)

Professional employment

2011–…	Hue University of Medicine and Pharmacy, Faculty of Pharmacy, Lecturer of Pharmaceutical Analysis
2008–2011	Hue University Branch in Quang Tri

Honours and awards

2012	The Consolation prize of Vietnam Fund for Supporting Technological Creations

List of publications in international peer-reviewed journals

1. Raal, A., Jaama, M., Utt, M., Püssa, T., Žvikas, V., Jakštas, V., Koshovyi, O., **Nguyen, K.V.**, & Nguyen, T.H., 2022. The phytochemical profile and anticancer activity of *Anthemis tinctoria* and *Angelica sylvestris* used in Estonian ethnomedicine. *Plants (Basel, Switzerland)*, 11(7), 994.
2. **Nguyen, K.V.**, Nguyen, T.O.T., Ho, DV, Heinämäki, J., Raal, A., Nguyen, H.T., 2021. *In-vitro* acetylcholinesterase inhibitory and antioxidant activity of *Alphonsea tonkinensis* A.DC. *Natural Product Communications*, 16 (9), 1–5.
3. **Nguyen, K.V.**, Ho, DV, Le, AT, Heinämäki, J., Raal, A, Nguyen, H.T., 2021. Secondary metabolites from *Alphonsea tonkinensis* A.DC. showing inhibition of nitric oxide production and cytotoxic activity. *Journal of Pharmacy & Pharmacognosy Research*, 9 (1), 24–32.
4. **Nguyen, K.V**., Ho, D.V., Nguyen, H.M., Do, T.T., Phan, K.V., Morita, H., Heinämäki, J., Raal, A., Nguyen, H.T., 2020. *chiro*-Inositol derivatives from *Chisocheton paniculatus* showing inhibition of nitric oxide production. *Journal of Natural Products*, 83 (4), 1201–1206.
5. Ho, D.V., Hoang, H.N.T., Vo, H.Q., **Nguyen, K.V.**, Pham, T.V., Le, A.T., Van Phan, K., Nguyen, H.M., Morita, H., & Nguyen, H.T. (2020). Three new steroidal saponins from *Aspidistra letreae* plants and their cytotoxic activities. *Journal of Natural Medicines*, *74*(3), 591–598.

6. **Nguyen, K.V.**, Ho, D.V., Le, N.T., Phan, K.V., Heinämäki, J., Raal, A., Nguyen, H.T., 2020. Flavonoids and alkaloids from the rhizomes of *Zephyranthes ajax* Hort. and their cytotoxicity. *Scientific Reports*, 10, 22193.
7. **Nguyen, K.V.**, Laidmäe, I., Kogermann, K., Lust A., Meos, A., Ho, D.V., Raal, A., Heinämäki, J., Nguyen, H.T., 2019. Preformulation study of electrospun haemanthamine-loaded amphiphilic nanofibers intended for a solid template for self-assembled liposomes. *Pharmaceutics*, 11, 499, 1–13.

ELULOOKIRJELDUS

Nimi	Khan Nguyen Viet
Sünniaeg	14. märts 1982
Aadress	Hue Meditsiini- ja Farmaatsiaülikooli farmaatsiateadukond, Ngo Quyen 6, Hue 530000, Vietnam
Telefon	+84 931771514
E-mail	nvietkhan@gmail.com, nvkhan@huemed-univ.edu.vn

Haridustee

2019–…	Tartu Ülikool, farmaatsia doktorantuur
2005–2007	Hue haridusülikool, analüütilise keemia magister
2000–2004	Hue haridusülikool, keemia bakalaureus

Töökäik

2011–…	Hue Meditsiini- ja Farmaatsiaülikooli farmaatsiateaduskond, farmatseutilise analüüsi lektor
2008–2011	Hue Ülikooli haruülikool Quang Tris, analüütilise keemia lektor

Teaduspreemiad ja tunnustused

2012	Vietnami tehnoloogilise loomingu toetamise fondi lohutusauhind

Publikatsioonid rahvusvahelistes eelretsenseeritavates ajakirjades

1. Raal, A., Jaama, M., Utt, M., Püssa, T., Žvikas, V., Jakštas, V., Koshovyi, O., **Nguyen, K.V.**, & Nguyen, T.H., 2022. The phytochemical profile and anticancer activity of *Anthemis tinctoria* and *Angelica sylvestris* used in Estonian ethnomedicine. *Plants (Basel, Switzerland)*, 11(7), 994.
2. **Nguyen, K.V.**, Nguyen, T.O.T., Ho, DV, Heinämäki, J., Raal, A., Nguyen, H.T., 2021. *In-vitro* acetylcholinesterase inhibitory and antioxidant activity of *Alphonsea tonkinensis* A.DC. *Natural Product Communications*, 16 (9), 1–5.
3. **Nguyen, K.V.**, Ho, DV, Le, AT, Heinämäki, J., Raal, A, Nguyen, H.T., 2021. Secondary metabolites from *Alphonsea tonkinensis* A.DC. showing inhibition of nitric oxide production and cytotoxic activity. *Journal of Pharmacy & Pharmacognosy Research*, 9 (1), 24–32.
4. **Nguyen, K.V**., Ho, D.V., Nguyen, H.M., Do, T.T., Phan, K.V., Morita, H., Heinämäki, J., Raal, A., Nguyen, H.T., 2020. *chiro*-Inositol derivatives from *Chisocheton paniculatus* showing inhibition of nitric oxide production. *Journal of Natural Products*, 83 (4), 1201–1206.
5. Ho, D.V., Hoang, H.N.T., Vo, H.Q., **Nguyen, K.V.**, Pham, T.V., Le, A.T., Van Phan, K., Nguyen, H.M., Morita, H., & Nguyen, H.T. (2020). Three new steroidal saponins from *Aspidistra letreae* plants and their cytotoxic activities. *Journal of Natural Medicines*, *74*(3), 591–598.

6. **Nguyen, K.V.**, Ho, D.V., Le, N.T., Phan, K.V., Heinämäki, J., Raal, A., Nguyen, H.T., 2020. Flavonoids and alkaloids from the rhizomes of *Zephyranthes ajax* Hort. and their cytotoxicity. *Scientific Reports*, 10, 22193.
7. **Nguyen, K.V.**, Laidmäe, I., Kogermann, K., Lust A., Meos, A., Ho, D.V., Raal, A., Heinämäki, J., Nguyen, H.T., 2019. Preformulation study of electrospun haemanthamine-loaded amphiphilic nanofibers intended for a solid template for self-assembled liposomes. *Pharmaceutics*, 11, 499, 1–13.

DISSERTATIONES MEDICINAE UNIVERSITATIS TARTUENSIS

1. **Heidi-Ingrid Maaroos**. The natural course of gastric ulcer in connection with chronic gastritis and *Helicobacter pylori*. Tartu, 1991.
2. **Mihkel Zilmer**. Na-pump in normal and tumorous brain tissues: Structural, functional and tumorigenesis aspects. Tartu, 1991.
3. **Eero Vasar**. Role of cholecystokinin receptors in the regulation of behaviour and in the action of haloperidol and diazepam. Tartu, 1992.
4. **Tiina Talvik**. Hypoxic-ischaemic brain damage in neonates (clinical, biochemical and brain computed tomographical investigation). Tartu, 1992.
5. **Ants Peetsalu**. Vagotomy in duodenal ulcer disease: A study of gastric acidity, serum pepsinogen I, gastric mucosal histology and *Helicobacter pylori*. Tartu, 1992.
6. **Marika Mikelsaar**. Evaluation of the gastrointestinal microbial ecosystem in health and disease. Tartu, 1992.
7. **Hele Everaus**. Immuno-hormonal interactions in chronic lymphocytic leukaemia and multiple myeloma. Tartu, 1993.
8. **Ruth Mikelsaar**. Etiological factors of diseases in genetically consulted children and newborn screening: dissertation for the commencement of the degree of doctor of medical sciences. Tartu, 1993.
9. **Agu Tamm**. On metabolic action of intestinal microflora: clinical aspects. Tartu, 1993.
10. **Katrin Gross**. Multiple sclerosis in South-Estonia (epidemiological and computed tomographical investigations). Tartu, 1993.
11. **Oivi Uibo**. Childhood coeliac disease in Estonia: occurrence, screening, diagnosis and clinical characterization. Tartu, 1994.
12. **Viiu Tuulik**. The functional disorders of central nervous system of chemistry workers. Tartu, 1994.
13. **Margus Viigimaa**. Primary haemostasis, antiaggregative and anticoagulant treatment of acute myocardial infarction. Tartu, 1994.
14. **Rein Kolk**. Atrial versus ventricular pacing in patients with sick sinus syndrome. Tartu, 1994.
15. **Toomas Podar**. Incidence of childhood onset type 1 diabetes mellitus in Estonia. Tartu, 1994.
16. **Kiira Subi**. The laboratory surveillance of the acute respiratory viral infections in Estonia. Tartu, 1995.
17. **Irja Lutsar**. Infections of the central nervous system in children (epidemiologic, diagnostic and therapeutic aspects, long term outcome). Tartu, 1995.
18. **Aavo Lang**. The role of dopamine, 5-hydroxytryptamine, sigma and NMDA receptors in the action of antipsychotic drugs. Tartu, 1995.
19. **Andrus Arak**. Factors influencing the survival of patients after radical surgery for gastric cancer. Tartu, 1996.

20. **Tõnis Karki**. Quantitative composition of the human lactoflora and method for its examination. Tartu, 1996.
21. **Reet Mändar**. Vaginal microflora during pregnancy and its transmission to newborn. Tartu, 1996.
22. **Triin Remmel**. Primary biliary cirrhosis in Estonia: epidemiology, clinical characterization and prognostication of the course of the disease. Tartu, 1996.
23. **Toomas Kivastik**. Mechanisms of drug addiction: focus on positive reinforcing properties of morphine. Tartu, 1996.
24. **Paavo Pokk**. Stress due to sleep deprivation: focus on $GABA_A$ receptor-chloride ionophore complex. Tartu, 1996.
25. **Kristina Allikmets**. Renin system activity in essential hypertension. Associations with atherothrombogenic cardiovascular risk factors and with the efficacy of calcium antagonist treatment. Tartu, 1996.
26. **Triin Parik**. Oxidative stress in essential hypertension: Associations with metabolic disturbances and the effects of calcium antagonist treatment. Tartu, 1996.
27. **Svetlana Päi**. Factors promoting heterogeneity of the course of rheumatoid arthritis. Tartu, 1997.
28. **Maarike Sallo**. Studies on habitual physical activity and aerobic fitness in 4 to 10 years old children. Tartu, 1997.
29. **Paul Naaber**. *Clostridium difficile* infection and intestinal microbial ecology. Tartu, 1997.
30. **Rein Pähkla**. Studies in pinoline pharmacology. Tartu, 1997.
31. **Andrus Juhan Voitk**. Outpatient laparoscopic cholecystectomy. Tartu, 1997.
32. **Joel Starkopf**. Oxidative stress and ischaemia-reperfusion of the heart. Tartu, 1997.
33. **Janika Kõrv**. Incidence, case-fatality and outcome of stroke. Tartu, 1998.
34. **Ülla Linnamägi**. Changes in local cerebral blood flow and lipid peroxidation following lead exposure in experiment. Tartu, 1998.
35. **Ave Minajeva**. Sarcoplasmic reticulum function: comparison of atrial and ventricular myocardium. Tartu, 1998.
36. **Oleg Milenin**. Reconstruction of cervical part of esophagus by revascularised ileal autografts in dogs. A new complex multistage method. Tartu, 1998.
37. **Sergei Pakriev**. Prevalence of depression, harmful use of alcohol and alcohol dependence among rural population in Udmurtia. Tartu, 1998.
38. **Allen Kaasik**. Thyroid hormone control over β-adrenergic signalling system in rat atria. Tartu, 1998.
39. **Vallo Matto**. Pharmacological studies on anxiogenic and antiaggressive properties of antidepressants. Tartu, 1998.
40. **Maire Vasar**. Allergic diseases and bronchial hyperreactivity in Estonian children in relation to environmental influences. Tartu, 1998.
41. **Kaja Julge**. Humoral immune responses to allergens in early childhood. Tartu, 1998.

42. **Heli Grünberg**. The cardiovascular risk of Estonian schoolchildren. A cross-sectional study of 9-, 12- and 15-year-old children. Tartu, 1998.
43. **Epp Sepp**. Formation of intestinal microbial ecosystem in children. Tartu, 1998.
44. **Mai Ots**. Characteristics of the progression of human and experimental glomerulopathies. Tartu, 1998.
45. **Tiina Ristimäe**. Heart rate variability in patients with coronary artery disease. Tartu, 1998.
46. **Leho Kõiv**. Reaction of the sympatho-adrenal and hypothalamo-pituitary-adrenocortical system in the acute stage of head injury. Tartu, 1998.
47. **Bela Adojaan**. Immune and genetic factors of childhood onset IDDM in Estonia. An epidemiological study. Tartu, 1999.
48. **Jakov Shlik**. Psychophysiological effects of cholecystokinin in humans. Tartu, 1999.
49. **Kai Kisand**. Autoantibodies against dehydrogenases of α-ketoacids. Tartu, 1999.
50. **Toomas Marandi**. Drug treatment of depression in Estonia. Tartu, 1999.
51. **Ants Kask**. Behavioural studies on neuropeptide Y. Tartu, 1999.
52. **Ello-Rahel Karelson**. Modulation of adenylate cyclase activity in the rat hippocampus by neuropeptide galanin and its chimeric analogs. Tartu, 1999.
53. **Tanel Laisaar**. Treatment of pleural empyema — special reference to intrapleural therapy with streptokinase and surgical treatment modalities. Tartu, 1999.
54. **Eve Pihl**. Cardiovascular risk factors in middle-aged former athletes. Tartu, 1999.
55. **Katrin Õunap**. Phenylketonuria in Estonia: incidence, newborn screening, diagnosis, clinical characterization and genotype/phenotype correlation. Tartu, 1999.
56. **Siiri Kõljalg**. *Acinetobacter* – an important nosocomial pathogen. Tartu, 1999.
57. **Helle Karro**. Reproductive health and pregnancy outcome in Estonia: association with different factors. Tartu, 1999.
58. **Heili Varendi**. Behavioral effects observed in human newborns during exposure to naturally occurring odors. Tartu, 1999.
59. **Anneli Beilmann**. Epidemiology of epilepsy in children and adolescents in Estonia. Prevalence, incidence, and clinical characteristics. Tartu, 1999.
60. **Vallo Volke**. Pharmacological and biochemical studies on nitric oxide in the regulation of behaviour. Tartu, 1999.
61. **Pilvi Ilves**. Hypoxic-ischaemic encephalopathy in asphyxiated term infants. A prospective clinical, biochemical, ultrasonographical study. Tartu, 1999.
62. **Anti Kalda**. Oxygen-glucose deprivation-induced neuronal death and its pharmacological prevention in cerebellar granule cells. Tartu, 1999.
63. **Eve-Irene Lepist**. Oral peptide prodrugs – studies on stability and absorption. Tartu, 2000.

64. **Jana Kivastik**. Lung function in Estonian schoolchildren: relationship with anthropometric indices and respiratory symptomas, reference values for dynamic spirometry. Tartu, 2000.
65. **Karin Kull**. Inflammatory bowel disease: an immunogenetic study. Tartu, 2000.
66. **Kaire Innos**. Epidemiological resources in Estonia: data sources, their quality and feasibility of cohort studies. Tartu, 2000.
67. **Tamara Vorobjova**. Immune response to *Helicobacter pylori* and its association with dynamics of chronic gastritis and epithelial cell turnover in antrum and corpus. Tartu, 2001.
68. **Ruth Kalda**. Structure and outcome of family practice quality in the changing health care system of Estonia. Tartu, 2001.
69. **Annika Krüüner**. *Mycobacterium tuberculosis* – spread and drug resistance in Estonia. Tartu, 2001.
70. **Marlit Veldi**. Obstructive Sleep Apnoea: Computerized Endopharyngeal Myotonometry of the Soft Palate and Lingual Musculature. Tartu, 2001.
71. **Anneli Uusküla**. Epidemiology of sexually transmitted diseases in Estonia in 1990–2000. Tartu, 2001.
72. **Ade Kallas**. Characterization of antibodies to coagulation factor VIII. Tartu, 2002.
73. **Heidi Annuk**. Selection of medicinal plants and intestinal lactobacilli as antimicrobil components for functional foods. Tartu, 2002.
74. **Aet Lukmann**. Early rehabilitation of patients with ischaemic heart disease after surgical revascularization of the myocardium: assessment of health-related quality of life, cardiopulmonary reserve and oxidative stress. A clinical study. Tartu, 2002.
75. **Maigi Eisen**. Pathogenesis of Contact Dermatitis: participation of Oxidative Stress. A clinical – biochemical study. Tartu, 2002.
76. **Piret Hussar**. Histology of the post-traumatic bone repair in rats. Elaboration and use of a new standardized experimental model – bicortical perforation of tibia compared to internal fracture and resection osteotomy. Tartu, 2002.
77. **Tõnu Rätsep**. Aneurysmal subarachnoid haemorrhage: Noninvasive monitoring of cerebral haemodynamics. Tartu, 2002.
78. **Marju Herodes**. Quality of life of people with epilepsy in Estonia. Tartu, 2003.
79. **Katre Maasalu**. Changes in bone quality due to age and genetic disorders and their clinical expressions in Estonia. Tartu, 2003.
80. **Toomas Sillakivi**. Perforated peptic ulcer in Estonia: epidemiology, risk factors and relations with *Helicobacter pylori*. Tartu, 2003.
81. **Leena Puksa**. Late responses in motor nerve conduction studies. F and A waves in normal subjects and patients with neuropathies. Tartu, 2003.
82. **Krista Lõivukene**. *Helicobacter pylori* in gastric microbial ecology and its antimicrobial susceptibility pattern. Tartu, 2003.

83. **Helgi Kolk**. Dyspepsia and *Helicobacter pylori* infection: the diagnostic value of symptoms, treatment and follow-up of patients referred for upper gastrointestinal endoscopy by family physicians. Tartu, 2003.
84. **Helena Soomer**. Validation of identification and age estimation methods in forensic odontology. Tartu, 2003.
85. **Kersti Oselin**. Studies on the human MDR1, MRP1, and MRP2 ABC transporters: functional relevance of the genetic polymorphisms in the *MDR1* and *MRP1* gene. Tartu, 2003.
86. **Jaan Soplepmann**. Peptic ulcer haemorrhage in Estonia: epidemiology, prognostic factors, treatment and outcome. Tartu, 2003.
87. **Margot Peetsalu**. Long-term follow-up after vagotomy in duodenal ulcer disease: recurrent ulcer, changes in the function, morphology and *Helicobacter pylori* colonisation of the gastric mucosa. Tartu, 2003.
88. **Kersti Klaamas**. Humoral immune response to *Helicobacter pylori* a study of host-dependent and microbial factors. Tartu, 2003.
89. **Pille Taba**. Epidemiology of Parkinson's disease in Tartu, Estonia. Prevalence, incidence, clinical characteristics, and pharmacoepidemiology. Tartu, 2003.
90. **Alar Veraksitš**. Characterization of behavioural and biochemical phenotype of cholecystokinin-2 receptor deficient mice: changes in the function of the dopamine and endopioidergic system. Tartu, 2003.
91. **Ingrid Kalev**. CC-chemokine receptor 5 (CCR5) gene polymorphism in Estonians and in patients with Type I and Type II diabetes mellitus. Tartu, 2003.
92. **Lumme Kadaja**. Molecular approach to the regulation of mitochondrial function in oxidative muscle cells. Tartu, 2003.
93. **Aive Liigant**. Epidemiology of primary central nervous system tumours in Estonia from 1986 to 1996. Clinical characteristics, incidence, survival and prognostic factors. Tartu, 2004.
94. **Andres, Kulla**. Molecular characteristics of mesenchymal stroma in human astrocytic gliomas. Tartu, 2004.
95. **Mari Järvelaid**. Health damaging risk behaviours in adolescence. Tartu, 2004.
96. **Ülle Pechter**. Progression prevention strategies in chronic renal failure and hypertension. An experimental and clinical study. Tartu, 2004.
97. **Gunnar Tasa**. Polymorphic glutathione S-transferases – biology and role in modifying genetic susceptibility to senile cataract and primary open angle glaucoma. Tartu, 2004.
98. **Tuuli Käämbre**. Intracellular energetic unit: structural and functional aspects. Tartu, 2004.
99. **Vitali Vassiljev**. Influence of nitric oxide syntase inhibitors on the effects of ethanol after acute and chronic ethanol administration and withdrawal. Tartu, 2004.

100. **Aune Rehema**. Assessment of nonhaem ferrous iron and glutathione redox ratio as markers of pathogeneticity of oxidative stress in different clinical groups. Tartu, 2004.
101. **Evelin Seppet**. Interaction of mitochondria and ATPases in oxidative muscle cells in normal and pathological conditions. Tartu, 2004.
102. **Eduard Maron**. Serotonin function in panic disorder: from clinical experiments to brain imaging and genetics. Tartu, 2004.
103. **Marje Oona**. *Helicobacter pylori* infection in children: epidemiological and therapeutic aspects. Tartu, 2004.
104. **Kersti Kokk**. Regulation of active and passive molecular transport in the testis. Tartu, 2005.
105. **Vladimir Järv**. Cross-sectional imaging for pretreatment evaluation and follow-up of pelvic malignant tumours. Tartu, 2005.
106. **Andre Õun**. Epidemiology of adult epilepsy in Tartu, Estonia. Incidence, prevalence and medical treatment. Tartu, 2005.
107. **Piibe Muda**. Homocysteine and hypertension: associations between homocysteine and essential hypertension in treated and untreated hypertensive patients with and without coronary artery disease. Tartu, 2005.
108. **Külli Kingo**. The interleukin-10 family cytokines gene polymorphisms in plaque psoriasis. Tartu, 2005.
109. **Mati Merila**. Anatomy and clinical relevance of the glenohumeral joint capsule and ligaments. Tartu, 2005.
110. **Epp Songisepp**. Evaluation of technological and functional properties of the new probiotic *Lactobacillus fermentum* ME-3. Tartu, 2005.
111. **Tiia Ainla**. Acute myocardial infarction in Estonia: clinical characteristics, management and outcome. Tartu, 2005.
112. **Andres Sell**. Determining the minimum local anaesthetic requirements for hip replacement surgery under spinal anaesthesia – a study employing a spinal catheter. Tartu, 2005.
113. **Tiia Tamme**. Epidemiology of odontogenic tumours in Estonia. Pathogenesis and clinical behaviour of ameloblastoma. Tartu, 2005.
114. **Triine Annus**. Allergy in Estonian schoolchildren: time trends and characteristics. Tartu, 2005.
115. **Tiia Voor**. Microorganisms in infancy and development of allergy: comparison of Estonian and Swedish children. Tartu, 2005.
116. **Priit Kasenõmm**. Indicators for tonsillectomy in adults with recurrent tonsillitis – clinical, microbiological and pathomorphological investigations. Tartu, 2005.
117. **Eva Zusinaite**. Hepatitis C virus: genotype identification and interactions between viral proteases. Tartu, 2005.
118. **Piret Kõll**. Oral lactoflora in chronic periodontitis and periodontal health. Tartu, 2006.
119. **Tiina Stelmach**. Epidemiology of cerebral palsy and unfavourable neurodevelopmental outcome in child population of Tartu city and county, Estonia Prevalence, clinical features and risk factors. Tartu, 2006.

120. **Katrin Pudersell**. Tropane alkaloid production and riboflavine excretion in the field and tissue cultures of henbane (*Hyoscyamus niger* L.). Tartu, 2006.
121. **Külli Jaako**. Studies on the role of neurogenesis in brain plasticity. Tartu, 2006.
122. **Aare Märtson**. Lower limb lengthening: experimental studies of bone regeneration and long-term clinical results. Tartu, 2006.
123. **Heli Tähepõld**. Patient consultation in family medicine. Tartu, 2006.
124. **Stanislav Liskmann**. Peri-implant disease: pathogenesis, diagnosis and treatment in view of both inflammation and oxidative stress profiling. Tartu, 2006.
125. **Ruth Rudissaar**. Neuropharmacology of atypical antipsychotics and an animal model of psychosis. Tartu, 2006.
126. **Helena Andreson**. Diversity of *Helicobacter pylori* genotypes in Estonian patients with chronic inflammatory gastric diseases. Tartu, 2006.
127. **Katrin Pruus**. Mechanism of action of antidepressants: aspects of serotoninergic system and its interaction with glutamate. Tartu, 2006.
128. **Priit Põder**. Clinical and experimental investigation: relationship of ischaemia/reperfusion injury with oxidative stress in abdominal aortic aneurysm repair and in extracranial brain artery endarterectomy and possibilities of protection against ischaemia using a glutathione analogue in a rat model of global brain ischaemia. Tartu, 2006.
129. **Marika Tammaru**. Patient-reported outcome measurement in rheumatoid arthritis. Tartu, 2006.
130. **Tiia Reimand**. Down syndrome in Estonia. Tartu, 2006.
131. **Diva Eensoo**. Risk-taking in traffic and Markers of Risk-Taking Behaviour in Schoolchildren and Car Drivers. Tartu, 2007.
132. **Riina Vibo**. The third stroke registry in Tartu, Estonia from 2001 to 2003: incidence, case-fatality, risk factors and long-term outcome. Tartu, 2007.
133. **Chris Pruunsild**. Juvenile idiopathic arthritis in children in Estonia. Tartu, 2007.
134. **Eve Õiglane-Šlik**. Angelman and Prader-Willi syndromes in Estonia. Tartu, 2007.
135. **Kadri Haller**. Antibodies to follicle stimulating hormone. Significance in female infertility. Tartu, 2007.
136. **Pille Ööpik**. Management of depression in family medicine. Tartu, 2007.
137. **Jaak Kals**. Endothelial function and arterial stiffness in patients with atherosclerosis and in healthy subjects. Tartu, 2007.
138. **Priit Kampus**. Impact of inflammation, oxidative stress and age on arterial stiffness and carotid artery intima-media thickness. Tartu, 2007.
139. **Margus Punab**. Male fertility and its risk factors in Estonia. Tartu, 2007.
140. **Alar Toom**. Heterotopic ossification after total hip arthroplasty: clinical and pathogenetic investigation. Tartu, 2007.

141. **Lea Pehme**. Epidemiology of tuberculosis in Estonia 1991–2003 with special regard to extrapulmonary tuberculosis and delay in diagnosis of pulmonary tuberculosis. Tartu, 2007.
142. **Juri Karjagin**. The pharmacokinetics of metronidazole and meropenem in septic shock. Tartu, 2007.
143. **Inga Talvik**. Inflicted traumatic brain injury shaken baby syndrome in Estonia – epidemiology and outcome. Tartu, 2007.
144. **Tarvo Rajasalu**. Autoimmune diabetes: an immunological study of type 1 diabetes in humans and in a model of experimental diabetes (in RIP-B7.1 mice). Tartu, 2007.
145. **Inga Karu**. Ischaemia-reperfusion injury of the heart during coronary surgery: a clinical study investigating the effect of hyperoxia. Tartu, 2007.
146. **Peeter Padrik**. Renal cell carcinoma: Changes in natural history and treatment of metastatic disease. Tartu, 2007.
147. **Neve Vendt**. Iron deficiency and iron deficiency anaemia in infants aged 9 to 12 months in Estonia. Tartu, 2008.
148. **Lenne-Triin Heidmets**. The effects of neurotoxins on brain plasticity: focus on neural Cell Adhesion Molecule. Tartu, 2008.
149. **Paul Korrovits**. Asymptomatic inflammatory prostatitis: prevalence, etiological factors, diagnostic tools. Tartu, 2008.
150. **Annika Reintam**. Gastrointestinal failure in intensive care patients. Tartu, 2008.
151. **Kristiina Roots**. Cationic regulation of Na-pump in the normal, Alzheimer's and CCK_2 receptor-deficient brain. Tartu, 2008.
152. **Helen Puusepp**. The genetic causes of mental retardation in Estonia: fragile X syndrome and creatine transporter defect. Tartu, 2009.
153. **Kristiina Rull**. Human chorionic gonadotropin beta genes and recurrent miscarriage: expression and variation study. Tartu, 2009.
154. **Margus Eimre**. Organization of energy transfer and feedback regulation in oxidative muscle cells. Tartu, 2009.
155. **Maire Link**. Transcription factors FoxP3 and AIRE: autoantibody associations. Tartu, 2009.
156. **Kai Haldre**. Sexual health and behaviour of young women in Estonia. Tartu, 2009.
157. **Kaur Liivak**. Classical form of congenital adrenal hyperplasia due to 21-hydroxylase deficiency in Estonia: incidence, genotype and phenotype with special attention to short-term growth and 24-hour blood pressure. Tartu, 2009.
158. **Kersti Ehrlich**. Antioxidative glutathione analogues (UPF peptides) – molecular design, structure-activity relationships and testing the protective properties. Tartu, 2009.
159. **Anneli Rätsep**. Type 2 diabetes care in family medicine. Tartu, 2009.
160. **Silver Türk**. Etiopathogenetic aspects of chronic prostatitis: role of mycoplasmas, coryneform bacteria and oxidative stress. Tartu, 2009.

161. **Kaire Heilman**. Risk markers for cardiovascular disease and low bone mineral density in children with type 1 diabetes. Tartu, 2009.
162. **Kristi Rüütel**. HIV-epidemic in Estonia: injecting drug use and quality of life of people living with HIV. Tartu, 2009.
163. **Triin Eller**. Immune markers in major depression and in antidepressive treatment. Tartu, 2009.
164. **Siim Suutre**. The role of TGF-β isoforms and osteoprogenitor cells in the pathogenesis of heterotopic ossification. An experimental and clinical study of hip arthroplasty. Tartu, 2010.
165. **Kai Kliiman**. Highly drug-resistant tuberculosis in Estonia: Risk factors and predictors of poor treatment outcome. Tartu, 2010.
166. **Inga Villa**. Cardiovascular health-related nutrition, physical activity and fitness in Estonia. Tartu, 2010.
167. **Tõnis Org**. Molecular function of the first PHD finger domain of Autoimmune Regulator protein. Tartu, 2010.
168. **Tuuli Metsvaht**. Optimal antibacterial therapy of neonates at risk of early onset sepsis. Tartu, 2010.
169. **Jaanus Kahu**. Kidney transplantation: Studies on donor risk factors and mycophenolate mofetil. Tartu, 2010.
170. **Koit Reimand**. Autoimmunity in reproductive failure: A study on associated autoantibodies and autoantigens. Tartu, 2010.
171. **Mart Kull**. Impact of vitamin D and hypolactasia on bone mineral density: a population based study in Estonia. Tartu, 2010.
172. **Rael Laugesaar**. Stroke in children – epidemiology and risk factors. Tartu, 2010.
173. **Mark Braschinsky**. Epidemiology and quality of life issues of hereditary spastic paraplegia in Estonia and implemention of genetic analysis in everyday neurologic practice. Tartu, 2010.
174. **Kadri Suija**. Major depression in family medicine: associated factors, recurrence and possible intervention. Tartu, 2010.
175. **Jarno Habicht**. Health care utilisation in Estonia: socioeconomic determinants and financial burden of out-of-pocket payments. Tartu, 2010.
176. **Kristi Abram**. The prevalence and risk factors of rosacea. Subjective disease perception of rosacea patients. Tartu, 2010.
177. **Malle Kuum**. Mitochondrial and endoplasmic reticulum cation fluxes: Novel roles in cellular physiology. Tartu, 2010.
178. **Rita Teek**. The genetic causes of early onset hearing loss in Estonian children. Tartu, 2010.
179. **Daisy Volmer**. The development of community pharmacy services in Estonia – public and professional perceptions 1993–2006. Tartu, 2010.
180. **Jelena Lissitsina**. Cytogenetic causes in male infertility. Tartu, 2011.
181. **Delia Lepik**. Comparison of gunshot injuries caused from Tokarev, Makarov and Glock 19 pistols at different firing distances. Tartu, 2011.
182. **Ene-Renate Pähkla**. Factors related to the efficiency of treatment of advanced periodontitis. Tartu, 2011.

183. **Maarja Krass**. L-Arginine pathways and antidepressant action. Tartu, 2011.
184. **Taavi Lai**. Population health measures to support evidence-based health policy in Estonia. Tartu, 2011.
185. **Tiit Salum**. Similarity and difference of temperature-dependence of the brain sodium pump in normal, different neuropathological, and aberrant conditions and its possible reasons. Tartu, 2011.
186. **Tõnu Vooder**. Molecular differences and similarities between histological subtypes of non-small cell lung cancer. Tartu, 2011.
187. **Jelena Štšepetova**. The characterisation of intestinal lactic acid bacteria using bacteriological, biochemical and molecular approaches. Tartu, 2011.
188. **Radko Avi**. Natural polymorphisms and transmitted drug resistance in Estonian HIV-1 CRF06_cpx and its recombinant viruses. Tartu, 2011, 116 p.
189. **Edward Laane**. Multiparameter flow cytometry in haematological malignancies. Tartu, 2011, 152 p.
190. **Triin Jagomägi**. A study of the genetic etiology of nonsyndromic cleft lip and palate. Tartu, 2011, 158 p.
191. **Ivo Laidmäe**. Fibrin glue of fish (*Salmo salar*) origin: immunological study and development of new pharmaceutical preparation. Tartu, 2012, 150 p.
192. **Ülle Parm**. Early mucosal colonisation and its role in prediction of invasive infection in neonates at risk of early onset sepsis. Tartu, 2012, 168 p.
193. **Kaupo Teesalu**. Autoantibodies against desmin and transglutaminase 2 in celiac disease: diagnostic and functional significance. Tartu, 2012, 142 p.
194. **Maksim Zagura**. Biochemical, functional and structural profiling of arterial damage in atherosclerosis. Tartu, 2012, 162 p.
195. **Vivian Kont**. Autoimmune regulator: characterization of thymic gene regulation and promoter methylation. Tartu, 2012, 134 p.
196. **Pirje Hütt**. Functional properties, persistence, safety and efficacy of potential probiotic lactobacilli. Tartu, 2012, 246 p.
197. **Innar Tõru**. Serotonergic modulation of CCK-4- induced panic. Tartu, 2012, 132 p.
198. **Sigrid Vorobjov**. Drug use, related risk behaviour and harm reduction interventions utilization among injecting drug users in Estonia: implications for drug policy. Tartu, 2012, 120 p.
199. **Martin Serg**. Therapeutic aspects of central haemodynamics, arterial stiffness and oxidative stress in hypertension. Tartu, 2012, 156 p.
200. **Jaanika Kumm**. Molecular markers of articular tissues in early knee osteoarthritis: a population-based longitudinal study in middle-aged subjects. Tartu, 2012, 159 p.
201. **Kertu Rünkorg**. Functional changes of dopamine, endopioid and endocannabinoid systems in CCK2 receptor deficient mice. Tartu, 2012, 125 p.
202. **Mai Blöndal**. Changes in the baseline characteristics, management and outcomes of acute myocardial infarction in Estonia. Tartu, 2012, 127 p.

203. **Jana Lass**. Epidemiological and clinical aspects of medicines use in children in Estonia. Tartu, 2012, 170 p.
204. **Kai Truusalu**. Probiotic lactobacilli in experimental persistent *Salmonella* infection. Tartu, 2013, 139 p.
205. **Oksana Jagur**. Temporomandibular joint diagnostic imaging in relation to pain and bone characteristics. Long-term results of arthroscopic treatment. Tartu, 2013, 126 p.
206. **Katrin Sikk**. Manganese-ephedrone intoxication – pathogenesis of neurological damage and clinical symptomatology. Tartu, 2013, 125 p.
207. **Kai Blöndal**. Tuberculosis in Estonia with special emphasis on drug-resistant tuberculosis: Notification rate, disease recurrence and mortality. Tartu, 2013, 151 p.
208. **Marju Puurand**. Oxidative phosphorylation in different diseases of gastric mucosa. Tartu, 2013, 123 p.
209. **Aili Tagoma**. Immune activation in female infertility: Significance of autoantibodies and inflammatory mediators. Tartu, 2013, 135 p.
210. **Liis Sabre**. Epidemiology of traumatic spinal cord injury in Estonia. Brain activation in the acute phase of traumatic spinal cord injury. Tartu, 2013, 135 p.
211. **Merit Lamp**. Genetic susceptibility factors in endometriosis. Tartu, 2013, 125 p.
212. **Erik Salum**. Beneficial effects of vitamin D and angiotensin II receptor blocker on arterial damage. Tartu, 2013, 167 p.
213. **Maire Karelson**. Vitiligo: clinical aspects, quality of life and the role of melanocortin system in pathogenesis. Tartu, 2013, 153 p.
214. **Kuldar Kaljurand**. Prevalence of exfoliation syndrome in Estonia and its clinical significance. Tartu, 2013, 113 p.
215. **Raido Paasma**. Clinical study of methanol poisoning: handling large outbreaks, treatment with antidotes, and long-term outcomes. Tartu, 2013, 96 p.
216. **Anne Kleinberg**. Major depression in Estonia: prevalence, associated factors, and use of health services. Tartu, 2013, 129 p.
217. **Triin Eglit**. Obesity, impaired glucose regulation, metabolic syndrome and their associations with high-molecular-weight adiponectin levels. Tartu, 2014, 115 p.
218. **Kristo Ausmees**. Reproductive function in middle-aged males: Associations with prostate, lifestyle and couple infertility status. Tartu, 2014, 125 p.
219. **Kristi Huik**. The influence of host genetic factors on the susceptibility to HIV and HCV infections among intravenous drug users. Tartu, 2014, 144 p.
220. **Liina Tserel**. Epigenetic profiles of monocytes, monocyte-derived macrophages and dendritic cells. Tartu, 2014, 143 p.
221. **Irina Kerna**. The contribution of *ADAM12* and *CILP* genes to the development of knee osteoarthritis. Tartu, 2014, 152 p.

222. **Ingrid Liiv**. Autoimmune regulator protein interaction with DNA-dependent protein kinase and its role in apoptosis. Tartu, 2014, 143 p.
223. **Liivi Maddison**. Tissue perfusion and metabolism during intra-abdominal hypertension. Tartu, 2014, 103 p.
224. **Krista Ress**. Childhood coeliac disease in Estonia, prevalence in atopic dermatitis and immunological characterisation of coexistence. Tartu, 2014, 124 p.
225. **Kai Muru**. Prenatal screening strategies, long-term outcome of children with marked changes in maternal screening tests and the most common syndromic heart anomalies in Estonia. Tartu, 2014, 189 p.
226. **Kaja Rahu**. Morbidity and mortality among Baltic Chernobyl cleanup workers: a register-based cohort study. Tartu, 2014, 155 p.
227. **Klari Noormets**. The development of diabetes mellitus, fertility and energy metabolism disturbances in a Wfs1-deficient mouse model of Wolfram syndrome. Tartu, 2014, 132 p.
228. **Liis Toome**. Very low gestational age infants in Estonia. Tartu, 2014, 183 p.
229. **Ceith Nikkolo**. Impact of different mesh parameters on chronic pain and foreign body feeling after open inguinal hernia repair. Tartu, 2014, 132 p.
230. **Vadim Brjalin**. Chronic hepatitis C: predictors of treatment response in Estonian patients. Tartu, 2014, 122 p.
231. **Vahur Metsna**. Anterior knee pain in patients following total knee arthroplasty: the prevalence, correlation with patellar cartilage impairment and aspects of patellofemoral congruence. Tartu, 2014, 130 p.
232. **Marju Kase**. Glioblastoma multiforme: possibilities to improve treatment efficacy. Tartu, 2015, 137 p.
233. **Riina Runnel**. Oral health among elementary school children and the effects of polyol candies on the prevention of dental caries. Tartu, 2015, 112 p.
234. **Made Laanpere**. Factors influencing women's sexual health and reproductive choices in Estonia. Tartu, 2015, 176 p.
235. **Andres Lust**. Water mediated solid state transformations of a polymorphic drug – effect on pharmaceutical product performance. Tartu, 2015, 134 p.
236. **Anna Klugman**. Functionality related characterization of pretreated wood lignin, cellulose and polyvinylpyrrolidone for pharmaceutical applications. Tartu, 2015, 156 p.
237. **Triin Laisk-Podar**. Genetic variation as a modulator of susceptibility to female infertility and a source for potential biomarkers. Tartu, 2015, 155 p.
238. **Mailis Tõnisson**. Clinical picture and biochemical changes in blood in children with acute alcohol intoxication. Tartu, 2015, 100 p.
239. **Kadri Tamme**. High volume haemodiafiltration in treatment of severe sepsis – impact on pharmacokinetics of antibiotics and inflammatory response. Tartu, 2015, 133 p.

240. **Kai Part**. Sexual health of young people in Estonia in a social context: the role of school-based sexuality education and youth-friendly counseling services. Tartu, 2015, 203 p.
241. **Urve Paaver**. New perspectives for the amorphization and physical stabilization of poorly water-soluble drugs and understanding their dissolution behavior. Tartu, 2015, 139 p.
242. **Aleksandr Peet**. Intrauterine and postnatal growth in children with HLA-conferred susceptibility to type 1 diabetes. Tartu. 2015, 146 p.
243. **Piret Mitt**. Healthcare-associated infections in Estonia – epidemiology and surveillance of bloodstream and surgical site infections. Tartu, 2015, 145 p.
244. **Merli Saare**. Molecular Profiling of Endometriotic Lesions and Endometria of Endometriosis Patients. Tartu, 2016, 129 p.
245. **Kaja-Triin Laisaar**. People living with HIV in Estonia: Engagement in medical care and methods of increasing adherence to antiretroviral therapy and safe sexual behavior. Tartu, 2016, 132 p.
246. **Eero Merilind**. Primary health care performance: impact of payment and practice-based characteristics. Tartu, 2016, 120 p.
247. **Jaanika Kärner**. Cytokine-specific autoantibodies in AIRE deficiency. Tartu, 2016, 182 p.
248. **Kaido Paapstel**. Metabolomic profile of arterial stiffness and early biomarkers of renal damage in atherosclerosis. Tartu, 2016, 173 p.
249. **Liidia Kiisk**. Long-term nutritional study: anthropometrical and clinico-laboratory assessments in renal replacement therapy patients after intensive nutritional counselling. Tartu, 2016, 207 p.
250. **Georgi Nellis**. The use of excipients in medicines administered to neonates in Europe. Tartu, 2017, 159 p.
251. **Aleksei Rakitin**. Metabolic effects of acute and chronic treatment with valproic acid in people with epilepsy. Tartu, 2017, 125 p.
252. **Eveli Kallas**. The influence of immunological markers to susceptibility to HIV, HBV, and HCV infections among persons who inject drugs. Tartu, 2017, 138 p.
253. **Tiina Freimann**. Musculoskeletal pain among nurses: prevalence, risk factors, and intervention. Tartu, 2017, 125 p.
254. **Evelyn Aaviksoo**. Sickness absence in Estonia: determinants and influence of the sick-pay cut reform. Tartu, 2017, 121 p.
255. **Kalev Nõupuu**. Autosomal-recessive Stargardt disease: phenotypic heterogeneity and genotype-phenotype associations. Tartu, 2017, 131 p.
256. **Ho Duy Binh**. Osteogenesis imperfecta in Vietnam. Tartu, 2017, 125 p.
257. **Uku Haljasorg**. Transcriptional mechanisms in thymic central tolerance. Tartu, 2017, 147 p.
258. **Živile Riispere**. IgA Nephropathy study according to the Oxford Classification: IgA Nephropathy clinical-morphological correlations, disease progression and the effect of renoprotective therapy. Tartu, 2017, 129 p.

259. **Hiie Soeorg**. Coagulase-negative staphylococci in gut of preterm neonates and in breast milk of their mothers. Tartu, 2017, 216 p.
260. **Anne-Mari Anton Willmore**. Silver nanoparticles for cancer research. Tartu, 2017, 132 p.
261. **Ott Laius**. Utilization of osteoporosis medicines, medication adherence and the trend in osteoporosis related hip fractures in Estonia. Tartu, 2017, 134 p.
262. **Alar Aab**. Insights into molecular mechanisms of asthma and atopic dermatitis. Tartu, 2017, 164 p.
263. **Sander Pajusalu**. Genome-wide diagnostics of Mendelian disorders: from chromosomal microarrays to next-generation sequencing. Tartu, 2017, 146 p.
264. **Mikk Jürisson**. Health and economic impact of hip fracture in Estonia. Tartu, 2017, 164 p.
265. **Kaspar Tootsi**. Cardiovascular and metabolomic profiling of osteoarthritis. Tartu, 2017, 150 p.
266. **Mario Saare**. The influence of AIRE on gene expression – studies of transcriptional regulatory mechanisms in cell culture systems. Tartu, 2017, 172 p.
267. **Piia Jõgi**. Epidemiological and clinical characteristics of pertussis in Estonia. Tartu, 2018, 168 p.
268. **Elle Põldoja**. Structure and blood supply of the superior part of the shoulder joint capsule. Tartu, 2018, 116 p.
269. **Minh Son Nguyen**. Oral health status and prevalence of temporomandibular disorders in 65–74-year-olds in Vietnam. Tartu, 2018, 182 p.
270. **Kristian Semjonov**. Development of pharmaceutical quench-cooled molten and melt-electrospun solid dispersions for poorly water-soluble indomethacin. Tartu, 2018, 125 p.
271. **Janne Tiigimäe-Saar**. Botulinum neurotoxin type A treatment for sialorrhea in central nervous system diseases. Tartu, 2018, 109 p.
272. **Veiko Vengerfeldt**. Apical periodontitis: prevalence and etiopathogenetic aspects. Tartu, 2018, 150 p.
273. **Rudolf Bichele**. TNF superfamily and AIRE at the crossroads of thymic differentiation and host protection against *Candida albicans* infection. Tartu, 2018, 153 p.
274. **Olga Tšuiko**. Unravelling Chromosomal Instability in Mammalian Preimplantation Embryos Using Single-Cell Genomics. Tartu, 2018, 169 p.
275. **Kärt Kriisa**. Profile of acylcarnitines, inflammation and oxidative stress in first-episode psychosis before and after antipsychotic treatment. Tartu, 2018, 145 p.
276. **Xuan Dung Ho**. Characterization of the genomic profile of osteosarcoma. Tartu, 2018, 144 p.
277. **Karit Reinson**. New Diagnostic Methods for Early Detection of Inborn Errors of Metabolism in Estonia. Tartu, 2018, 201 p.

278. **Mari-Anne Vals**. Congenital N-glycosylation Disorders in Estonia. Tartu, 2019, 148 p.
279. **Liis Kadastik-Eerme**. Parkinson's disease in Estonia: epidemiology, quality of life, clinical characteristics and pharmacotherapy. Tartu, 2019, 202 p.
280. **Hedi Hunt**. Precision targeting of intraperitoneal tumors with peptide-guided nanocarriers. Tartu, 2019, 179 p.
281. **Rando Porosk**. The role of oxidative stress in Wolfram syndrome 1 and hypothermia. Tartu, 2019, 123 p.
282. **Ene-Ly Jõgeda**. The influence of coinfections and host genetic factor on the susceptibility to HIV infection among people who inject drugs. Tartu, 2019, 126 p.
283. **Kristel Ehala-Aleksejev**. The associations between body composition, obesity and obesity-related health and lifestyle conditions with male reproductive function. Tartu, 2019, 138 p.
284. **Aigar Ottas**. The metabolomic profiling of psoriasis, atopic dermatitis and atherosclerosis. Tartu, 2019, 136 p.
285. **Elmira Gurbanova**. Specific characteristics of tuberculosis in low default, but high multidrug–resistance prison setting. Tartu, 2019, 129 p.
286. **Van Thai Nguyeni**. The first study of the treatment outcomes of patients with cleft lip and palate in Central Vietnam. Tartu, 2019, 144 p.
287. **Maria Yakoreva**. Imprinting Disorders in Estonia. Tartu, 2019, 187 p.
288. **Kadri Rekker**. The putative role of microRNAs in endometriosis pathogenesis and potential in diagnostics. Tartu, 2019, 140 p.
289. **Ülle Võhma**. Association between personality traits, clinical characteristics and pharmacological treatment response in panic disorder. Tartu, 2019, 121 p.
290. **Aet Saar**. Acute myocardial infarction in Estonia 2001–2014: towards risk-based prevention and management. Tartu, 2019, 124 p.
291. **Toomas Toomsoo**. Transcranial brain sonography in the Estonian cohort of Parkinson's disease. Tartu, 2019, 114 p.
292. **Lidiia Zhytnik**. Inter- and intrafamilial diversity based on genotype and phenotype correlations of Osteogenesis Imperfecta. Tartu, 2019, 224 p.
293. **Pilleriin Soodla**. Newly HIV-infected people in Estonia: estimation of incidence and transmitted drug resistance. Tartu, 2019, 194 p.
294. **Kristiina Ojamaa**. Epidemiology of gynecological cancer in Estonia. Tartu, 2020, 133 p.
295. **Marianne Saard**. Modern Cognitive and Social Intervention Techniques in Paediatric Neurorehabilitation for Children with Acquired Brain Injury. Tartu, 2020, 168 p.
296. **Julia Maslovskaja**. The importance of DNA binding and DNA breaks for AIRE-mediated transcriptional activation. Tartu, 2020, 162 p.
297. **Natalia Lobanovskaya**. The role of PSA-NCAM in the survival of retinal ganglion cells. Tartu, 2020, 105 p.

298. **Madis Rahu**. Structure and blood supply of the postero-superior part of the shoulder joint capsule with implementation of surgical treatment after anterior traumatic dislocation. Tartu, 2020, 104 p.
299. **Helen Zirnask**. Luteinizing hormone (LH) receptor expression in the penis and its possible role in pathogenesis of erectile disturbances. Tartu, 2020, 87 p.
300. **Kadri Toome**. Homing peptides for targeting of brain diseases. Tartu, 2020, 152 p.
301. **Maarja Hallik**. Pharmacokinetics and pharmacodynamics of inotropic drugs in neonates. Tartu, 2020, 172 p.
302. **Raili Müller**. Cardiometabolic risk profile and body composition in early rheumatoid arthritis. Tartu, 2020, 133 p.
303. **Sergo Kasvandik**. The role of proteomic changes in endometrial cells – from the perspective of fertility and endometriosis. Tartu, 2020, 191 p.
304. **Epp Kaleviste**. Genetic variants revealing the role of STAT1/STAT3 signaling cytokines in immune protection and pathology. Tartu, 2020, 189 p.
305. **Sten Saar**. Epidemiology of severe injuries in Estonia. Tartu, 2020, 104 p.
306. **Kati Braschinsky**. Epidemiology of primary headaches in Estonia and applicability of web-based solutions in headache epidemiology research. Tartu, 2020, 129 p.
307. **Helen Vaher**. MicroRNAs in the regulation of keratinocyte responses in *psoriasis vulgaris* and atopic dermatitis. Tartu, 2020, 242 p.
308. **Liisi Raam**. Molecular Alterations in the Pathogenesis of Two Chronic Dermatoses – Vitiligo and Psoriasis. Tartu, 2020, 164 p.
309. **Artur Vetkas**. Long-term quality of life, emotional health, and associated factors in patients after aneurysmal subarachnoid haemorrhage. Tartu, 2020, 127 p.
310. **Teele Kasepalu**. Effects of remote ischaemic preconditioning on organ damage and acylcarnitines' metabolism in vascular surgery. Tartu, 2020, 130 p.
311. **Prakash Lingasamy**. Development of multitargeted tumor penetrating peptides. Tartu, 2020, 246 p.
312. **Lille Kurvits.** Parkinson's disease as a multisystem disorder: whole transcriptome study in Parkinson's disease patients' skin and blood. Tartu, 2021, 142 p.
313. **Mariliis Põld.** Smoking, attitudes towards smoking behaviour, and nicotine dependence among physicians in Estonia: cross-sectional surveys 1982–2014. Tartu, 2021, 172 p.
314. **Triin Kikas**. Single nucleotide variants affecting placental gene expression and pregnancy outcome. Tartu, 2021, 160 p.
315. **Hedda Lippus-Metsaots**. Interpersonal violence in Estonia: prevalence, impact on health and health behaviour. Tartu, 2021, 172 p.

316. **Georgi Dzaparidze.** Quantification and evaluation of the diagnostic significance of adenocarcinoma-associated microenvironmental changes in the prostate using modern digital pathology solutions. Tartu, 2021, 132 p.
317. **Tuuli Sedman.** New avenues for GLP1 receptor agonists in the treatment of diabetes. Tartu, 2021, 118 p.
318. **Martin Padar.** Enteral nutrition, gastrointestinal dysfunction and intestinal biomarkers in critically ill patients. Tartu, 2021, 189 p.
319. **Siim Schneider.** Risk factors, etiology and long-term outcome in young ischemic stroke patients in Estonia. Tartu, 2021, 131 p.
320. **Konstantin Ridnõi.** Implementation and effectiveness of new prenatal diagnostic strategies in Estonia. Tartu, 2021, 191 p.
321. **Risto Vaikjärv.** Etiopathogenetic and clinical aspects of peritonsillar abscess. Tartu, 2021, 115 p.
322. **Liis Preem.** Design and characterization of antibacterial electrospun drug delivery systems for wound infections. Tartu, 2022, 220 p.
323. **Keerthie Dissanayake.** Preimplantation embryo-derived extracellular vesicles: potential as an embryo quality marker and their role during the embryo-maternal communication. Tartu, 2022, 203 p.
324. **Laura Viidik.** 3D printing in pharmaceutics: a new avenue for fabricating therapeutic drug delivery systems. Tartu, 2022, 139 p.
325. **Kasun Godakumara.** Extracellular vesicle mediated embryo-maternal communication – A tool for evaluating functional competency of preimplantation embryos. Tartu, 2022, 176 p.
326. **Hindrek Teder.** Developing computational methods and workflows for targeted and whole-genome sequencing based non-invasive prenatal testing. Tartu, 2022, 138 p.
327. **Jana Tuusov.** Deaths caused by alcohol, psychotropic and other substances in Estonia: evidence based on forensic autopsies. Tartu, 2022, 157 p.
328. **Heigo Reima.** Colorectal cancer care and outcomes – evaluation and possibilities for improvement in Estonia. Tartu, 2022, 146 p.
329. **Liisa Kuhi.** A contribution of biomarker collagen type II neoepitope C2C in urine to the diagnosis and prognosis of knee osteoarthritis. Tartu, 2022, 157 p.
330. **Reeli Tamme.** Associations between pubertal hormones and physical activity levels, and subsequent bone mineral characteristics: a longitudinal study of boys aged 12–18. Tartu, 2022, 118 p.
331. **Deniss Sõritsa.** The impact of endometriosis and physical activity on female reproduction. Tartu, 2022, 152 p.
332. **Mohammad Mehedi Hasan.** Characterization of follicular fluid-derived extracellular vesicles and their contribution to periconception environment. Tartu, 2022, 194 p.
333. **Priya Kulkarni.** Osteoarthritis pathogenesis: an immunological passage through synovium-synovial fluid axis. Tartu, 2022, 268 p.

334. **Nigul Ilves.** Brain plasticity and network reorganization in children with perinatal stroke: a functional magnetic resonance imaging study. Tartu, 2022, 169 p.
335. **Marko Murruste.** Short- and long-term outcomes of surgical management of chronic pancreatitis. Tartu, 2022, 180 p.
336. **Marilin Ivask.** Transcriptomic and metabolic changes in the WFS1-deficient mouse model. Tartu, 2022, 158 p.
337. **Jüri Lieberg.** Results of surgical treatment and role of biomarkers in pathogenesis and risk prediction in patients with abdominal aortic aneurysm and peripheral artery disease. Tartu, 2022, 160 p.
338. **Sanna Puusepp.** Comparison of molecular genetics and morphological findings of childhood-onset neuromuscular disorders. Tartu, 2022, 216 p.